

APPLICATION OF TOPOLOGY OPTIMIZATION IN THE DESIGN OF CONCRETE STRUCTURES

Thesis

Submitted in partial fulfillment of the requirements for the
degree of

DOCTOR OF PHILOSOPHY

by

RESMY V R



**DEPARTMENT OF CIVIL ENGINEERING
NATIONAL INSTITUTE OF TECHNOLOGY KARNATAKA
SURATHKAL, MANGALORE - 575 025**

May,2024

APPLICATION OF TOPOLOGY OPTIMIZATION IN THE DESIGN OF CONCRETE STRUCTURES

Thesis

Submitted in partial fulfilment of the requirements for the
degree of

DOCTOR OF PHILOSOPHY

by

RESMY V R

(CV16F16)

Under the guidance of

DR. RAJASEKARAN C.



**DEPARTMENT OF CIVIL ENGINEERING
NATIONAL INSTITUTE OF TECHNOLOGY KARNATAKA
SURATHKAL, MANGALORE - 575 025**

May,2024

DECLARATION

By the Ph.D. Research Scholar

I hereby declare that the Research Thesis entitled “**Application of Topology Optimization in the Design of Concrete Structures**” which is being submitted to the National Institute of Technology Karnataka, Surathkal in partial fulfillment of the requirements for the award of the Degree of **Doctor of Philosophy in Civil Engineering** is a *bonafide report of the research work carried out by me*. The material contained in this Research Thesis has not been submitted to any University or Institution for the award of any degree.



Resmy V R

CV16F16

Department of Civil Engineering

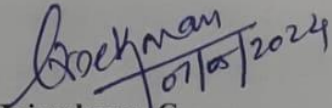
National Institute of Technology Karnataka, Surathkal

Place: NITK, Surathkal

Date: May 7, 2024

CERTIFICATE

This is to certify that the Research Thesis entitled “**Application of Topology Optimization in the Design of Concrete Structures**” submitted by **Ms.RESMY V R** (Register Number:165112CV16F16) as the record of research work carried out by her, is accepted as Research Thesis submission in partial fulfillment of the requirements for the award of the degree of Doctor of Philosophy.

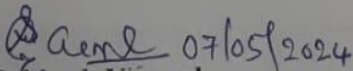

07/05/2024
Dr. Rajasekaran C.

Research Guide

Assistant Professor

Department of Civil Engineering

NITK Surathkal - 575025


07/05/2024
Dr. Subhash Yaragal

Chairperson - DRPC

Chairman (DRPC)

Department of Civil Engineering
National Institute of Technology Karnataka
Surathkal, Mangalore - 575 025, Karnataka, INDIA



ACKNOWLEDGMENT

First and foremost, I express gratitude to God for guiding and inspiring me to embark on this research journey, which has been profoundly enriching. I am delighted and honored to have successfully completed the research journey.

With a deep sense of gratitude, I express my heartfelt thanks to my research supervisor **Dr. Rajasekaran, C.** Associate Professor, Department of Civil Engineering, NITK Surathkal for his invaluable guidance, encouragement, and motivation throughout my research work. I consider myself incredibly fortunate and grateful to be his protege, and I am forever indebted to him for his care, support, and affection.

I am also thankful to the RPAC Panel members **Dr. Katta Venkataramana**, Professor, Department of Civil Engineering, NITK, Surathkal, and **Dr. P.Sam Johnson**, Associate Professor, Department of Mathematics and Computational Sciences, NITK, Surathkal, for their valuable guidance and suggestions throughout my work. I am also thankful to **Prof. Subhash Yaragal**, Head of the Department of Civil Engineering and Chairman - DRPC, **Dr. Mithun Mohan** Secretary - DRPC and **Dr. T. Palanisamy** Former Secretary - DRPC, Department of Civil Engineering, NITK-Surathkal, for their support and guidance throughout my work. I would like to thank **Prof. B.R. Jayalekshmi**, Former Head of the Department of Civil Engineering, NITK Surathkal for all the support throughout my work. I owe my special thanks to **Dr. M.C. Narasimhan**, Professor, Department of Civil Engineering, NITK Surathkal for the support in my research work.

I extend my thankfulness to the external examiners **Dr. Konjengbam Darunkumar Singh**, Professor, Department of Civil Engineering, Indian Institute of Technology Guwahati, and **Dr. P. Ratish Kumar**, Professor, Department of Civil Engineering, NIT Warangal for their valuable comments which helped me to improve the quality of the thesis.

I would like to express my gratitude to the faculty and staff of the Civil Engineering department at the Institute for their unwavering support. The fellowship from the Institute, the TEQIP-III fund, and the contingency grants have greatly assisted me in meeting the requirements for attending conferences during my research period.

I would like to give special recognition to my dear friends for creating a positive working space with their support and affection. I am grateful for the invaluable moral support and assistance generously offered by my fellow research colleagues throughout this endeavor.

Their informal encouragement and backing have been immensely significant. I appreciate all who aided and motivated me during this research endeavor.

Life wouldn't have been easy without the care and support of my family for which I express my deepest sense of gratitude, love and reverence toward each and everyone of them.

RESMY V R

ABSTRACT

Structural optimization involves arranging components efficiently to meet load-bearing requirements, with constraints serving as performance indicators and objective functions. The Finite Element (FE) method enables topology optimization techniques for weight reduction in aerospace, automotive, and mechanical engineering, but its application in civil and structural engineering is less prevalent. However, in the era of renewable and robust infrastructure, optimizing structural designs becomes essential for efficiency enhancement in unique civil-structural engineering projects. The study applied optimization procedures to different concrete structures with different objectives and constraints using Material Interpolation scheme SIMP(Solid isotropic material with penalization)method. The study explores the use of higher-order elements and multiple constrained problems, particularly focusing on stress and deflection. Stress levels are maintained within safety limits, and deflection control is implemented to ensure structural aesthetics.

The optimization capability of FEM software ABAQUS has been utilized for this study. Compliance minimization with volume constraints was used for static problems while maximizing first-order eigenfrequency was applied for free vibration cases. Topology optimization of concrete dapped beams is performed using the Bidirectional evolutionary structural optimization(BESO) method in ABAQUS software. High-stress concentration occurs at reentrant corners of dapped beams due to their geometrical nonlinearity, necessitating proper reinforcement to prevent failure. Concrete damage plasticity model in ABAQUS enhances the modelling of concrete beams by incorporating tension and compression damage. The findings also shed light on the benefits of topology optimization in addressing specific challenges. Strut and Tie modeling, a commonly used method for modeling discontinuity regions, can be enhanced through the application of topology optimization. This approach not only avoids inaccuracies associated with Strut and Tie modeling but also provides more accurate results based on load path methods. The study showcases the potential of topology optimization to solve various civil engineering problems by generating optimized layouts that satisfy both functional constraints and material-saving objectives.

Keywords: Topology optimization, SIMP, BESO, Strut and Tie model

Contents

List of figures	ix
List of tables	xi
1 INTRODUCTION	1
1.1 CLASSIFICATIONS OF STRUCTURAL OPTIMIZATION	1
1.1.1 Sizing optimization	2
1.1.2 Shape optimization	2
1.1.3 Topology optimization	2
1.1.4 MATHEMATICAL FORM OF A STRUCTURAL OPTIMIZATION PROBLEM	4
1.2 TOPOLOGY OPTIMIZATION IN STRUCTURAL ENGINEERING AND ARCHITECTURE	5
1.3 METHODS OF TOPOLOGY OPTIMIZATION	7
1.3.1 Gradient based methods	7
1.3.2 Non-gradient based methods	9
1.4 STRUT AND TIE MODELING	10
1.5 ORGANIZATION OF THESIS	10
2 LITERATURE REVIEW	11
2.1 INTRODUCTION	11
2.2 HISTORY OF TOPOLOGY OPTIMIZATION	13
2.3 SOLUTION APPROACHES OF TOPOLOGY OPTIMIZATION	15
2.3.1 Homogenization	15
2.3.2 Solid Isotropic Material with Penalization	15
2.3.3 Evolutionary Structural Optimization	17

2.3.4	Evolutionary Algorithms	18
2.3.5	Level Set method	19
2.4	TOPOLOGY OPTIMIZATION IN STRUT AND TIE MODELING	20
2.5	STRESS OPTIMIZATION IN CONCRETE	22
2.6	SUMMARY OF LITERATURE SURVEY	24
2.7	SCOPE OF THE STUDY	25
2.8	Objectives	26
3	METHODOLOGY	27
3.1	FORMULATION OF OPTIMIZATION PROBLEM	27
3.1.1	Static problems	27
3.1.2	Dynamic Problems	28
3.1.3	Sensitivity analysis	29
3.1.4	Optimality Criteria	30
3.1.5	Bidirectional Evolutionary Structural Optimization	30
3.1.6	Filtering	31
3.2	Application of Topology Optimization in different Engineering Problems	31
3.2.1	Concrete dapped beams with multiple constraints	32
3.2.2	Different load cases in Dapped Beams	34
3.2.3	Topology Optimization with Concrete Damaged Plasticity model	35
3.2.4	TO using Higher order elements	37
	Stiffness matrix formulation	38
	Shape functions	40
3.2.5	Displacement constrained optimization	41
	Lagrange function	41
3.3	Stress Constrained Optimization	42
3.3.1	Drucker-Prager Yield Criteria	45
4	RESULTS AND DISCUSSION	47
4.1	STATIC AND DYNAMIC PROBLEMS	47
4.1.1	Numerical Examples	47
4.1.2	Comparison of different algorithms in static and dynamic problems	49
	Compliance minimization for a 2D-Cantilever beam	50

	Compliance minimization for a 2D-Simply supported beam	50
	Eigenfrequency maximization	51
4.2	Application of TO in different engineering problems	52
4.2.1	Concrete dapped beams with multiple constraints	52
	Problem 1	52
	Problem 2	54
	Problem 3	54
	Problem 4	55
4.2.2	Dapped beams with different loads	57
	Load case 1	57
	Load case 2	57
	Load case 3	59
	Load case 4	59
4.2.3	Topology Optimization with Concrete Damaged Plasticity model	61
4.2.4	Higher order Elements	62
4.2.5	Displacement constrained optimization	64
4.3	Stress Constrained Optimization	66
	Cantilever beam	68
	Simply supported beam	69
4.3.1	Drucker-prager stress criterion	70
4.3.2	Strut and Tie modeling	70
	Steps of Strut and Tie modeling	72
5	CONCLUSIONS	75
5.1	Future scope of research	76
5.2	PUBLICATIONS	77
	Bibliography	77

List of Figures

1.1	Structural optimization classifications: size, shape and topology optimization	3
1.2	Representation of fictitious 2-D design space with constraint surfaces [Engineering optimization: Theory and Practice by S.S.Rao,2009]	5
1.3	a) An office building in Japan with topology optimized Walls b) A topology optimized support structure(Source:Wikipedia)	6
2.1	Michell truss under the influence of force F at location A and a fixed circular support at point B, after Michell (1904)	14
3.1	Topology optimization using the SIMP algorithm	29
3.2	Dimensions and boundary conditions of Dapped beam)	32
3.3	Finite element model of Dapped beam	33
3.4	Dimensions and boundary conditions of Dapped beams	35
3.5	Different Load Cases	35
3.6	Four noded, Eight noded and Nine noded elements	39
3.7	BESO algorithm with displacement constraint	43
4.1	Dimensions and Boundary conditions of Cantilever beam)	48
4.2	Optimization history of Cantilever beam in Static case	48
4.3	Optimization history of Cantilever beam in Dynamic case	48
4.4	Optimum material layout in Static case and Dynamic case	49
4.5	Optimum material layout for Corbel	49
4.6	Optimum material layout for L-beam	50
4.7	Optimum material layout for Cantilever beam	51
4.8	Convergence history of Cantilever beam	51
4.9	Optimum material layout of SSB	52
4.10	Convergence history of SSB	53

4.11 Optimum material layout of fixed beam	53
4.12 Optimization history with displacement as Constraint-2	54
4.13 Optimum material layout)	54
4.14 Optimization history with Eigen frequency as Constraint-2	55
4.15 Optimum material layout	55
4.16 Optimization history with Stress as Constraint-2	56
4.17 Optimum material layout	56
4.18 Optimum material layout	56
4.19 Objective history of Load case 1 in BESO	57
4.20 Objective history of Load case 1 in ABAQUS	58
4.21 Optimum material layout in Load case 1	58
4.22 Objective history of Load case 2 in BESO	58
4.23 Objective history of Load case 2 in ABAQUS	59
4.24 Optimum material layout in Load case 2	59
4.25 Objective history of Load case 3 in BESO	60
4.26 Objective history of Load case 3 in ABAQUS	60
4.27 Converged layout in Load case 3	60
4.28 Objective history of Load case 4 in BESO	61
4.29 Objective history of Load case 4 in ABAQUS	61
4.30 Converged layout in Load case 4	61
4.31 Stress-Strain behaviour in Compression	62
4.32 Stress-Strain behaviour in Tension	63
4.33 Convergence history of CDP model and linear model in ABAQUS	63
4.34 Final layout in ABAQUS (a)CDP model (b)Linear model	64
4.35 Convergence history of BESO method in higher order elements	65
4.36 Optimum Topology of BESO method (a)4-noded element (b)Higher order elements	65
4.37 Convergence history and Optimum topology of OC method	66
4.38 Convergence history and Optimum topology of MMA method	66
4.39 Example for displacement constrained problem	66
4.40 Convergence history of optimization (a) with displacement constraint (b) without displacement constraint	67

4.41 (a) Variation of lambda (b) Optimum layout in displacement constrained problem	68
4.42 Optimum topology of Cantilever beam with volume constraint (a) and stress constraint (b)	69
4.43 Optimum topology of Simply supported beam with (a)volume constraint (b) and stress constraint	70
4.44 Variation of stress and number of constraints	71
4.45 MBB using Drucker-Prager yield criteria	71
4.46 Linear Analysis and Topology optimization results from IDEA Statica	72
4.47 Experimental set up from Abdul-Razzaq and Jebur (2017)	72
4.48 Identification of truss within beam	73
4.49 Member forces from the Method of joints	73

List of Tables

4.1	Comparison of Higher Order Elements without filter	67
4.2	Von Mises stress and Deflection values for cantilever beam	69
4.3	Von Mises stress and Deflection values for simply supported beam	70

SYMBOLS AND ACRONYMS

Here are the main symbols and acronyms from the text for easy access. Any unusual or specialized notations will be clarified within the text at the time they are used.

TO	: Topology Optimization
SIMP	: Solid Isotropic material with Penalization
MMA	: Method of moving asymptotes
BESO	: Bi-directional Evolutionary Structural Optimization
ER	: Evolutionary ratio
STM	: Strut and Tie Modeling
ACI	: American Concrete Institute
OC	: Optimality Criteria
x_i	: i^{th} design variable
p	: Penalization exponent
E^0	: Modulus of Elasticity of solid material
D-region	: Discontinuity region
V^*	: Imposed volume fraction
C	: Compliance
u	: Displacement vector
K	: Global stiffness matrix
M	: Global mass matrix
α	: Sensitivity
ω_n	: n^{th} mode Eigen frequency
r_{\min}	: radius of filtration
σ^n	: Stress of the n^{th} element
μ	: Lagrange multiplier
J_1	: First stress invariant
J_{2D}	: Second deviatoric stress

CHAPTER 1

INTRODUCTION

The process of achieving the best solution with respect to prescribed criteria under different alternatives is termed as optimization. It is a common practice to maximize or minimize the objective function by methodically selecting the input values from the prescribed set. Structural optimization deals with the efficient arrangement of structural components to satisfy the required condition to withstand loads in the best way. Constraints can be anything that evaluates the performance of the structure. These can also be treated as the indicators of best, as objective functions. The structural performance can be evaluated in terms of geometrical parameters, stresses, critical load, buckling load, stiffness, weight, and displacement. Maximisation or minimization of an objective function with respect to particular constraints characterizes an optimization problem. A feasible domain can be defined with respect to boundary conditions. Vast varieties of solution methods have emerged with advancements in the field of mathematical programming and computational methods. No unique efficient solution methodology can solve all optimization problems. Minimizing a function with several variables subjected to different sets of constraints, programming techniques are efficient. For accessing issues characterised by a set of random variables with known probability distributions, stochastic process approaches can be utilized.

1.1 CLASSIFICATIONS OF STRUCTURAL OPTIMIZATION

Structural optimization can be categorized into various strategies, such as those dependent on input variables, the type of desired output, and the ultimate goal of the optimization process. The structural model must be constructed using design variables, (Pedersen, 2003). Node locations and areas of cross section are the variables in the case of truss. Either continuous or discrete variables can choose to describe the system. Different strategies are related to structural optimization depending on their types of goals. The three main classes

are sizing, shape, and topology optimization (Figure 1.1). Material topology optimization is usually related to one of these strategies. Solutions of real world problems often require the combination of all these optimizations.

1.1.1 Sizing optimization

Cross-sectional dimensions of already defined structural elements are changed to an optimum design in size optimization. Discrete variables are optimized to achieve gains in the predefined design space. Economic savings from the weight savings of individual elements can be defined as the main objective of size optimization. Size optimization has been applied to revise the cross-section during the construction of the National Military Museum in Soesterberg, Netherlands after fixing the span and height of the truss. Individual bar elements have to be optimized such that size optimization is mainly applied to steel structures with numerous repetitions.

1.1.2 Shape optimization

As the name implies shape optimization alters the shape of the body by choosing x as the domain variables. x indicates the shape or contour of a section of the boundary that belongs to the structural domain. Consider a solid material whose state can be explained by a set of partial differential equations. Shape optimization is the optimal way of selecting the integration domain and introducing more freedoms in the configuration of connections between members without affecting connectivity. Definitions of constraints of size optimization is modified to adjust with the design variables. Shape optimizations are applicable in the case of free-formed structures, where fundamental shapes are predefined. The objective of truss shape optimisation is to identify the ideal node placements for a particular truss with a given number of nodes, bars, and bar connections.

1.1.3 Topology optimization

The functional performance of structure can be influenced by the optimization of topology and geometry. As a common form of structural optimization, topology optimization modifies the connectivity of the members other than the size and shape of members. This represents the most comprehensive form of structural optimization, encompassing not only the size and shape of individual members but also considering how these members are interconnected with each other. The concept of topology optimization is eliminating unnecessary material from the initial structure to make it optimal. Discretizing the domain or design space

is the initial step of topology optimization. Each mesh can be treated as design variables with similar constraints of sizing and shape optimization. Topology optimizations are often quite rough and serve as inspiration for the actual form of the structure. It is normal to demand that the solution for improving the topology of a structure consists of distinct and separate materials and void, preferably with a material distribution that can be manufactured. State of an element either material or void demand the usage of a discrete variable. Effective mathematical programming approaches are more applicable to continuous variables. The problem with the formulation of the most general topology optimization problem is that there is no real solution. This is because, while optimising the average stiffness, improving the mesh will always result in a topologically better solution for a given problem (Bends et al., 2003)

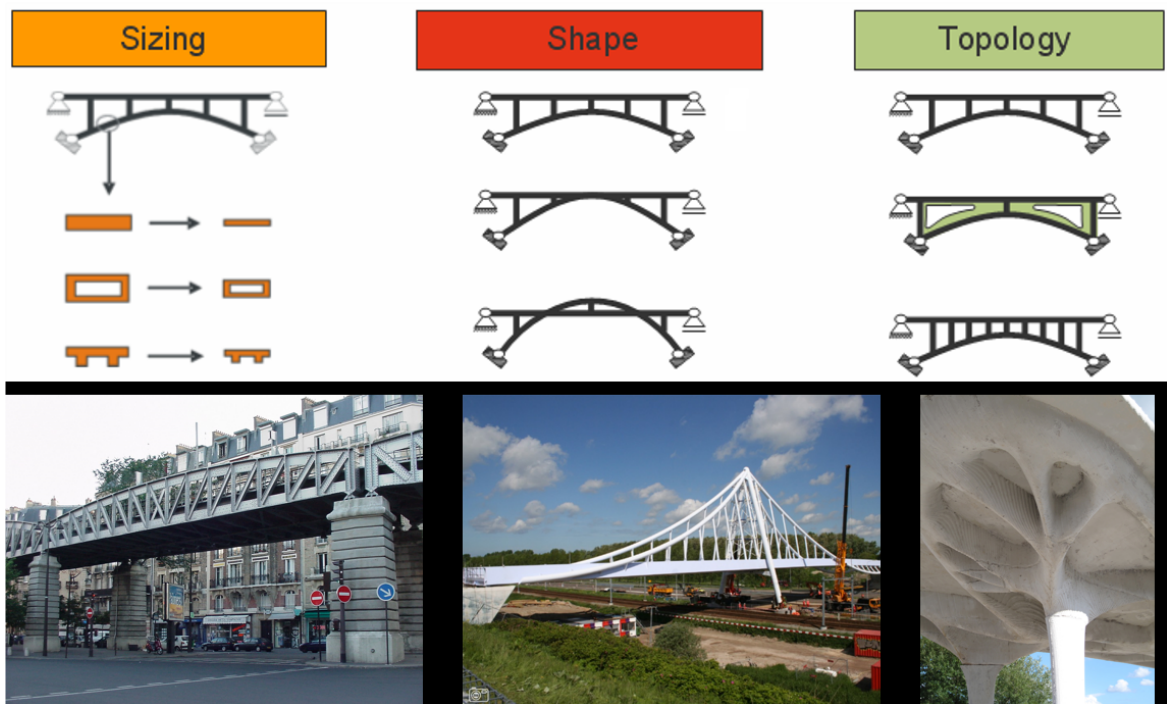


Figure 1.1: Structural optimization classifications: size, shape and topology optimization

1.1.4 MATHEMATICAL FORM OF A STRUCTURAL OPTIMIZATION PROBLEM

Mathematical formulation of an optimization problem can be defined as

$$\text{Find } X = \left\{ \begin{array}{c} x_1 \\ x_2 \\ \dots \\ x_n \end{array} \right\} \text{ which minimizes } f(X) \quad (1.1)$$

with constraints

$$l_j(X) = 0, j = 1, 2, \dots, m$$

$$g_j(X) \leq 0, j = 1, 2, \dots, n$$

X represents design vector of n dimension such that n represents a number of variables and m denotes the count of constraints. $f(X)$ represents the objective function with equality constraints $g_j(x)$ and inequality constraints $f_j(x)$. The above equation denotes constrained optimization problem. If there is no involvement of constraints in the optimization problem, it can be treated as unconstrained optimization. Behavior or functional constraints restrict the performance or functionality of the structure. Physical limitations on the design variables represent geometric or side constraints.

Take into account the optimization problem with inequality constraint $g_i(X) \leq 0$. This constraint equation creates a boundary surface in the design space based on the values of x satisfying the equation. Boundary surface is the constraint surface which separates the feasible region with $g_i(X) \leq 0$ and infeasible region with $g_i(X) > 0$. The values of x satisfying $g_i(X) = 0$ lie on the boundary surface. Figure 1.2 illustrates different kinds of design points. According to whether a specific design point is in the acceptable or undesirable region, it can be classified as one of the four kinds are identified. They are Bound and acceptable point, Bound and unacceptable point, Free and acceptable point and Free and unacceptable point. A bound point is a design point that is on one or more constraint surfaces, and the corresponding constraint is termed as an active constraint. Free points are design points that

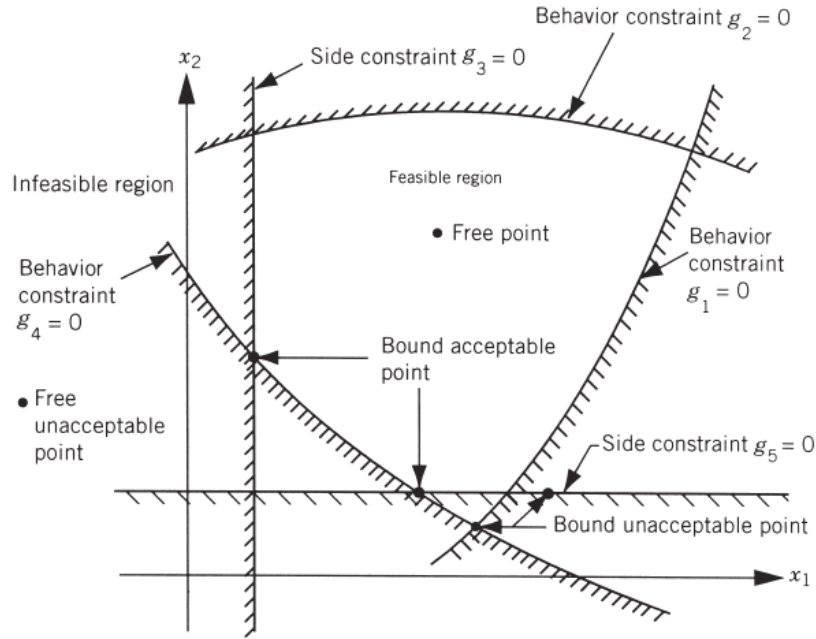


Figure 1.2: Representation of fictitious 2-D design space with constraint surfaces [Engineering optimization: Theory and Practice by S.S.Rao,2009]

are not bound under any constraints. Based on whether a specific design point falls within the acceptable or unacceptable region, it can be categorized into one of four types.

1.2 TOPOLOGY OPTIMIZATION IN STRUCTURAL ENGINEERING AND ARCHITECTURE

Topology optimization techniques have been significantly enhanced by the relatively recent development of the Finite Element (FE) method, enabling their application to a wide range of generalized problems. Topology optimization has been effectively used by engineers in the aerospace, automotive, and mechanical fields to reduce the weight of structures. It is commonly acknowledged that there is less interest in topology optimization in the fields of civil or structural engineering, where weight reductions are less important due to the uniqueness of building structures (Pucker and Grabe, 2011). During the period of renewable and robust infrastructure, design of structures is a process of recurrence. It is very important to reevaluate each structure to maximize its efficiency. Since each civil-structural engineering project is unique, it is essential to utilize optimization approaches to increase efficiency on complicated projects.

Availability of large computational ability enables designers to incorporate structural optimization. Different developing and novel optimization approaches encourage the process of simulation. Traditional gradient-based mathematical programming algorithms are being su-



Figure 1.3: a) An office building in Japan with topology optimized Walls b) A topology optimized support structure(Source:Wikipedia)

perseded in many cases by unique and effective heuristic methods motivated by biological, chemical, or physical mechanisms. Because of their adaptability and simple numerical execution, these approaches are effective methods for structural optimization. One example of a real-world design is the support structure for a canopy in Doha (Tsavdaridis, 2015). There are numerous applications for topology optimization in the design of tall buildings with reference to shape (Beghini et al., 2014) and in bridge constructions (Zhao and Wang, 2014). Topology optimization is regarded as an optimization tactic rather than a structural design technique. It is really effective of conveying the sense of optimization in structural shapes. In an office building in Japan close to the Takatsuki JR Station, topology optimization was utilized to determine the optimal number, position, and shape of holes (Ohmori, 2011). The rectangular plate model walls were optimized for combinations of vertical and horizontal loads. The outcome (Figure 1.3a) was evaluated to be both aesthetically attractive and robust. Structural requirements obtained from Topology optimization are capable of influencing the architecture of the entire building. Geometry of the canopy support structure (Figure 1.3b) was based on Topology optimization studies. The formwork for such a geometrically difficult topological form was made using computer numerical controlled (CNC) milling technology. It is important to realize that when topology optimized designs are to be used on a larger scale, sophisticated production techniques are necessary.

1.3 METHODS OF TOPOLOGY OPTIMIZATION

Either gradient-based mathematical programming approaches or non-gradient-based procedures are used to optimize the design. In gradient based methods, the redesign of each element is based on some gradient value or at least the value of the response parameter for the considered element. Most non-gradient based methods are based on heuristics.

1.3.1 Gradient based methods

Methods that use gradients typically reach convergence in a limited number of steps. Gradient methods are suitable for situations where the functions involved are continuous and differentiable, and their computation is not overly complicated. These methods typically rely on the Taylor series for their algorithms. First-order methods exclusively consider gradient functions, while second-order techniques incorporate Hessian functions and so forth. **Ground structure approach** is one of the discrete topology optimization techniques. The Ground Structure approach, initially introduced by (Dorn, 1964) offers a way to simplify the complexity of a topology optimization problem. It achieves this by employing a predetermined grid of nodes with initially strong connections. These connections represent potential structural elements that can exist in binary states (on/off) or be gradually assigned section sizes. If a connection is determined to be underutilized, such as having a section size below a specified minimum, it can be removed from the structure entirely. Different approaches have been employed to derive a streamlined and "optimal" structural layout from the initial system. However, it is important to acknowledge that superior solutions might exist beyond the limitations imposed by the grid framework. Many implementations do not allow node movement or the addition of nodes and elements. This approach is best suited for addressing problems of moderate scale rather than intricate structural designs. By incorporating elements with intermediate densities into the optimization problem, it becomes possible to ensure the existence of a solution. However, the real challenge lies in comprehending the consequences of this innovative material interpretation.

The **homogenization method** employs a model of composite material, comprising numerous tiny unit cells that contain either material or void or two distinct materials (Bends et al., 2003). The goal is to optimize the porosity of the overall structure based on a specific objective function. Every unit cell has the flexibility to possess its unique size and orientation. Typically, intermediate densities are discouraged to encourage the elements to be either completely solid or completely empty. A desired volume fraction is usually established, and

adjusting various modeling parameters allows for a range of possible solutions, including truss-like structures and plate-like solutions to composites, and reinforced composites. The **Solid Isotropic Microstructure with Penalization (SIMP)** is widely utilized for structural topology optimization. In SIMP, there is a design variable, $x \in [0, 1]$, associated with each element in the finite element discretization, typically interpreted as a density ratio (Bends et al., 2003). This means that prior to commencing the optimization process, a design domain is defined to enclose the desired final structure. Initially, this domain contains elements with random density distributions. Elements with maximum density are typically represented as black, while elements with zero density, which implies their removal in a physical sense, are represented as white. Intermediate densities are often depicted using various shades of grey. In the literature, the SIMP model is commonly referred to as the Artificial or Fictitious material model or interpolation scheme.

One of the commonly used techniques for optimizing the design of structures is **Evolutionary Structural Optimization (ESO)**. Despite its name, ESO does not follow the same evolutionary principles as Evolutionary Algorithms that are based on Darwinian concepts, and it is not strictly focused on optimization. Instead, it is a design approach that aims to achieve uniformity of structural parameters, such as stress or strain energy density. ESO operates on the principle that a structure progresses towards an optimal state by progressively removing the least stressed elements in each iteration. To apply ESO, it is necessary to define an initially over-dimensioned structure along with its boundary conditions before performing the analysis. Another variant of ESO is the additive evolutionary structural optimization (AESO) method. AESO combines the original ESO approach with the capability to add elements to the structure as well. Building upon this, the bidirectional evolutionary structural optimization (BESO) method was revealed. BESO allows for both the addition and removal of elements during the optimization process. Furthermore, BESO (Bi-directional Evolutionary Structural Optimization) provides the option to start iterations with either a minimal initial structure, where material is predominantly added, or with a maximal design domain, from which material is primarily removed.

The underlying idea behind **level-set methods** is to represent the volume of a structure using an auxiliary continuous function, where the number of variables in the function corresponds to the number of spatial dimensions. In this approach, the optimization objective becomes the function itself, rather than the physical design volume. By parameterizing a con-

tinuous function instead of an arbitrary domain, the traditional challenges related to material continuity in topology optimization are eliminated. While it is still possible to encounter infeasible solutions where continuous but disconnected areas form, dealing with such situations is much simpler compared to other optimization techniques. If the boundary lines or surfaces are permitted to create new topologies, the topology optimisation techniques can also be employed for shapes. However, a challenge arises when re-parameterizing the boundary due to the merging, splitting, appearance, or disappearance of lines or surfaces. To address this issue, a different approach can be taken. Rather than explicitly defining a two-dimensional geometry with boundary lines or a contour line in three dimensions, the boundary surface of a three-dimensional structure can be defined using an isoline from a two-dimensional scalar field or an isosurface from a three-dimensional scalar field. This alternative representation offers more flexibility and facilitates the handling of topological changes during the optimization process.

1.3.2 Non-gradient based methods

These methods are often claimed to be ‘global methods’, supposedly guaranteeing global convergence, but this claim is unproven. There exist truly global methods such as enumeration methods but most non-gradient techniques are based on heuristics. Some of these methods are also termed ‘nature-inspired’, ‘biomimicry’, ‘metaheuristic’, or ‘population type’ algorithms and usually some random process. The best-established nature-inspired method is the Genetic Algorithm (GA) method. **Genetic Algorithm** is a direct search algorithm that draws inspiration from the principles of natural genetics and natural selection. Genetic Algorithm (GA) is founded on the concept of “survival of the fittest.” It operates by creating a new generation ($i+1$) through the combination of the “surviving” individuals from the previous generation. Many practical optimization problems involve a combination of continuous and discrete variables, along with non-convex and discontinuous design spaces. When traditional nonlinear programming techniques are applied to such problems, they often prove inefficient, and computationally expensive and tend to converge to a local optimum closest to the starting point. In contrast, GA is well-suited for tackling these types of problems and has a higher probability of discovering the global optimum solution. Being a population-based algorithm, GA explores a set of candidate solutions, denoted as “generation i ,” before determining the next generation ($i+1$). By employing various genetic operators, such as selection, crossover, and mutation, GA evolves the population towards increasingly better solutions over succes-

sive generations. In certain scenarios, parallel computing can be employed to solve multiple generations simultaneously, thereby enhancing computational efficiency and reducing the overall optimization time.

1.4 STRUT AND TIE MODELING

The conventional method for designing reinforced concrete flexural members involves using a sectional moment design with Whitney's stress block, which is based on the assumption that a plane section before bending remains plane after bending (Bernoulli hypothesis). This method assumes linear strains in the section and refers to the sections where this assumption holds true as B-regions (B for Bernoulli). However, there are parts of a beam, particularly near supports, concentrated loads, and discontinuities, where the strains do not follow this assumption and exhibit non-linear behavior across the section. These sections are called D-regions (D for discontinuity or disturbed). For the design of B-regions, either sectional analysis or strut-and-tie modeling (STM) can be employed. STM is an accepted design method by American Association of State Highway and Transportation Officials (AASHTO) for dealing with D-regions as it simplifies the non-linear stresses into a truss model composed of struts and ties. This truss model represents the flow of stresses at failure and ensures equilibrium while keeping the stresses in the struts, ties, and nodal zones below the strength limits. By satisfying the requirements of the lower bound theorem of plasticity, this model meets the design criteria.

1.5 ORGANIZATION OF THESIS

The thesis consists of five chapters, each of which is thoroughly explained in detail with its enclosed content described as follows. In the first chapter, a comprehensive overview is presented of different optimization techniques and general formulations. A concise introduction of different solution approaches of topology optimization and its application in concrete structures is presented. In Chapter 2, a thorough examination of pertinent literature, research goals, and the scope of the project is presented. Chapter 3 outlines the adopted methodology for achieving the set of objectives. Chapter 4 encompasses the results and discussions in detail obtained based on the methods adopted. Chapter 5 contains overall conclusions drawn from the current study. Finally, a list of publications and references is appended at the end.

CHAPTER 2

LITERATURE REVIEW

2.1 INTRODUCTION

Nowadays structural optimization is becoming a wide concept and the diversified outcomes of structural optimization is due to the choice of constraints and the desired objective of optimization. Both the economic and aesthetic aspects can be the incentive to fix the optimization goal. Accompanying the reliable methods of structural analysis with growing digital computing technologies catalyze the research in structural optimization. A.G.M. Michell, in the early 19th century, published a paper titled "The Limits of Economy of Material in Frame-Structure," which discussed structural optimization ([Michell, 1904](#)). With the availability of the high-speed digital computer together with the advancement of finite element method has begun in the mid-1950. During the initial decade or more, significant amounts of money were allocated for research endeavors focused on transforming this into a functional tool for engineering analysis. As a result, by 1970, the method had achieved a reasonably advanced stage of development, and various software options were emerging in the market for commercial use. In 1960, Schmit introduced a combination of finite element analysis and nonlinear numerical optimization, which he referred to as structural synthesis at that time. [Vanderplaats \(1993\)](#) investigated the history of modern structural optimization begins with the landmark paper of Schmit in 1960. The progress of structural optimization gradually evolved from its application in discrete structures to shape or topology optimization in more complex continuum structures. [Pedersen \(2003\)](#) extensively investigated and explored numerous concepts and significant applications within the field of structural optimization.

[Duysinx et al. \(2008\)](#) integrates stress constraints into the topology optimization problem to obtain an optimal structural configuration that is most suitable. He demonstrated a particular

character of stress design in two different situations such as multiple load cases and unequal stress limits in tension and compression are involved. The aim of the optimization is most often to minimize or maximize some kind of physical property of the structure, which are all either load-dependent properties or load-independent properties. The primary objective of optimization is usually to maximize or minimize a specific characteristic of the structure, which can be either influenced by external load or not influenced by external load .

Deterministic methods can be used for solving sizing optimization as it can be easily expressed mathematically. The Fully Stressed Design method is primarily employed for structures where strength considerations take precedence over stiffness, typically found in smaller to medium-sized frames. [Maxwell \(1864\)](#)'s analysis identifies every member in a statically indeterminate structure that is subjected to the maximum allowable stress in the design with the least possible weight. Traditional methods follow a process of increasing the size of overstressed members and decreasing the size of under-stressed members, repeating this cycle until convergence is achieved. However, [Mueller and Burns \(2001\)](#) demonstrated that this approach overlooks a group of fully stressed designs that repel this adjustment, as some members respond to an increase in size by attracting more stress. On the other hand, [Borkowski and Jendo \(1990\)](#) applies an iterative approach in mathematical programming methods to find an optimal solution. This involves calculating a search direction within the design space and determining the step size, which refers to the distance to be traveled in that direction. A collection of conditions that are both necessary and sufficient is developed to define the optimal solutions for convex problems. When applied to sizing structural sections, optimal solutions are found through an iterative process that includes reanalysis to account for variations in load distribution. [Rozvany \(2012\)](#) provides a detailed overview of optimality criteria methods in structural optimization. Even though optimizing the size of individual sections is relatively easier, there is a compelling reason to prioritize optimization before this stage. Estimates indicate that a significant portion, approximately four-fifths, of the overall resources in an engineering project are allocated during the initial design phases ([Deiman, 1993](#)). [Grierson and Chan \(1993\)](#) introduces a specialized approach specifically designed for the efficient design of tall buildings. One advantage of OC methods compared to mathematical programming techniques is their ability to explore solutions beyond local optimality near the initial design. However, in structures that possess a high level of statical indeterminacy, even with changes in load distribution, the existing approach may still strug-

gle to identify the global optimum. As a result, the hybrid OC-GA method was developed to address this limitation. This method, introduced in the work by [Chan and Liu \(2000\)](#), combines the robustness of Genetic Algorithms (GA) with the computational efficiency of OC, aiming to overcome the challenges posed by load distribution variations. In the context of shape optimization, the focus is on optimizing the shape of structural members, including potential voids within them, as described in [Haftka and Grandhi \(1986\)](#). It is important to note that this optimization process does not involve the addition of new connections or holes, nor does it entail the removal of existing members or voids. Shape optimization is particularly effective in eliminating areas of high stress concentration. Its primary application arises when there is no need or desire to alter the topology of the structure.

2.2 HISTORY OF TOPOLOGY OPTIMIZATION

Topology optimization can be categorized into two main types depend on the nature of optimized objects: continuum topology optimization and discrete topology optimization. The origins of discrete structural topology optimization can be traced back to the research conducted by [Michell \(1904\)](#), where he developed equations for structures with minimal weight while satisfying stress constraints within different design domains. For instance, when considering a cantilever truss under a point load with a circular support, neglecting the weight of joints, the minimum weight configuration corresponds to a truss-like continuum with an infinite number of bars and joints. The illustration of this optimal structure can be observed in [Figure 2.1](#).

[Prager and Rozvany \(1977\)](#) introduced a limited quantity of joints by incorporating into the overall weight of the structure that needs to be reduced, not just the weight of their connections, which is presumed to be directly related to the number of joints. [Bendsøe \(1989\)](#) proposed the homogenization method based on studies of the existence of solutions. In the homogenization method, materials with microstructure are used. The material is a composite that is constructed by a unit cell consisting of one or more holes that are period repeated. The homogenization method is used to determine the material properties and the optimal distribution of material can be found. The method has the drawback that the optimal microstructures and their orientations are difficult to solve or unsolvable and the absence of specific length scales in the resulting microstructures renders it impossible to construct the structure. The approach remains applicable for comprehending the theoretical performance of structures ([Sigmund, 2001](#)). When optimizing the structure's topology, it is reasonable to require that

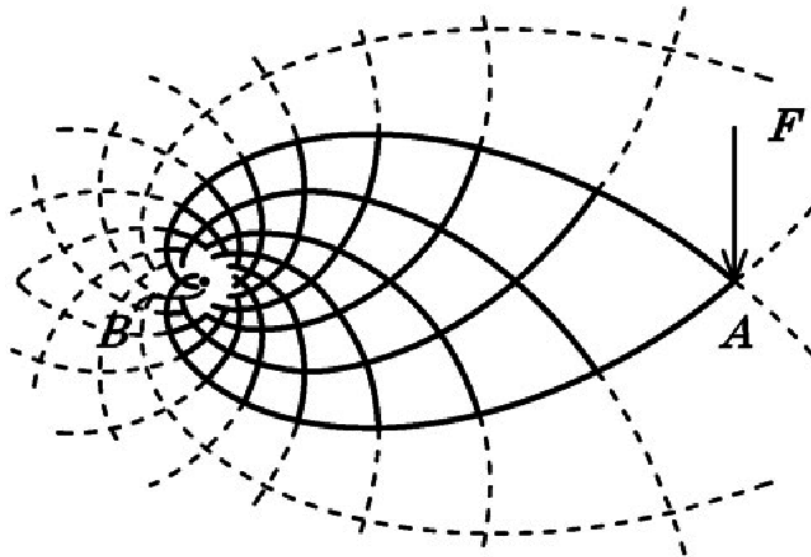


Figure 2.1: Michell truss under the influence of force F at location A and a fixed circular support at point B , after Michell (1904)

the solution comprises distinct material and void regions, ideally with a manufacturable material distribution. This necessitates the utilization of discrete variables to represent the state of each element, either as material or void. The SIMP method permits the presence of intermediate densities that lack physical significance. Gray regions that emerge can be eliminated by imposing a penalty on these intermediate states. Although it is still feasible to utilize discrete variables, as mentioned in [Beckers \(1999\)](#), such approaches have thus far proven to be inefficient or limited to specific problem formulations, as indicated in [Bendsoe and Querind \(2003\)](#). Evolutionary Structural Optimization was first proposed in the early 1990's. The method is based on a simple approach where inefficient material is slowly removed from the structure leaving the only necessary material. In the late 1990's an extension of the Evolutionary Structural Optimization method was made called Bi-directional Evolutionary Structural Optimization. Besides removing inefficient material the method also allowed the material to be added to locations where it was most needed. Level sets offer an alternative method for depicting the topology of a structure. In this approach, an implicit function assigns positive values to regions with material and negative values to regions without material within the design domain. Consequently, the level set represents the boundary of the structure, consisting of points where this function equals zero. By modifying the implicit function, it becomes possible to discover an optimal structure. In 2010, Challis published an instructive article that included a concise MATLAB code for conducting topology optimization using a level-set approach.

2.3 SOLUTION APPROACHES OF TOPOLOGY OPTIMIZATION

Topology optimization can be categorized into two groups: discrete and continuous approaches. Indiscrete approaches an element is removed by a "hard-kill" method and the element cannot reappear. Evolutionary Structural Optimization is a discrete approach. Under continuous approaches are elements never completely removed and can reappear in later iterations. The density-based methods, Solid Isotropic Material with Penalization method and the Homogenization method fall under the continuous approaches.

2.3.1 Homogenization

The homogenization method, initially introduced by [Bendsøe \(1989\)](#) and extensively discussed by Bendsøe and Sigmund (2004), assigns distinct materials to individual elements in the mesh, each containing an infinite number of microscopic voids. [Tenek and Hagiwara \(1993\)](#) utilized homogenization techniques to maximize the fundamental eigenfrequency of both isotropic and composite plates, employing SLP (Sequential Linear Programming) for optimization. In a well-known industrial case of topology optimization, [Larsen et al. \(1997\)](#) devised compliant mechanisms and developed a microstructure with a negative Poisson's ratio. Additionally, [Maar and Schulz \(2000\)](#) employed multi-grid methods within a homogenization framework for structural optimization.

2.3.2 Solid Isotropic Material with Penalization

Prior to 1989, only whole numbers were employed as design variables in structural optimization functions. However, in his 1989 paper, Bendsøe introduced a technique for introducing continuous variations to the design variables, leading to a non-discrete solution. To achieve a non-discrete solution that closely resembled a discrete solution, the mathematical model used for structural analysis was modified to minimize the impact of intermediate variable values. This approach eventually became known as Solid Isotropic Microstructure with Penalization (SIMP). [Buhl et al. \(2000\)](#) utilized the SIMP approach in conjunction with the Method of Moving Asymptotes (MMA) to minimize diverse objective functions for geometrically nonlinear structures while adhering to volume constraints. In 2001, Rietz demonstrated that the penalty function employed in the SIMP method could yield discrete solutions under certain conditions. Additionally, in the same year, Stolpe and Svanberg explored the utilization of a continuation method to gradually enhance the penalty parameter

in the SIMP method. They concluded that this approach helps evade numerous local minima that may arise when using a constant penalty parameter, albeit at the cost of increased computational complexity. Furthermore, they discovered specific instances where the solution would contain intermediate densities regardless of the magnitude of the penalty parameter. In 2001, Sigmund released a publicly accessible code for topology optimization, which was a concise MATLAB code. This code relied on the SIMP formulation to iteratively update the structure, aiming to achieve the specified optimality criteria (OC) while minimizing compliance within the constraints of a volume problem. Presently, it is widely utilized in numerous commercial optimization software packages (Rozvany, 2009). The equation representing the element stiffness within the SIMP model is as follows [Equation 2.1]:

$$E_{ijkl} = x^p E_{ijkl}^0, p > 1 \quad (2.1)$$

where E_{ijkl} represents a material property of the base material, typically its stiffness. The penalization exponent, denoted as p , and the design variable x are also involved. The penalization exponent determines the cost associated with intermediate densities, with a value of $p = 1$ indicating no penalization. Increasing the penalization exponent leads to the penalization of intermediate densities, causing the stiffness to deviate from a linear relationship. To achieve a binary solution where only black-and-white values are present, a penalization exponent greater than $p = 3$ is often necessary, Bendsoe and Querind (2003). According to Rozvany (2009), it is recommended to gradually increase the penalization starting from $p = 1$ in order to avoid rushing the optimization process and prevent getting trapped at local optima. Despite the presence of penalization, the optimized results often include grey material, which can be much more efficient. While Rozvany states that the SIMP method is likely to find a true optimal solution, Stolpe and Svanberg (2001) has demonstrated that this is not always the case. Under certain conditions, SIMP may fail to reach the global optimum regardless of how slowly the penalization exponent is increased. Additionally, the research by Stolpe and Svanberg (2001) also reveals that SIMP, even with significant penalization, sometimes fails to produce a black-and-white solution.

2.3.3 Evolutionary Structural Optimization

Evolutionary Structural Optimization (ESO) offers an alternative approach for solving structural optimization problems and was initially developed by [Xie and Steven \(1993\)](#). The fundamental principle of ESO involves systematically eliminating material that appears to be of least significance to the structure. Initially, stress was used as the criterion function, but it has been discovered that optimizing based on stress alone can lead to structures with sub-optimal stiffness. To address this issue, [Chu et al. \(1996\)](#) introduced an alternative criterion function called elemental strain criterion or element compliance within ESO. This modified criterion retains the same core concept as ESO but allows for the reintroduction of material into the structure. In order to identify elements with the least element strains, a sensitivity analysis is conducted, which involves calculating a sensitivity number for each element i . Following the sensitivity analysis, the elements in ESO are either completely removed or left untouched based on their sensitivity numbers. This binary approach means that no intermediate densities are present in the resulting structure. Unlike other topology optimization methods like SIMP, ESO doesn't require penalizing intermediate densities. Furthermore, ESO, in its original form, is considered a one-way method or a "hard-kill" method. It means that elements can only be removed, and no elements can be added. Once an element is removed, it becomes permanent, and even previously removed elements cannot be reintroduced into the structure, ([Querin et al., 1998](#)). Several advancements have been made to the original ESO method. Additive Evolutionary Structural Optimization (AESO), introduced by [Querin et al. \(2000\)](#), involves the addition of new elements adjacent to the existing perimeter elements. This extension allows for boundary problems to be addressed through shape optimization. However, AESO is less applicable to building design due to its focus on shape optimization rather than structural optimization. Another development is Bi-directional Evolutionary Structural Optimization (BESO), also proposed by [huang et al. \(2000\)](#). BESO allows for both the removal and addition of elements. The addition of elements can be achieved either by extrapolating the "sensitivity number" or by considering the sensitivity number of perimeter elements. BESO, and its convergent variant, have found widespread adoption in both academic research and engineering applications due to its efficiency and robustness [[Xia et al. \(2017\)](#), [Xia et al. \(2018a\)](#), [Huang and Xie \(2007\)](#)]. The bi-directional capability of BESO methods provides a notable advantage over the original ESO method by increasing the flexibility of the optimization process. A key benefit is that BESO

allows for the replacement of material that was removed in the early stages of the evolutionary process if it is later determined to be structurally beneficial. This feature enhances design space exploration, enabling a wider range of possibilities to be considered and increasing the likelihood of discovering globally optimal solutions. Due to the bi-directionality feature, it is expected that a higher number of iterations will be necessary for BESO compared to the basic algorithm. Extended Evolutionary Structural Optimization (XESO), introduced by Cui et al. in 2003, operates by creating stress contour lines or contour lines of another property within the designable domain during each iteration. Material with stress values below a critical threshold is eliminated, while the material is added in regions where extrapolated contour lines indicate high-stress values. To accommodate these changes, the finite element model is updated by re-meshing at each step of the process. Genetic ESO (GESO), as presented by Liu et al. (2008), incorporates the concepts of survival of the fittest and probability into the BESO method. GESO introduces a binary string of variable length for each element, which is not present in the original BESO method. At the beginning of the process, the binary string representing all elements is initialized with all digits set to 1, signifying that they are filled with material. After each iteration and sensitivity analysis, genetic algorithms are employed, utilizing the aforementioned concepts, to update the binary string. Based on the likelihood of elements being necessary in the later stages of the iteration process, a bit in the string is changed to 1 or 0. An element marked with a single 0 is temporarily removed, and if the binary string contains only 0s, the element is permanently eliminated. This removal is based on the low probability of the element being useful later in the iteration process.

2.3.4 Evolutionary Algorithms

While not strictly classified as pure optimization algorithms (Jh, 1975), Evolutionary Algorithms (EAs) are versatile and stochastic problem-solving methods that are often grouped under the umbrella term of Evolutionary Computing (EC). These methods are named as such because they emulate the principles of natural biological evolution initially proposed by Charles Darwin in 1859. Typically, a population of individual solutions is evaluated based on one or more quantifiable criteria to assess their performance in solving a given problem. In EAs, an individual's performance, often referred to as fitness, influences their chances of contributing to the subsequent generation of solutions through genetic operators like reproduction, crossover, and mutation. Three distinct sub-classes of EAs emerged independently in the 1960s: Genetic Algorithms (GA) (Jh, 1975), Evolutionary Programming

(EP) (Fogel, 1998), and Evolutionary Strategies (ES) (Rechenberg, 1965). However, these sub-classes were not unified under the umbrella term of EAs until the 1990s. Another subclass, known as Genetic Programming (GP) (Koza, 1994), also emerged in the 1990s. Due to their population-based approach and stochastic nature, Evolutionary Algorithms (EAs) require significant computational resources and are generally not as effective as numerical methods in tasks such as standard continuous parametric optimization (Eiben and Schoenauer, 2002).

2.3.5 Level Set method

The level set method was initially developed by Osher and Sethian (1988). In the early 2000s, this method was introduced into the field of topology optimization and gained significant popularity. The level set-based approach offers a convenient way to handle topology changes in structures. It is also an appealing method for achieving topology design in multi-material structures. Typically, the level set model employs higher-order surfaces to represent the structural boundaries implicitly, particularly using zero-level sets. Shape modifications and potential topology changes in structures are accomplished through the emergence and splitting of moving boundaries. There are two methods available for tracking these moving boundaries: one involves solving the Hamilton-Jacobi equation, while the other updates the parameterization coefficients using mathematical programming algorithms (Luo et al., 2008). The concept of the level set description was first introduced to topology optimization by Sethian in their work Sethian and Wiegmann (2000). Following this, Wang et al. (2003) and Allaire et al. (2004) further advanced level-set-based methods for topology and shape optimization, integrating shape-sensitivity analysis into their approaches. The level set description was initially introduced into topology optimization by Sethian and Wiegmann (2000). Subsequently, Wang et al. (2003) and Allaire et al. (2004) developed level-set-based methods for topology and shape optimization, incorporating shape-sensitivity analysis. The level set method has been recognized for its benefits, including smooth boundary representation, distinct interface handling, and the ability to integrate topology and shape optimization. Alternative level set approaches have been put forth for single-material design issues to improve optimization behaviour, lower computing costs, or accomplish particular objectives (Makhija and Maute, 2014). Over time, level set-based approaches have found extensive application in various design problems, such as eigenvalue maximization (Allaire and Jouve, 2005), stress minimization (Allaire and Jouve, 2008), and designs involving geometrical un-

certainties ([Chen and Chen, 2011](#)).

2.4 TOPOLOGY OPTIMIZATION IN STRUT AND TIE MODELING

Strut and tie models is based on truss analogy which adequately expresses complex stress patterns as triangulated models. It can be used as an effective method for the design of D-regions (disturbed or discontinuity regions) where normal beam theory does not necessarily apply. Types of D-regions include deep beams, connections, beams with holes, corbels, brackets, pile caps and shear critical walls. An STM is an internal truss, comprising concrete struts and steel ties that are connected at nodes to transfer applied loads through D-regions to the supports ([Liang et al., 2002](#)).

The concept of utilizing strut and tie modeling in structural design can be traced back to the late 1890s when German civil engineer Wilhelm Ritter introduced the idea. Ritter proposed that concrete beams could be designed by applying a truss analogy, with reinforcing steel wires or bars carrying tensile forces and concrete carrying compressive forces. Until the 1970s, design practices predominantly involved using bent-up bars at the beam ends, with limited development beyond Ritter's truss analogy. In the 1980s, Schlaich and his colleagues made significant advancements in the application of the truss analogy for designing entire beams and structures. Their seminal work, "Toward a Consistent Design of Structural Concrete," advocated for the establishment of standardized procedures and rules for employing the truss analogy, also known as strut-and-tie modeling. The article highlighted the limitations of traditional sectional analysis methods near regions of static and geometric discontinuities, as the stresses and strains in these areas deviated from the rest of the beam. According to Schlaich and his colleagues (1987), traditional design practices were often reliant on test results, rules of thumb, and past experience rather than a comprehensive understanding of mechanics, resulting in inefficient designs. In response to this issue, strut-and-tie models (STMs) were introduced into the AASHTO (American Association of State Highway and Transportation Officials) code in 1994 and the ACI 318 (American Concrete Institute) code in 2002 as an appendix. The design code and procedure utilized in this paper adhere to the AASHTO LRFD (Load and Resistance Factor Design) Specifications. The strength requirements for struts, ties, and nodal zones provided in the AASHTO LRFD Specifications closely align with the proposals put forth by [Schlaich et al. \(1987\)](#).

An innovative technique for creating strut-and-tie models using topology optimization was introduced by [Xie and Steven \(1993\)](#). In their evolutionary structural optimization (ESO) method. Building on this foundation, [Yang \(1999\)](#) further developed the bidirectional evolutionary optimization (BESO) method. A pioneering approach for generating strut-and-tie models through topology optimization was presented by [Xie and Steven \(1993\)](#) in their evolutionary structural optimization (ESO) method. Building upon this method, [Yang et al. \(1999\)](#) developed a bidirectional evolutionary optimization (BESO) method. Additionally, [Liang et al. \(2002\)](#) proposed a performance-based optimization method using level-set-based techniques specifically for strut-and-tie modeling. Over time, the strut-and-tie modeling technique underwent rapid development, with various algorithmic versions being introduced. [Liang et al. \(2002\)](#) focused on computing the stiffness of struts and ties based on an evolved topology of a finite element model, allowing for the solution of statically indeterminate strut-and-tie problems in three-dimensional concrete structures. Over the past six years, the research field concerning strut-and-tie modeling has made significant progress, witnessing the emergence of several new procedures. Some notable advancements include the full homogenization (FH) optimization method ([Herranz et al., 2012](#)), the smooth evolutionary structural optimization (SESO) method ([Almeida et al., 2013](#)), the different material properties method ([Liu and Qiao, 2011](#)), and hybrid techniques that combine various methods ([Palmisano and Elia, 2015](#)). Additionally, [Nagarajan and Pillai \(2008\)](#) contributed to the development of strut and tie models for simply supported deep beams using topology optimization. In their work, [Bruggi \(2009\)](#) put forward a methodology that addresses the generation of truss-like designs, capable of deriving preliminary strut-and-tie models. The novelty of their approach lies in extending this methodology beyond the conventional two-dimensional context, allowing it to be applied in a three-dimensional environment as well. In 2010, James and Christopher introduced a methodology aimed at deriving truss models with maximum stiffness or minimum total strain energy for a general concrete member. Their optimization routine, implemented through a freely available computer program, generates strut and tie geometries that follow the elastic tensile and compressive stress paths. As a result, this approach leads to steel reinforcement layouts that have the potential to minimize crack widths. [Amir and ole Sigmundd \(2013\)](#) focuses on determining the distribution of ties in strut-and-tie models (STMs) through a conceptual optimization procedure. On the other hand, [Bruggi and Zordan](#) in their work [Bruggi \(2016\)](#) introduced a numerical method

specifically focused on generating strut-only models. Their aim was to discover optimal and consistent Strut-and-Tie Models (STMs) for concrete structures. Additionally, various practical computer-aided design tools have been developed to facilitate the STM-based design process, offering a user-friendly graphical interface (GUI) environment. [Tjhin and Kuchma \(2002\)](#) introduced such tools to facilitate the creation of strut-and-tie models. [Lee et al. \(2012\)](#) utilized material topology optimization techniques to determine the optimal layout of reinforcement within a specified volume, aiming to maximize stiffness given a specific set of loads and boundary conditions. In their work, [Zhong et al. \(2017\)](#) introduced an evaluation system for assessing the performance of D-regions designed with various STMs. This evaluation system utilizes the ANSYS parametric design language (APDL) and the computer-aided strut-and-tie (CAST) design tool to implement the numerical procedure. This evaluation system not only identifies the best STM among various options but also enables the examination of individual strut-and-tie models and the numerical prediction of their load-carrying capacity, eliminating the need for experimental testing.

2.5 STRESS OPTIMIZATION IN CONCRETE

Stress-based topology optimization has been acknowledged as a challenging problem and has consistently attracted research attention since the pioneering work by [Duysinx and Bendsoe \(1998\)](#). However, upon reviewing the literature, it becomes evident that there are relatively few studies considering stress constraints, in contrast to the numerous ones focusing on stiffness problems ([\(Pereira et al., 2004\)](#), [\(Stolpe and Svanberg, 2001\)](#), [\(Duysinx and Bendsoe, 1998\)](#)). One noteworthy attempt by [Baumgartner et al. \(1992\)](#) utilized a biological growth concept and an optimality criteria approach to determine the optimal topology for reducing structural peak stress. The method involved varying Young's moduli as functions of stress to achieve a fully stress-designed structure. However, its limitation lies in lacking generality. In industrial applications of topology optimization, it is of utmost importance to incorporate stress constraints. This ensures that the optimal design not only meets all engineering requirements but also avoids significant modifications that would deviate from the original optimized outcome. [Rozvany et al. \(1992\)](#) discusses how the Solid Isotropic Material with Penalization (SIMP) method can handle stress constraints. In the field of topology optimization, there have been two primary approaches for incorporating stress constraints into the finite element discretization of the problem. The first approach, used, for instance, in the work by [\(Duysinx and Bendsoe, 1998\)](#), involves implementing local stress controls

within each finite element of the discretized domain. This method ensures robustness but can be computationally expensive due to the need to account for material failure on a fine scale. Researchers such as [Van Miegroet and Duysinx \(2007\)](#) have included local stress constraints as design limitations. However, there is an alternative approach presented by [Yang and Chen \(1996\)](#) which replaces these local stress restrictions with one or several integrated stress criteria. By doing so, they formulate the optimization problems with a reduced set of global constraints. This alternative procedure allows for a more efficient and streamlined optimization process compared to dealing with numerous local constraints.

[Le et al. \(2010\)](#) identified three main challenges associated with stress-based topology optimization. The "singularity" problem, which was initially observed in truss layout designs ([Kirsch, 1990](#)), ([Cheng and Jiang, 1992](#)). [Cheng and Guo \(1997\)](#) introduced a novel approach known as the ε -relaxation technique to address this issue. This technique helps overcome the singularity phenomenon that arises when stress constraints are applied. In density-based methods, this phenomenon occurs when elements with low densities still exhibit high stress values, leading to difficulties in removing them during the optimization process. To tackle this, subsequent approaches proposed remedy schemes that relax stress constraints, allowing element stress and density to decrease simultaneously [([Duysinx and Sigmund, 1998](#)), ([Bruggi, 2008](#)), ([Bruggi, 2008](#))]. The local nature of stress, poses a challenge as stress is a property that varies at a small scale. This localized behavior can make it challenging to obtain a smooth and continuous stress distribution throughout the design. The highly non-linear stress behavior, which adds complexity to the optimization process, as the relationship between stress and material properties is not linear. This nonlinearity can complicate the convergence and stability of the optimization algorithm. To address the "singularity" problem in stress-based topology optimization, [Xia et al. \(2018b\)](#) employ the Bi-Directional Evolutionary Structural Optimization (BESO) method. Additionally, the level set approach, another technique for topology optimization, has been utilized to tackle stress-constrained problems as demonstrated by [Guo et al. \(2011\)](#) and [Xia et al. \(2012\)](#). The second challenge in stress-based topology optimization arises from stress being a local quantity. This means that stress needs to be controlled at each point throughout the structure, resulting in a large number of constraints that must be considered. One way to address this problem is by using global measures like the p-norm and the Kresselmeier-Steinhauser (KS) functions to estimate the maximum stress. These methods, as proposed by [Yang and Chen \(1996\)](#) and [Duysinx and](#)

[Bendsøe \(1998\)](#), are computationally efficient for sensitivity evaluation. However, it's worth noting that these global stress measures may not provide enough control over the local stress behavior, and this compromise in accuracy is made to achieve faster computational speed. The code given by [Yang and Chen \(1996\)](#) comprises 146 lines and encompasses finite element analysis along with p-norm stress sensitivity analysis utilizing the adjoint method. Importantly, by utilizing discrete topology optimization techniques like level-set methods and ESO-type methods as suggested by ([Xie and Steven, 1993](#)), the issue of "singularity" can be naturally avoided. Over the years, several computational programs for topology optimization have been made available for educational purposes. One notable formulation, presented by [Senhora et al. \(2020\)](#), offers a consistent approach for topology optimization focused on mass minimization with local stress constraints. This method utilizes the augmented Lagrangian method and is referred to as an aggregation-free approach. Among the different variants of topology optimization methods, the bi-directional evolutionary structural optimization (BESO) method stands out for its convergence, mesh independence, and ability to handle both material removal and addition. The stress sensitivity analysis is based on the adjoint method as described by [Deng et al. \(2021\)](#). The 146 lines of code that were provided consist of implementations for both finite element analysis and p-norm stress sensitivity analysis. [Xia et al. \(2018b\)](#) extended the ESO method to its BESO variant for stress minimization designs.

2.6 SUMMARY OF LITERATURE SURVEY

An overview of various kinds of structural optimization (size, shape, and topology) has been provided. When performing structural optimization and topology optimization, the goal is to achieve a structure that with a given amount of material performs best while satisfying the necessary constraints. Since the 1980's the rapidly-growing incensement and availability of computer capacity made it possible to perform more and more complex finite element modelling. This combined with the improvements in algorithms for design optimization has moved the field of topology optimization. Application of topology optimization in discrete as well as continuum structures has been presented. A detailed review on solution approaches of topology optimization was also made. Among many different algorithms for optimization, the best suitable algorithm can be selected based on many factors such as type of problem, formulation of objective, number, and complexity of variables, and available computational resources. The existing literature suggests that topology optimization is a widely recognized

design technique that can also be utilized for generating optimal strut and tie models. The combination of strut and tie model design with SIMP topology optimization has shown great potential as a comprehensive and automated approach for strut and tie model design (Lee et al., 2012). Problems of topology optimization use the mathematical background for the better aesthetical appearance of structural forms with improved weight-to-stiffness ratio using SIMP technique. It is identified that only a limited number of studies have been carried out for the conventional design of concrete structures for discontinuous regions (D-regions) enabling material topology optimization.

2.7 SCOPE OF THE STUDY

Optimization has been one of the most active domains of modern mathematical research for over a century. Optimization research is engaged in the development of fundamental mathematical theory for the creation of new optimization techniques. Structural optimization is a wide field with applications in all disciplines of engineering. The development of reinforced concrete can be linked to optimization goals such as an increase in strength and cost reduction. During the period of durable and resilient infrastructures, It is very crucial to reconsider optimizing each and every structure to its maximum efficiency for satisfying the idea of redundancy. While rigorous optimization techniques are necessary to improve efficiency in complex civil and structural engineering projects, it is also essential to consider the unique characteristics of each project. Reinforcement around D regions, which are regions where Bernoulli's hypothesis does not hold due to geometric discontinuities or variations in load patterns, is typically designed based on experience or expert decisions. Strut and tie models provide an alternative approach to the non-quantitative reinforcement design of D regions, offering a more robust and reliable solution. Stress concentrations occur in discontinuous regions and in deep beams. D regions refer to weak positions in a structure where there is a higher likelihood of structural damage, such as the formation of cracks. To ensure structural safety, it is necessary to reinforce these D regions by incorporating steel or fiber elements to prevent crack propagation. Initially, the strut and tie model was introduced as a means to address transverse reinforcement for the shear design of beams. Over time, it has been further developed and extended to encompass the design of D regions in general. The basis of strut and tie modeling is the assumption that concrete primarily carries compressive stresses, while steel reinforcement is responsible for handling tensile stress. Nevertheless, traditional strut-and-tie model designs typically involve a trial-and-error process to

determine the appropriate reinforcement design for a specific structure. In order to achieve a more quantitative and consistent reinforcement design, there is a need for a scientific and automated tool, as opposed to relying solely on the conventional human trial-and-error method. Therefore, there is a research opportunity to develop a quantitative approach for designing discontinuous regions (D-regions). This study aims to address these gaps in the existing literature by focusing on the aforementioned objectives.

2.8 Objectives

1. Formulate and apply Topology optimization in static and dynamic problems
2. To ascertain the applicability of topology optimization in the design of concrete structures.
3. Implementing Topology optimization by incorporating quasi-brittle property of concrete

CHAPTER 3

METHODOLOGY

This chapter discusses the overview of the detailed methodology to be adopted in this research work. The methodology includes general topology optimization formulations of different kinds of problems and solution algorithms.

3.1 FORMULATION OF OPTIMIZATION PROBLEM

Problem formulation of both static as well as dynamic problems is presented. An artificial material law is implemented to link together stiffness and density. Algorithm for topology optimization using SIMP has been presented. Different steps involved in the basic algorithm is listed and explained in this section.

3.1.1 Static problems

Based on the principle of minimum potential energy, the objective function is formulated as the minimization of compliance. The minimum compliance problem seeks to design the stiffest structure while considering a fixed load, specific support conditions, and limitations on the volume of material utilized within the designated design space.

$$\text{Minimum Strain Energy } SE = \sum_{e=1}^N \rho_e^p u_e^T k_e u_e \quad (3.1)$$

$$\text{Minimize } C = u^T K u$$

$$\sum x_i v_i - V^* = 0$$

$$K u = F$$

The inequality optimization constraint, represented as $0 \leq x_i \leq 1$, ensures that the density of each element, denoted by x_i , remains within the prescribed bounds. This constraint effectively controls the volume of the material used and the volume fraction in the optimization process as follows.

$$\frac{V(x)}{V_0} = f \quad (3.2)$$

3.1.2 Dynamic Problems

The dynamic behavior of structural systems can be assessed through Eigen frequency, which characterizes the stiffness of the structure. As the stiffness of a structure is directly related to its Eigen frequency, maximizing the first-order Eigen frequency can serve as an objective for dynamic optimization problems. The dynamic design problem can be formulated as follows:

$$\text{Maximize : } \omega_1^2 = \frac{u_1^T K u_1}{u_1^T M u_1} \quad (3.3)$$

$$\text{Subject to: } \frac{V(x)}{V_0} \leq f$$

$$[K - M\omega_1^2]u_i = 0$$

$$0 \leq x_{min} \leq x_i \leq x_{max}$$

The objective is to maximize the first-order Eigen frequency denoted by ω_1 . The design variables are represented by x_i , and the global stiffness matrix is denoted by K , while M represents the global mass matrix. Additionally, the variable f is used to denote the ratio between the obtained volume and the volume constraint in the optimization process.

Topology optimization aims to achieve the most efficient material distribution within the design space. This is achieved by dividing the design space into finite elements and then identifying the elements that should be included in the final solution. The process of topology optimization, specifically using the Solid Isotropic Material with Penalization (SIMP) method, is depicted in the provided Figure 3.1. In the conventional SIMP approach, the densities x_e are bounded by a lower limit slightly larger than zero to avoid elements with zero stiffness. However, in the modified SIMP approach proposed by Bendsøe and Sigmund (Bends et al., 2003), a minimum modulus of elasticity E_{min} is assigned to void regions. This

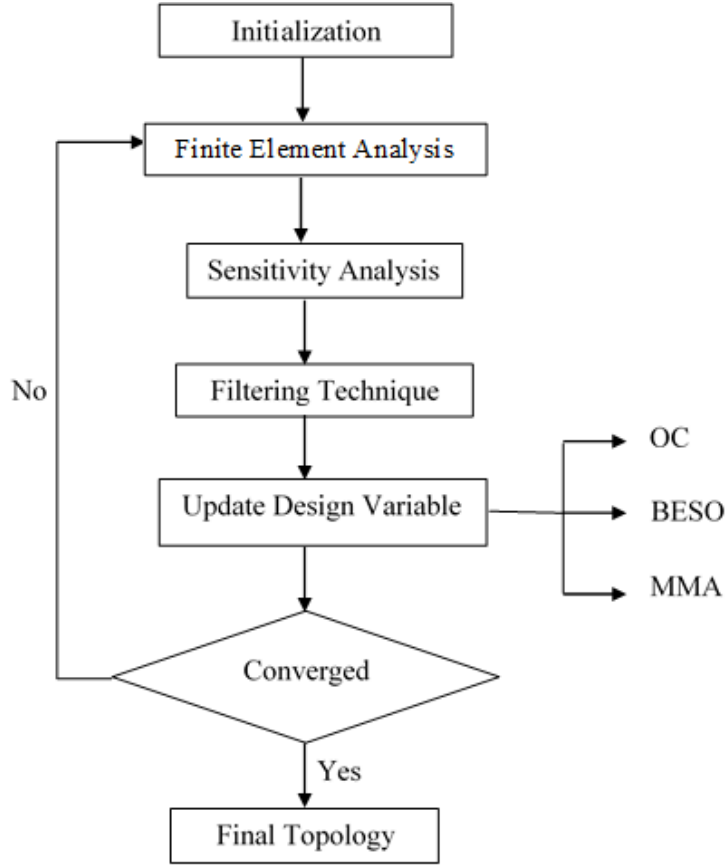


Figure 3.1: Topology optimization using the SIMP algorithm

modification is aimed at preventing the stiffness matrix from becoming singular. Additionally, the introduction of a penalization factor, denoted as p , is incorporated in Equation (3.4) to ensure the generation of black-and-white solutions.

$$E_e(x_e) = E_{min} + x_e^p(E_0 - E_{min}) \quad (3.4)$$

3.1.3 Sensitivity analysis

Sensitivity of the objective function, Compliance is given in Equation(3.5).SIMP interpolation scheme is taken as $E(x_i) = x_i^p E_0$.

$$\alpha_i = \begin{cases} u_i^T K_i^0 u_i & \text{when } x_i = 1 \\ x_{min}^{p-1} u_i^T K_i^0 u_i & \text{when } x_i = x_{min} \end{cases} \quad (3.5)$$

Dynamic Problem: Applying the SIMP (Solid Isotropic Material with Penalization) model directly to frequency optimization problems poses challenges. The main obstacle lies in the significant disparity in penalization between mass and stiffness when dealing with small values of x_i . This discrepancy results in the occurrence of artificial localized modes in regions with low density, which can adversely affect the optimization process. To address this issue, an alternative material interpolation scheme is introduced in Equation (3.6).

$$\rho(x_i) = x_i \rho \quad E(x_i) = \left[\frac{x_{min} - x_{min}^p}{1 - x_{min}^p} (1 - x_i^p) + x_i^p \right] \quad (3.6)$$

$$\alpha_i = \begin{cases} \frac{1}{2\omega_i} u_i^T \left(\frac{1-x_{min}}{1-x_{min}^p} K_i^0 - \frac{\omega^2}{p} M_i^0 \right) u_i & \text{when } x_i = 1 \\ \frac{1}{2\omega_i} u_i^T \left(\frac{x_{min}^{p-1} - x_{min}^p}{1-x_{min}^p} K_i^0 - \frac{\omega^2}{p} M_i^0 \right) u_i & \text{when } x_i = x_{min} \end{cases}$$

3.1.4 Optimality Criteria

arious approaches can be employed to solve the optimization problem and update the variable density. One such method is the use of optimality criteria, which is formulated in Equation (3.7). The optimality criteria provide a heuristic updating scheme for the design variables, proving to be effective in solving structural topology optimization problems (Bends et al., 2003).

$$x_e^{new} = \begin{cases} \max(x_{min}, x_e - m), & \text{if } x_e B_e^\eta \leq \max(x_{min}, x_e - m) \\ x_e B_e^\eta, & \text{if } \max(x_{min}, x_e - m) \leq x_e B_e^\eta < \min(1, x_e + m) \\ \min(1, x_e + m), & \text{if } \min(1, x_e + m) \leq x_e B_e^\eta \end{cases} \quad (3.7)$$

3.1.5 Bidirectional Evolutionary Structural Optimization

The element variables are defined using the element sensitivity number, as shown in Equation (3.9). A small percentage of volume that can be added or subtracted in each iteration is termed as an evolutionary ratio(ER).

$$\alpha_i = -\frac{p}{x_i} x_i^p u_i^T k_i^0 u_i = -p \frac{E_i}{x_i} \quad (3.8)$$

The target volume for the next iteration V^{*+1} is determined using Equation(3.9).

$$V^{*+1} = V^*(1 \pm ER) \quad (3.9)$$

3.1.6 Filtering

To guarantee the existence of solutions in the topology optimization problem and prevent the formation of checkerboard patterns, certain constraints on the design need to be imposed. One commonly used approach is the application of a filter to either the sensitivities or the densities. The mesh independency filter operates by adjusting the element sensitivities according to Equation (3.10). This filter helps in achieving mesh-independent results, enhancing the convergence and stability of the optimization process, while also mitigating issues related to checkerboard patterns in the final design.

$$\frac{\partial c}{\partial x_e} = \frac{1}{x_e \sum_{f=1}^N H_f} \sum_{f=1}^N H_f x_f \frac{\partial c}{\partial x_f} \quad (3.10)$$

$$\text{where } H_f = r_{min} - \text{dis}(e,f) \quad (3.11)$$

In the given equation, the operator $\text{dist}(e,f)$ represents the distance between the centers of element e and element f. The convolution operator H_f is utilized within the filter area, where it is non-zero. As the distance from element f increases, the convolution operator decays linearly, resulting in a reduced influence on elements that are farther away from f.

3.2 Application of Topology Optimization in different Engineering Problems

Multiple constrained problems have been applied to Concrete dapped beams using ABAQUS software. BESO method incorporates in the ABAQUS input file to simulate Dapped beams with different load cases. Topology Optimization using higher order elements and concrete Damaged Plasticity model(CDP) have been included in this section. An algorithm for optimization problems with displacement as a constraint is formulated. Reinforced concrete dapped end beams (RC-DEB) are commonly utilized in concrete bridge girders and precast concrete buildings. The inclusion of dapped beams offers the advantage of enhanced lateral stability, which allows for the efficient assembly of precast members. This lateral stability is achieved through the presence of an isolated dapped end beam, which provides more struc-

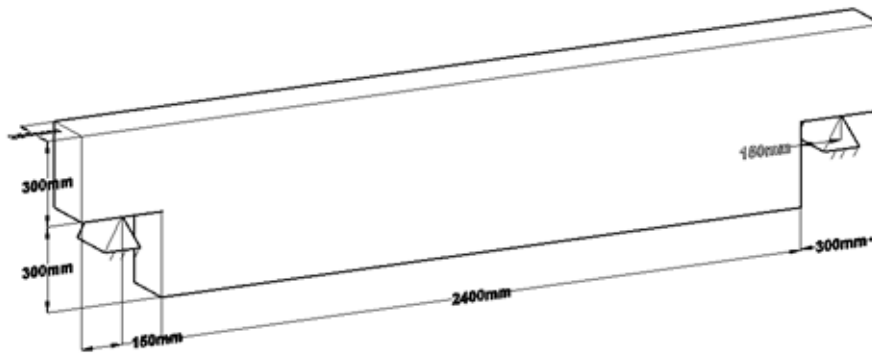


Figure 3.2: Dimensions and boundary conditions of Dapped beam)

tural support compared to using only isolated beams. In certain cases, the nib of a dapped end beam resembles an inverted corbel. However, due to the geometrical nonlinearity, these dapped beams experience high-stress concentration at their reentrant corners, necessitating proper reinforcement to prevent failure (Huang and Nanni, 2006). For the analysis, the model dimensions and boundary conditions are depicted in Figure 3.2, with symmetrical loading and boundary conditions applied. A concrete grade of M30 with a Poisson's ratio of 0.15 has been selected. The ABAQUS software is utilized to model the beam with a mesh size of 40mm, adopting the SIMP material interpolation scheme and a penalty factor of 3. The initial design undergoes convergence to an optimal topology through finite element analysis, sensitivity analysis, and design variable updating using the optimality criteria method. The finite element model, along with the load and boundary conditions, is presented in Figure 3.3

3.2.1 Concrete dapped beams with multiple constraints

Four distinct optimization problems are considered for simulation. Compliance is an inverse indicator of stiffness. To derive the stiffest layout of a structure for a given set of loadings and boundary conditions, minimization of compliance can be selected as an objective function. To obtain a truss-like pattern for beams, the optimization approach chosen involves minimizing compliance while considering three distinct constraints, in addition to a volume constraint. To derive a lightweight structure, volume-based topology optimization, where the goal is to minimize the overall weight of the structure while ensuring that stresses remain within acceptable limits. This section centers on conducting topology optimization for Concrete Dapped beams using the ABAQUS finite element software, while accounting

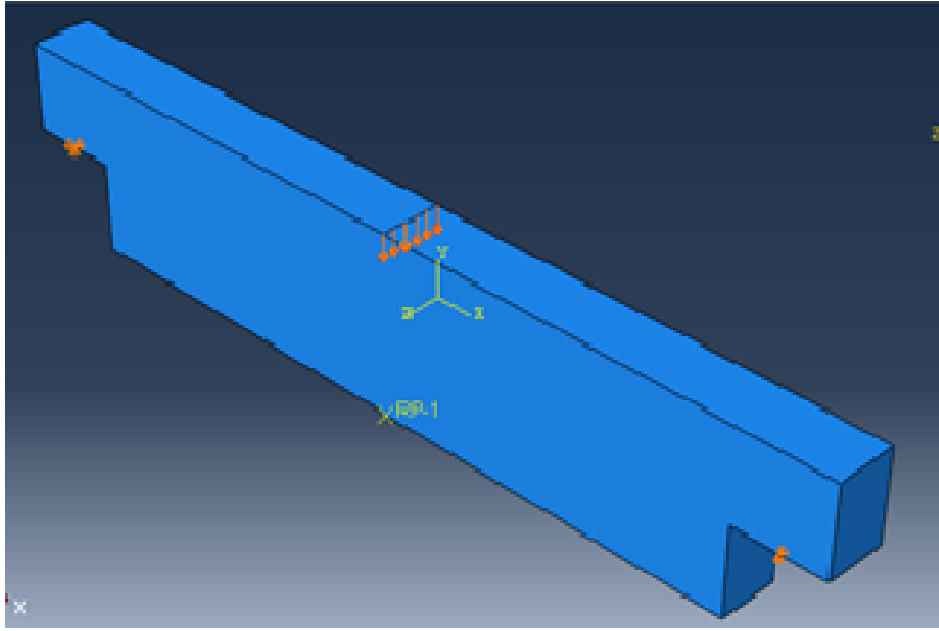


Figure 3.3: Finite element model of Dapped beam

for multiple constraints.

$$\text{Problem 1: Minimize } C = C(x) = \frac{1}{2}u^TKu \quad (3.12)$$

$$\text{Subject to : } d_j(x) - d^* \leq 0$$

$$\frac{V(x)}{V^*} = f$$

$$\text{Problem 2: Minimize } C = C(x) = \frac{1}{2}u^TKu \quad (3.13)$$

$$\text{Subject to : } \omega^* - \omega_n(x) \leq 0$$

$$\frac{V(x)}{V^*} = f$$

$$\text{Problem 3: Minimize } C = C(x) = \frac{1}{2}u^TKu \quad (3.14)$$

$$\text{Subject to : } \sigma_n(x) - \sigma^* \leq 0$$

$$\frac{V(x)}{V^*} = f$$

Problem 4: Minimize Volume (3.15)

$$\text{Subject to : } \sigma_n(x) - \sigma^* \leq 0$$

In the optimization problem, the vector of design variables is represented by x , while u denotes the displacement vector, and K stands for the global stiffness matrix. The mean compliance is denoted by C , and d_j represents the magnitude of the displacement vector at the j^{th} node. Additionally, ω_n corresponds to the natural frequency of the n^{th} mode, and σ_n stands for the stress of the n^{th} element. The objective function for the first three problems is to minimize compliance while adhering to the volume constraint. Here, the material volume is represented by V , and V denotes the volume of the design domain. The specified volume fraction is denoted by f , and d , ω , and σ are the values of the imposed constraints. Equation (3.12) presents the optimization formulation involving compliance minimization and the addition of a displacement constraint. For the second problem (Equation (3.13)), the constraint is Eigen frequency, while for the third problem (Equation (3.14)), the constraints involve stress. Finally, the fourth problem aims to achieve a lightweight structure by using stress as the primary constraint. The objective function for the first three problems is to minimize compliance, while satisfying the volume constraint. The material volume is represented by V , and V is the volume of the design domain. The prescribed volume fraction is denoted by f , and d , ω , and σ are the imposed constraint values.

3.2.2 Different load cases in Dapped Beams

The main focus of this section is on performing topology optimization for 3D Concrete dapped beams using the BESO (Bi-directional Evolutionary Structural Optimization) method within the ABAQUS finite element software environment. The model dimensions and boundary conditions are illustrated in Figure 3.4. The optimization process involves considering four different load cases, which are depicted in Figure 3.5 for simulation.

Load case-1: A Concentrated load at a distance of 430mm from the left support

Load case- 2: Uniformly distributed load throughout the effective span

Load case -3: Uniformly distributed load in the mid third of effective span

Load case- 4: Lateral load at the both ends of beam

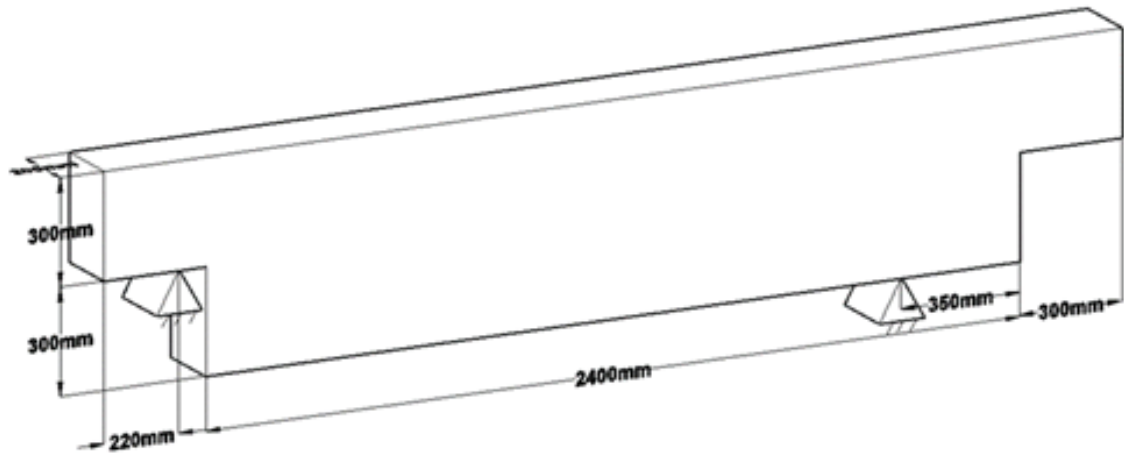


Figure 3.4: Dimensions and boundary conditions of Dapped beams

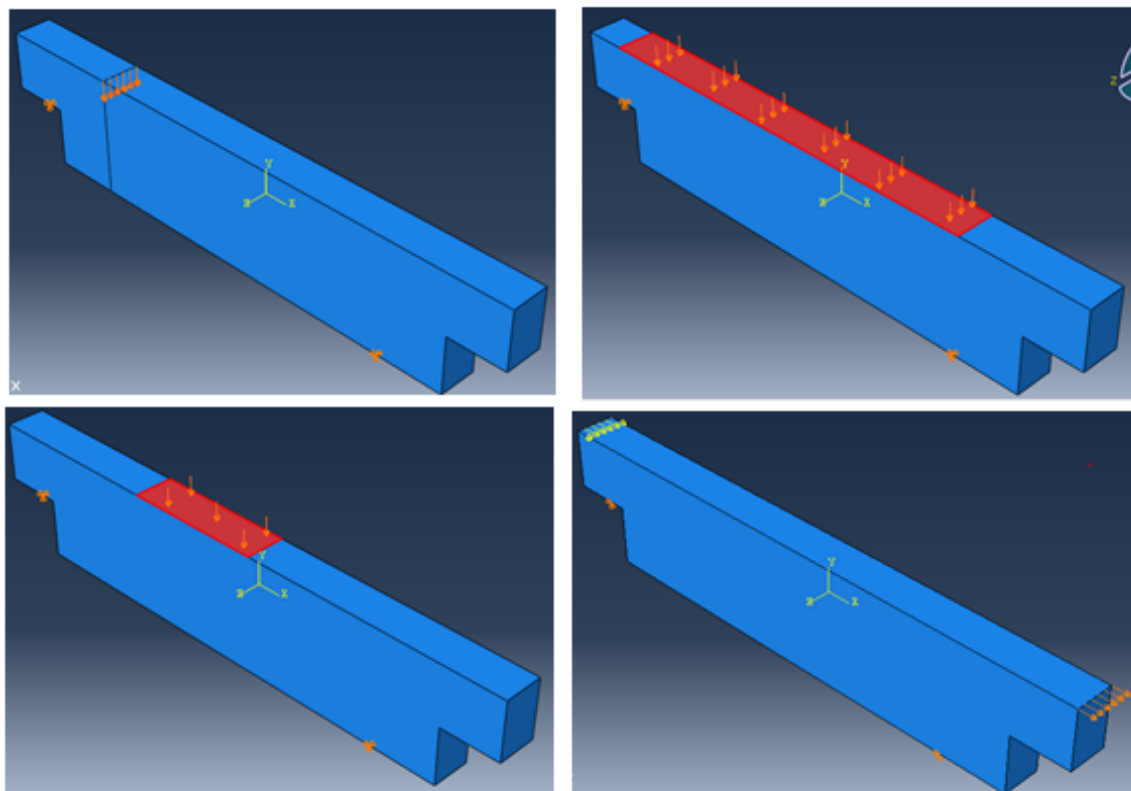


Figure 3.5: Different Load Cases

3.2.3 Topology Optimization with Concrete Damaged Plasticity model

The Concrete Damaged Plasticity (CDP) model is a suitable choice for simulating concrete and other quasi-brittle materials. It combines isotropic damaged elasticity with isotropic tensile and compressive plasticity to accurately represent the inelastic behavior of concrete. ABAQUS finite element software has the capability to incorporate damage modeling in con-

crete elements using the CDP model. To define the CDP model in ABAQUS, various parameters need to be specified, including ζ , ε , K , $\frac{\sigma_{ho}}{\sigma_{co}}$, and μ . Here, ζ represents the dilation angle, ε is the flow potential eccentricity, $\frac{\sigma_{ho}}{\sigma_{co}}$ denotes the ratio of the second stress invariant on the tensile meridian to that on the compressive meridian, and μ stands for the viscosity parameter. These parameters play a crucial role in accurately capturing the mechanical behavior of concrete and other similar materials when subjected to different loading conditions. Compressive behaviour of concrete is modelled based on the work by [Hsu and Hsu \(1994\)](#) and [Hognestad \(1951\)](#). Tensile behaviour is simulated using the material model developed by [Aslani and Jowkarmeimandi \(2012\)](#).

Compressive behavior of Concrete using Hsu and Hsu (1994)

For $0 \leq \varepsilon \leq \varepsilon_{c,lim}$

$$\frac{\sigma_c}{\sigma_{cu}} = \frac{\beta \left(\frac{\varepsilon_c}{\varepsilon_0}\right)}{\beta - 1 + \left(\frac{\varepsilon_c}{\varepsilon_0}\right)^\beta} \quad (3.16)$$

$$\text{Elastic strain, } \varepsilon_c^e = \frac{\sigma_c}{E} \quad (3.17)$$

$$\text{Inelastic strain, } \varepsilon_c^{in} = \varepsilon_c - \varepsilon_c^e \quad (3.18)$$

where σ_{cu} is the ultimate compressive stress and ε_c is the total strain. β parameter depends on the shape of the stress-strain curve. ε_0 and β can be calculated using Equation 3.19 and Equation 3.20. The value of σ_{cu} is in MPa.

$$\varepsilon_0 = (1680 + 7.1\sigma_{cu}) * 10^{(-6)} \quad (3.19)$$

$$\beta = \left(\frac{\sigma_{cu}}{65.23}\right)^3 + 2.59 \quad (3.20)$$

$\varepsilon_{c,limit}$ =strain at $0.3\sigma_{cu}$ in the falling branch of stress-strain curve

Compressive behavior of Concrete using Hognestad (1951)

This model predicts good results for concrete with compressive strength $< 60MPa$.

$$\sigma_c = \sigma_{cu} \left[2 \left(\frac{\varepsilon}{\varepsilon_0} \right) - \left(\frac{\varepsilon}{\varepsilon_0} \right)^2 \right] \quad (3.21)$$

where strain at peak stress, $\varepsilon_0 = 0.002$ and ultimate strain, $\varepsilon_{cu} = 0.0035$

Tensile behavior of concrete using Aslani and Jowkarmeimandi (2012)

$$\sigma_{t0} = 0.33\sqrt{\sigma_{cu}} \quad (3.22)$$

$$\sigma_t = \sigma_{t0} * \left[\frac{\varepsilon_{t0}}{\varepsilon_t} \right]^{0.85} \quad (3.23)$$

$$\text{where } \varepsilon_{t0} = \frac{\sigma_{t0}}{E}$$

$$\text{Elastic strain, } \varepsilon_t^e = \frac{\sigma_t}{E} \quad (3.24)$$

$$\text{cracking strain, } \varepsilon_t^{ck} = \varepsilon_t - \varepsilon_t^e \quad (3.25)$$

where σ_{t0} is the maximum tensile stress, ε_t is the total stress and σ_{cu} is the ultimate compressive strength. Damage parameter in tension(d_t) and compression(d_c) can be find out using Equation 3.26 and Equation 3.27.

$$d_t = \frac{\varepsilon_{cr}}{\varepsilon_t} \quad (3.26)$$

$$d_c = \frac{\varepsilon_{in}}{\varepsilon_c} \quad (3.27)$$

ABAQUS checks the correctness of damage curve by calculating plastic strain values in compression and tension. Plastic strain values should neither be negative nor decreasing with increased stress. Declining plastic strain values are indicators of inaccurate damage curve. Plastic strain values can be calculated by Equation 3.28

$$\varepsilon^{plastic} = \varepsilon^{in/cr} - \frac{d_{c/t}}{1 - d_{c/t}} * \frac{\sigma_{c/t}}{E_0} \quad (3.28)$$

3.2.4 TO using Higher order elements

Four node square elements, Eight node square elements and Nine node square elements have been used in this study. The elements used are shown in Figure 3.6. The purpose of using higher order elements is to check whether it changes optimum layout of the struc-

ture. Anyway computation time is higher for the higher order elements with relatively more number of iteration to converge.

Stiffness matrix formulation

Shape functions of higher order elements can be derived by extra nodes on the sides of linear element. Following steps are required to develop a stiffness matrix. Select the shape functions for each type of element. Determine the strains which can be expressed as derivatives of displacement with respect to x and y as Equation 3.29.

$$\begin{Bmatrix} \varepsilon_x \\ \varepsilon_y \\ \gamma_{xy} \end{Bmatrix} = \begin{bmatrix} \frac{\partial()}{\partial x} & 0 \\ 0 & \frac{\partial()}{\partial x} \\ \frac{\partial()}{\partial y} & \frac{\partial()}{\partial x} \end{bmatrix} \begin{Bmatrix} u \\ v \end{Bmatrix} \quad (3.29)$$

$$\text{Element Strains, } \{\varepsilon\} = [B]\{d\} \quad (3.30)$$

Individual elements of the strain matrix is evaluated by Equation 3.31 and Equation 3.32

$$\frac{\partial()}{\partial x} = \frac{1}{|[J]|} \left[\frac{\partial y}{\partial \eta} \frac{\partial()}{\partial \xi} - \frac{\partial y}{\partial \xi} \frac{\partial()}{\partial \eta} \right] \quad (3.31)$$

$$\frac{\partial()}{\partial y} = \frac{1}{|[J]|} \left[\frac{\partial x}{\partial \xi} \frac{\partial()}{\partial \eta} - \frac{\partial x}{\partial \eta} \frac{\partial()}{\partial \xi} \right] \quad (3.32)$$

where Jacobian matrix $[J]$ is

$$[J] = \begin{bmatrix} \frac{\partial x}{\partial \xi} & \frac{\partial y}{\partial \xi} \\ \frac{\partial x}{\partial \eta} & \frac{\partial y}{\partial \eta} \end{bmatrix} \quad (3.33)$$

Strains can be expressed in terms of natural coordinates ξ and η as in Equation 3.34

$$\begin{Bmatrix} \varepsilon_x \\ \varepsilon_y \\ \gamma_{xy} \end{Bmatrix} = \frac{1}{|[J]|} \begin{bmatrix} \frac{\partial y}{\partial \eta} \frac{\partial()}{\partial \xi} - \frac{\partial y}{\partial \xi} \frac{\partial()}{\partial \eta} & 0 \\ 0 & \frac{\partial x}{\partial \xi} \frac{\partial()}{\partial \eta} - \frac{\partial x}{\partial \eta} \frac{\partial()}{\partial \xi} \\ \frac{\partial x}{\partial \xi} \frac{\partial()}{\partial \eta} - \frac{\partial x}{\partial \eta} \frac{\partial()}{\partial \xi} & \frac{\partial y}{\partial \eta} \frac{\partial()}{\partial \xi} - \frac{\partial y}{\partial \xi} \frac{\partial()}{\partial \eta} \end{bmatrix} \begin{Bmatrix} u \\ v \end{Bmatrix} \quad (3.34)$$

$$\{\varepsilon\} = [D'] [N] \{d\} \quad (3.35)$$

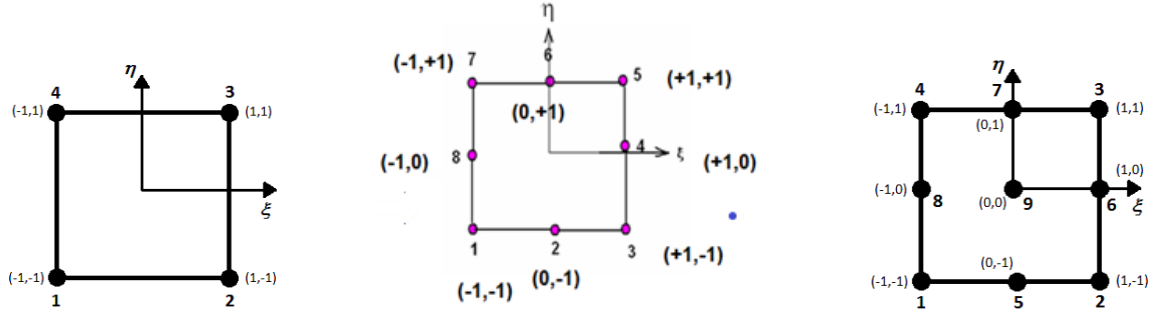


Figure 3.6: Four noded, Eight noded and Nine noded elements

Formulate Element matrix $[B]$ to evaluate $[k]$ such that $[B] = [D'] [N]$

$$[B(\zeta, \eta)] = \frac{1}{|[J]|} [[B_1] [B_2] \dots [B_n]] \quad (3.36)$$

where submatrices $[B]$ are

$$[B_i] = \frac{1}{|[J]|} \begin{bmatrix} \frac{\partial y}{\partial \eta} \frac{\partial(N_i)}{\partial \zeta} - \frac{\partial y}{\partial \zeta} \frac{\partial(N_i)}{\partial \eta} & 0 \\ 0 & \frac{\partial x}{\partial \zeta} \frac{\partial(N_i)}{\partial \eta} - \frac{\partial x}{\partial \eta} \frac{\partial(N_i)}{\partial \zeta} \\ \frac{\partial x}{\partial \zeta} \frac{\partial(N_i)}{\partial \eta} - \frac{\partial x}{\partial \eta} \frac{\partial(N_i)}{\partial \zeta} & \frac{\partial y}{\partial \eta} \frac{\partial(N_i)}{\partial \zeta} - \frac{\partial y}{\partial \zeta} \frac{\partial(N_i)}{\partial \eta} \end{bmatrix} \begin{Bmatrix} u \\ v \end{Bmatrix} \quad (3.37)$$

where $i= 1$ to n and n is number of nodes in the element

Stiffness matrix of an element with constant thickness h

$$[k] = \int \int_A [B]^T [D] [B] h dx dy \quad (3.38)$$

Express the stiffness matrix in terms of ζ and η by general type of transformation as in Equation 3.39.

$$\int \int_A f(x, y) dx dy = \int \int_A f(\zeta, \eta) |J| d\zeta d\eta \quad (3.39)$$

After applying transformation equation, $[k]$ can be written as Equation 3.40

$$[k] = \int_{-1}^1 \int_{-1}^1 [B]^T [D] [B] h |J| d\zeta d\eta \quad (3.40)$$

Shape functions

Shape functions are the functions which interpolates the solution at any point based on the discrete values at the nodes in the mesh.

Quadrilateral Element

The ξ - η coordinates can be related to global coordinates x and y by the Equation 3.41 and Equation 3.42.

$$x = a_1 + a_2\xi + a_3\eta + a_4\xi\eta \quad (3.41)$$

$$y = a_5 + a_6\xi + a_7\eta + a_8\xi\eta \quad (3.42)$$

Shape functions of four node square elements are:

$$N_1 = \frac{(1 - \xi)(1 - \eta)}{4}$$

$$N_2 = \frac{(1 + \xi)(1 - \eta)}{4}$$

$$N_3 = \frac{(1 + \xi)(1 + \eta)}{4}$$

$$N_4 = \frac{(1 - \xi)(1 + \eta)}{4}$$

Eight noded Quadratic square element

Shape functions are based on incomplete cubic polynomials. Global coordinates are given in Equation 3.43 and Equation 3.44.

$$x = a_1 + a_2\xi + a_3\eta + a_4\xi\eta + a_5\xi^2 + a_6\eta^2 + a_7\xi^2\eta + a_8\xi\eta^2 \quad (3.43)$$

$$y = a_9 + a_{10}\xi + a_{11}\eta + a_{12}\xi\eta + a_{13}\xi^2 + a_{14}\eta^2 + a_{15}\xi^2\eta + a_{16}\xi\eta^2 \quad (3.44)$$

Shape functions:

$$N_1 = \frac{-(1 - \xi)(1 - \eta)(1 + \xi + \eta)}{4}$$

$$N_2 = \frac{-(1 + \xi)(1 - \eta)(1 - \xi + \eta)}{4}$$

$$N_3 = \frac{-(1 + \xi)(1 + \eta)(1 - \xi - \eta)}{4}$$

$$N_4 = \frac{-(1 - \xi)(1 + \eta)(1 + \xi - \eta)}{4}$$

$$N_5 = \frac{(1 - \xi^2)(1 - \eta)}{2}$$

$$N_6 = \frac{(1 + \xi)(1 - \eta^2)}{2}$$

$$N_7 = \frac{(1 - \xi^2)(1 + \eta)}{2}$$

$$N_8 = \frac{(1 - \xi)(1 - \eta^2)}{2}$$

Nine noded square element

Global coordinates can be obtained by adding $a_{17}\xi^2\eta^2$ and $a_{18}\xi^2\eta^2$ respectively in x and y coordinates of 8-noded element. Shape functions are given below.

$$\begin{aligned}
 N_1 &= \frac{\xi\eta(1-\xi)(1-\eta)}{4} & N_2 &= \frac{-\xi\eta(1+\xi)(1-\eta)}{4} \\
 N_3 &= \frac{\xi\eta(1+\xi)(1+\eta)}{4} & N_4 &= \frac{-(\xi\eta(1-\xi)(1+\eta))}{4} \\
 N_5 &= \frac{-\eta(1-\xi^2)(1-\eta)}{2} & N_6 &= \frac{\xi(1+\xi)(1-\eta^2)}{2} \\
 N_7 &= \frac{\eta(1-\xi^2)(1+\eta)}{2} & N_8 &= \frac{-\xi(1-\xi)(1-\eta^2)}{2} \\
 N_9 &= \frac{(1-\xi^2)(1-\eta^2)}{2}
 \end{aligned}$$

3.2.5 Displacement constrained optimization

The stiffness maximization problem with volume and displacement constraint is formulated as Equation 3.45

$$\text{Minimize } C = u^T K u \quad (3.45)$$

$$\text{Subject to: } d_j(x) - d^* < 0$$

$$\sum x_i v_i - V^* = 0$$

$$K u = f$$

where K is the stiffness matrix, u is the displacement vector and d_j is the magnitude of the displacement in the j^{th} node. d^* and V^* is the imposed value of displacement and volume constraint.

Lagrange function

The inequality constraint of local displacement can be relaxed by using Lagrange function (Equation 3.46)

$$L(x, \lambda_v, \mu) = C(x) + \lambda_v \left(\sum_1^n x_i v_i - V^* \right) + \mu_1 [d_j - d^* + S_1^2] \quad (3.46)$$

Overall element sensitivity is represented as Equation 3.47

$$\alpha_i = \frac{\partial L}{\partial x_i} - \lambda_v v = \frac{\partial C}{\partial x_i} + \mu_1 \frac{\partial d_j}{\partial x_i} \quad (3.47)$$

Element sensitivity for the mean compliance can be written as (Huang and Xie, 2009)

$$\alpha_i^{objective} = \frac{\partial C}{\partial x_i} = -\frac{px_i^{p-1}}{2} u_i^T K_i^0 u_i \quad (3.48)$$

Element sensitivity of the displacement constraint can be written as

$$\alpha_i^{dis} = \frac{\partial d_j}{\partial x_i} = -px_i^{p-1} u_{ij}^T K_i^0 u_i \quad (3.49)$$

u_{ij} is the element displacement vector under a virtual load. It can be calculated as providing a unit virtual load at the j^{th} node where the displacement value has to be restrained. The displacement in the next iteration, d_j^{i+1} can be estimated by using the displacement in the current iteration. The relation is expressed in Equation 3.50

$$d_j^{i+1} \approx d_j^i + \sum \frac{\partial d_j}{\partial x_i} \Delta x_i \quad (3.50)$$

if the value of $d_j^{i+1} > d^*$, increase the value of Lagrange multiplier μ by 20%. Otherwise reduce the effect of constraint in the sensitivity analysis by declining the value of μ by 20%. The Algorithm for solving Displacement constrained problem using BESO method is shown in Figure 3.7.

3.3 Stress Constrained Optimization

Minimizing compliance such that maximum value of stress anywhere in the structure will not exceed the constrained value. Von Mises stress value is taken into consideration. The problem is formulated as Equation 3.51

$$\begin{aligned} \text{Minimize } & C = u^T K u \\ \text{such that : } & K u = f \\ & \{\sigma_i\} \leq \sigma_c \text{ if } \rho > 0 \\ & 0 \leq \rho_{min} \leq \rho_i \leq \rho_{max} \leq 1 \end{aligned} \quad (3.51)$$

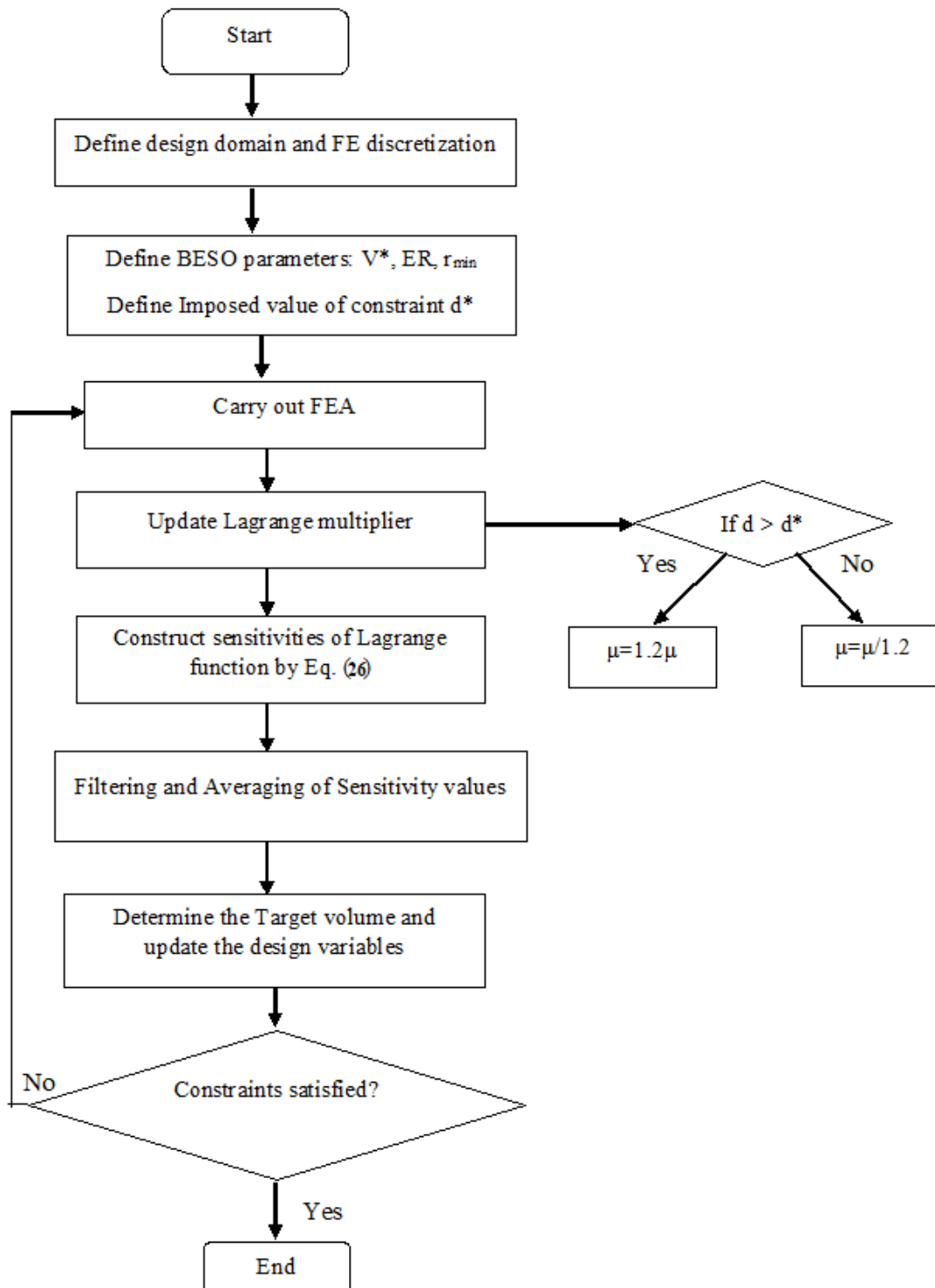


Figure 3.7: BESO algorithm with displacement constraint

VonMises stress of a 2-D plane stress quadrilateral elements can be calculated using Equation 3.52

$$\sigma_{vm} = \sqrt{\sigma_x^2 + \sigma_y^2 - \sigma_x\sigma_y + 3\sigma_{xy}^2} \quad (3.52)$$

2-D stress tensor is expressed as $\sigma = \begin{Bmatrix} \sigma_x \\ \sigma_y \\ \sigma_{xy} \end{Bmatrix}$ (3.53)

$$\begin{Bmatrix} \sigma_x \\ \sigma_y \\ \sigma_{xy} \end{Bmatrix} = [D] \begin{Bmatrix} \varepsilon_x \\ \varepsilon_y \\ \varepsilon_{xy} \end{Bmatrix} \quad (3.54)$$

$$\sigma = DBd \text{ where } \{\varepsilon\} = [B]\{d\}$$

where B is the shape function derivative matrix, D is the constitutive matrix and d is the displacement vector. Calculation of constitutive matrix involves the terms Young's modulus (E) and the Poisson's ratio (ν).

$$D = \frac{E}{1-\nu^2} \begin{bmatrix} 1 & \nu & 0 \\ \nu & 1 & 0 \\ 0 & 0 & (1-\nu)/2 \end{bmatrix} \quad (3.55)$$

B matrix for a 2-D 4-noded square element with length L is given in Equation 3.56

$$B = \frac{1}{2L} \begin{bmatrix} -1 & 0 & 1 & 0 & 1 & 0 & -1 & 0 \\ 0 & -1 & 0 & -1 & 0 & 1 & 0 & 1 \\ -1 & -1 & -1 & 1 & 1 & 1 & 1 & -1 \end{bmatrix} \quad (3.56)$$

Displacement vector can be represented in terms of x and y translations

3.3.1 Drucker-Prager Yield Criteria

The Drucker-Prager failure criterion is employed to handle materials that exhibit different tension-compression behaviors. Additionally, a relaxed equivalent stress measure is incorporated to address singularity issues that may arise during the analysis of such materials.

$$\sigma^{eq} = \frac{s+1}{2s} \sqrt{3J_{2D}} + \frac{s-1}{2s} J_1 \leq \sigma_{Lt} \quad (3.57)$$

$$J_1 = \sigma_{11} + \sigma_{22} \quad (3.58)$$

$$3J_{2D} = \sigma_{11}^2 + \sigma_{22}^2 - \sigma_{11}\sigma_{22} + 3\sigma_{12}^2 \quad (3.59)$$

First stress invariant is denoted as J_1 and second deviatoric stress constraint is denoted as J_{2D} and s is the compressive strength to tensile strength ratio. Employing some algebraic transformations, the invariants for the e -th finite element can be expressed using a "hydrostatic stress matrix" denoted as H_e^0 and a "von Mises stress matrix" represented as M_e^0 .

$$J_{1,e} = x_e^p H_e^0 U_e \quad (3.60)$$

$$3J_{2D,e} = x_e^{2p} U_e^T M_e^0 U_e \quad (3.61)$$

The equivalent Drucker-Prager stress measure for the e -th finite element

$$\sigma_{eq} = x_e^p \left(\frac{s+1}{2s} \sqrt{U_e^T M_e^0 U_e} + \frac{s-1}{2s} H_e^0 U_e \right) = x_e^p \tilde{\sigma}_e^{eq} \quad (3.62)$$

As suggested by Duysinx and Bendsøe in 1998, a suitable failure criterion for the porous SIMP material should be defined based on the apparent "local" stress (σ_{ij}), which can be derived as $(\sigma_{ij}) = \frac{\sigma_{ij}}{x_e^q}$, with $q > 1$. To implement the Drucker-Prager stress criterion in conjunction with the SIMP model on the e -th finite element, the following form is appropriate:

$$x_e^{(p-q)} \frac{\tilde{\sigma}_e^{eq}(s)}{\sigma_{Lt}} \leq 1 \quad (3.63)$$

Further computational work is required to account for the sensitivities of stress limitations.

$$\frac{\partial \tilde{\sigma}_e^{eq'}}{\partial x_k} = \rho_{ek} (p-q) x_e^{p-q-1} \tilde{\sigma}_e^{eq} + \frac{\partial \sigma_e^{eq}}{\partial x_k} x_e^{p-q} \quad (3.64)$$

Due to the fact that the number of active stress constraints, denoted as N_a , is usually smaller than the number of design variables, denoted as N , the adjoint method is favored over the direct approach for computing the derivative of σ_e^{eq} . To compute \tilde{U}^T , one extra load case is needed.

$$\frac{\partial \tilde{\sigma}_e^{eq}}{\partial x_k} = -\tilde{U}^T \frac{\partial K}{\partial x_k} U \quad (3.65)$$

$$K\tilde{U} = \left[\frac{s+1}{2s} (U^T M_e^0 U)^{-\frac{1}{2}} M_0^e U + \frac{s-1}{2s} H_e^0 \right] \quad (3.66)$$

CHAPTER 4

RESULTS AND DISCUSSION

This chapter discusses converged optimum material layouts and convergence history of structural members in different kinds of Topology optimization problems

4.1 STATIC AND DYNAMIC PROBLEMS

Define the 3D structural concrete, loads, boundary conditions, Finite element discretization and optimization procedure in ABAQUS software environment. For static problems strain energy was selected as an objective. Volume fraction of 0.3 was set as constraint for both static and dynamic problems. For free vibration problems first order Eigen-frequency was maximized. Concrete grade of M30 with density of $2400\text{kg}/\text{m}^3$ was selected for simulation. The Young's modulus of concrete, $E_c = 27386.127\text{MPa}$ and Poisson's ratio = 0.15 were defined during analysis.

4.1.1 Numerical Examples

Numerical examples demonstrate the optimum material layout of the concrete structure in static and free vibration problems. Three structural members were selected to evaluate the capability of ABAQUS to derive the truss pattern by satisfying given objective and constraint. The penalty parameter of SIMP material was entered as 3.

The dimensions and boundary conditions of cantilever beam is shown in Figure 4.1. A load of 1000N was applied at the free end of cantilever beam and a mesh size of 3mm had applied. The Iteration history of objective function and constraint is plotted Figure 4.2 and Figure 4.3. Mat-Prop-Normalized is the output variable in ABAQUS which is displayed after topology optimization. It is the element based normalized material value. Optimal material layouts in both cases are shown in Figure 4.4. Similar kinds of material layout obtained for other two examples. The optimum material layout for corbel and L-beam. The optimum layout is shown in Figure 4.5 and Figure 4.6.

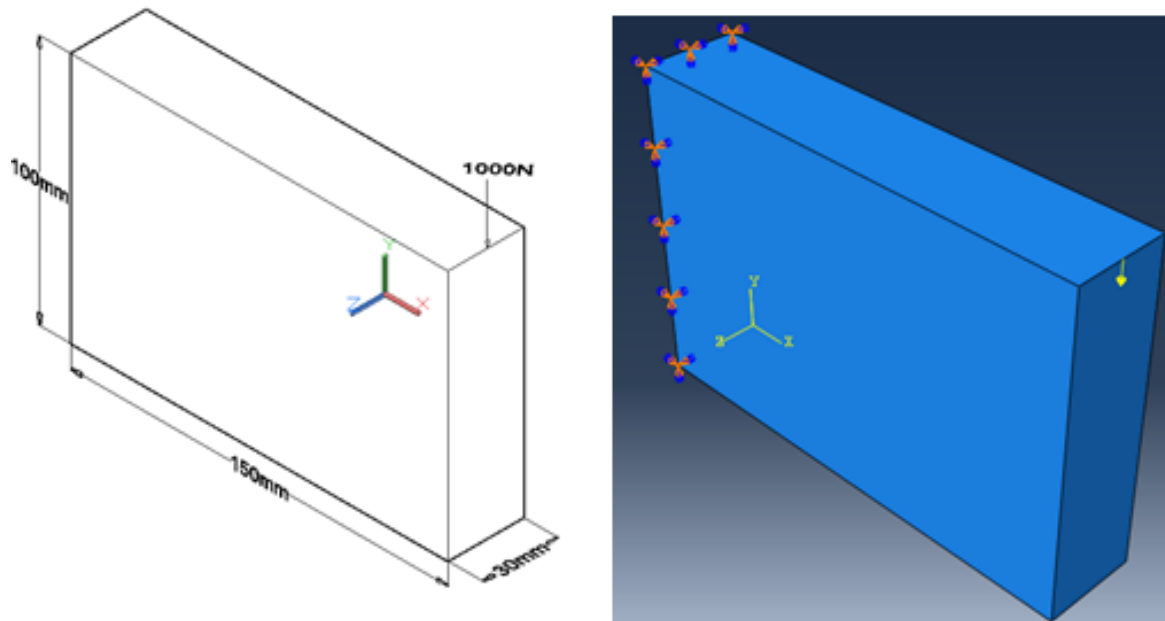


Figure 4.1: Dimensions and Boundary conditions of Cantilever beam)

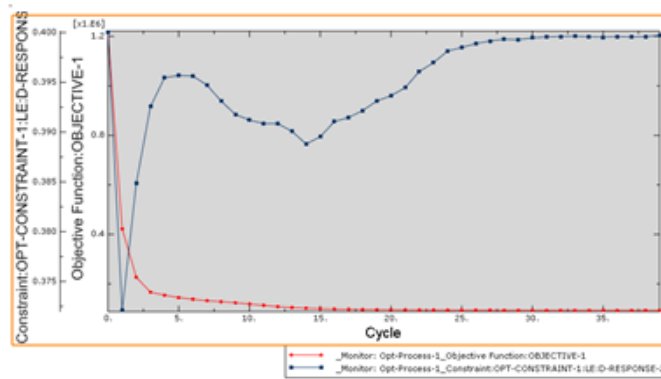


Figure 4.2: Optimization history of Cantilever beam in Static case

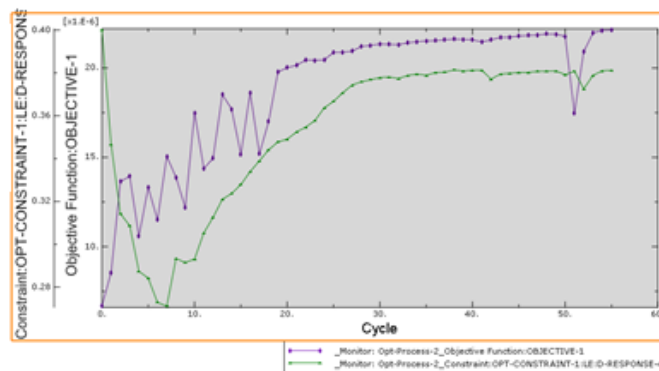


Figure 4.3: Optimization history of Cantilever beam in Dynamic case

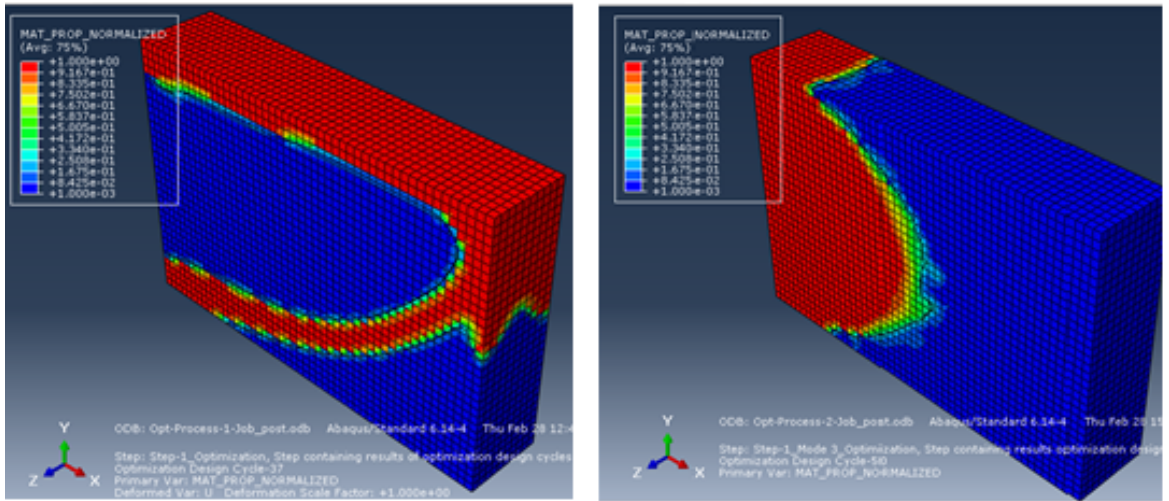


Figure 4.4: Optimum material layout in Static case and Dynamic case

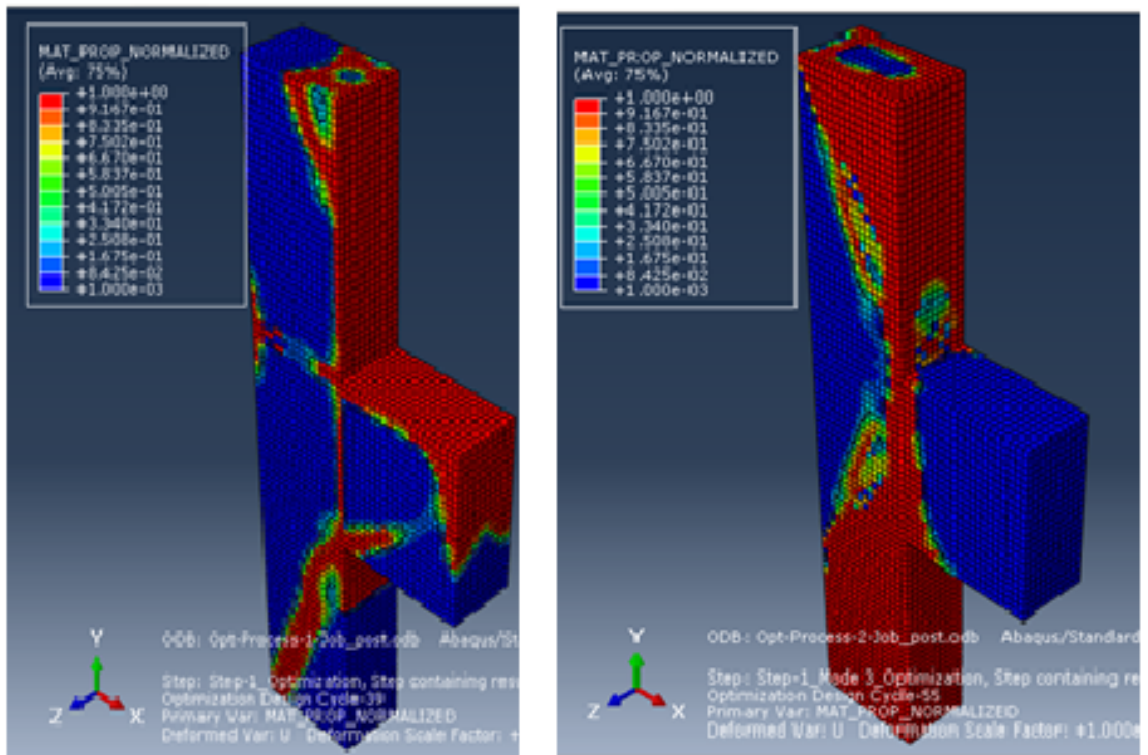


Figure 4.5: Optimum material layout for Corbel

4.1.2 Comparison of different algorithms in static and dynamic problems

For static problems, simply supported beam with central loading and a cantilever beam with end loading has been selected to implement the BESO code and the results are validated with Optimality Criteria method and Method of Moving Asymptotes (MMA by Swanberg,

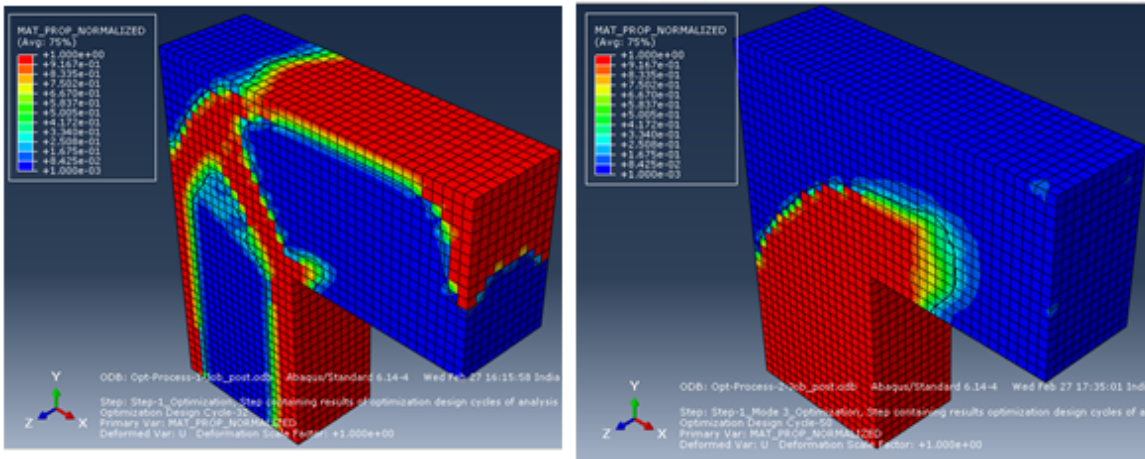


Figure 4.6: Optimum material layout for L-beam

1987). 32MPa Concrete with Poisson ratio of 0.15 and Mass density of 2400kg/m³ has been taken for the entire simulation. For dynamic problems, two support conditions have been chosen. Results of both 2D, as well as 3D structures, have been presented. For the whole problem, a volume fraction of 0.5 with an Evolutionary ratio, of 0.02 has been chosen. A filter radius of 3 (3*Lx/No.of.elements in the x-direction) has been taken to simulate static problems where Lx is the length of the structural element.

Compliance minimization for a 2D-Cantilever beam

A Cantilever beam with dimensions 60 x 20mm with a plane stress condition. A load of 10kN is applied at the free end of the cantilever. A simply supported beam with a central loading of 10kN. The objective function got converged at 43rd iteration with a value of 23.87Nmm in BESO algorithm. Using the Optimality criteria and MMA method, the objective function required more number of iterations and converged at a value of 28.5Nmm and 30.9Nmm respectively. Optimum material layout in the three algorithms is shown in Figure 4.7. The iteration history of Objective and volume fraction in BESO, OC and MMA has shown in Figure 4.8.

Compliance minimization for a 2D-Simply supported beam

For simply supported beam with a central loading of 10kN, objective function got converged at a value of 1.66 Nmm in 42 iterations. The iteration history of BESO method is shown in Figure 8. The converged value of the objective function is 1.86Nmm and 1.96Nmm in OC and MMA methods, respectively. Corresponding iteration history is shown in Figure 9. The optimum topology in the three algorithms is compared in Figure 10. A variation of 11% has shown by the converged value of BESO algorithm than that of OC method. Opti-

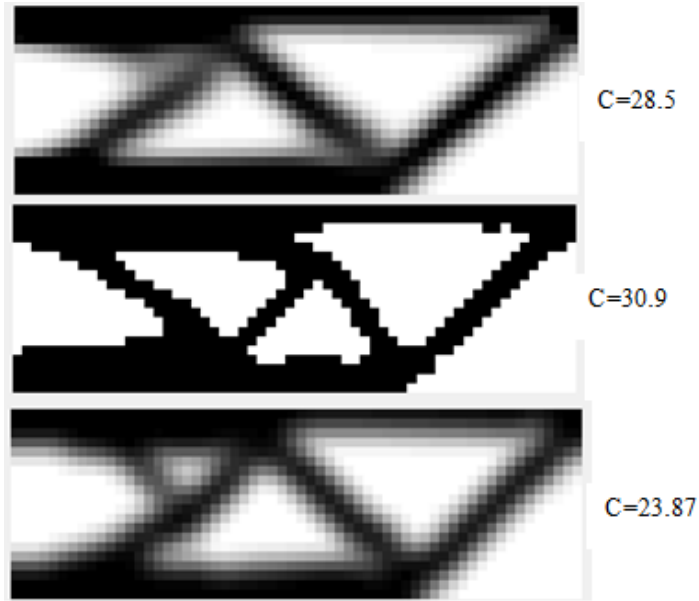


Figure 4.7: Optimum material layout for Cantilever beam

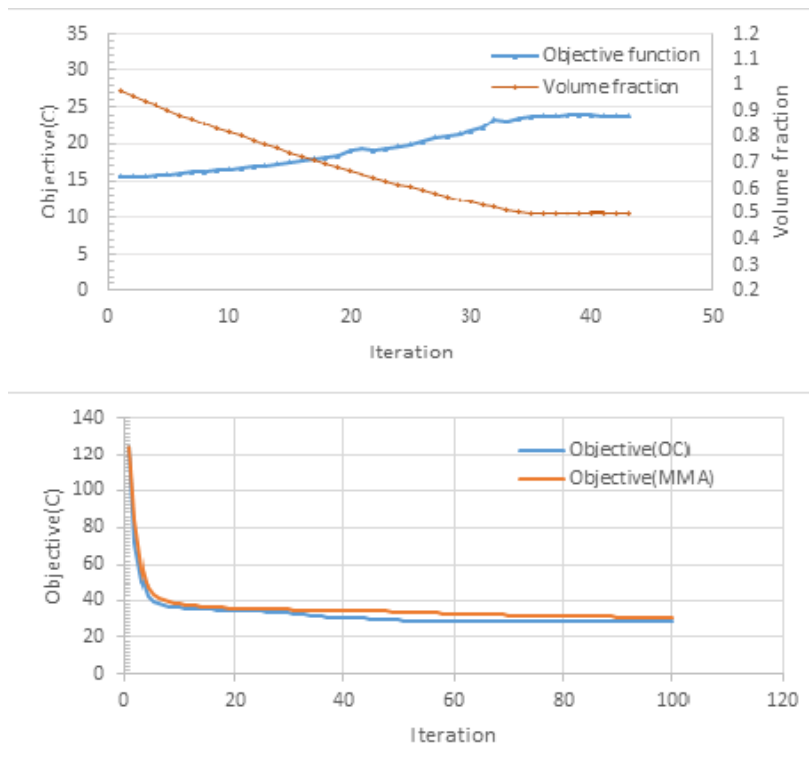


Figure 4.8: Convergence history of Cantilever beam

imum material layout in the three algorithms is shown in Figure 4.9. The iteration history of Objective and volume fraction in BESO, OC and MMA has shown in Figure 4.10.

Eigenfrequency maximization

Fixed beam with dimensions 8m x 1m with plane stress condition is equally divided into 160 x 20 4-noded bilinear plane stress elements in the example problems. A filter radius



Figure 4.9: Optimum material layout of SSB

of 0.15m (3 x 8/160) has been taken for simulation. A concrete grade of M35 with a mass density of 2400kg/m³ is adopted for simulation. The first mode Eigenfrequency for fixed beam using Equation 4.1 is 354.203rad/s and 324.621rad/s in ABAQUS. Optimum design is converged at a first mode Eigen frequency of 566.8rad/sec from 456.5rad/s. Figure 4.11 represents the optimum topology of the fixed beam in BESO algorithm which can be compared with OC and MMA method.

$$\omega = 2\pi C \sqrt{\frac{EI}{mL^3}} \quad (4.1)$$

ω is the eigenfrequency in rad/s, C (1.57 for simply supported and 3.56 for fixed beam) is the constant depending on the boundary conditions, m is the mass in kg, L is the length of the beam in m, E is in N/m² and moment of Inertia I is in m⁴.

4.2 Application of TO in different engineering problems

Various engineering problems with different objectives and constraints are presented.

4.2.1 Concrete dapped beams with multiple constraints

In all compliance minimization problems, a volume fraction of 30% is chosen as the volume constraint. The simply supported concrete dapped beam is subjected to a central load of 60KN.

Problem 1

The optimization process includes a displacement constraint of not exceeding 1mm at the center of the bottom surface, covering all nodes. The figure displaying the optimization

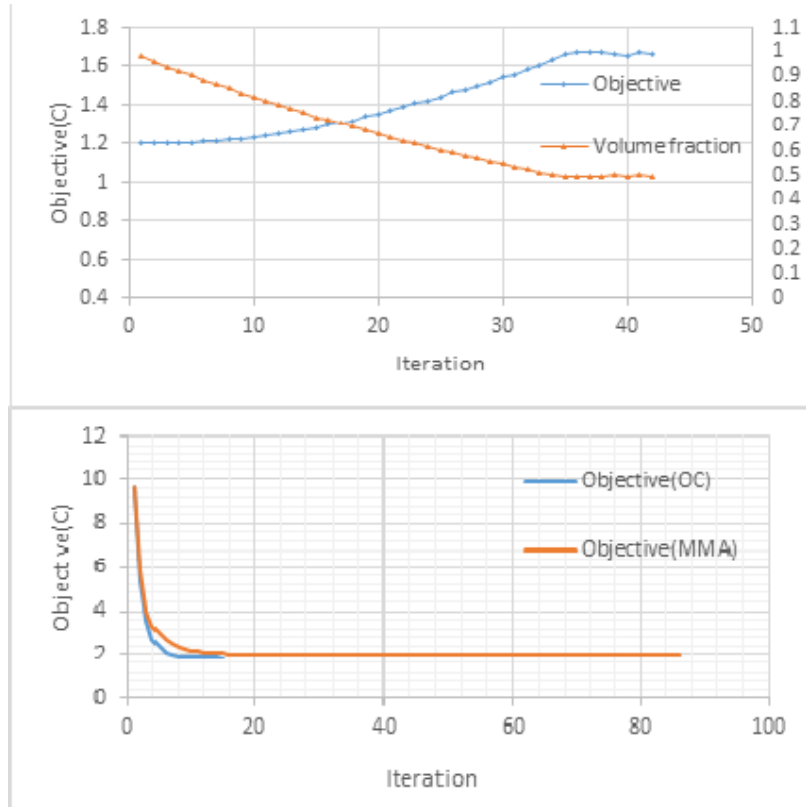


Figure 4.10: Convergence history of SSB

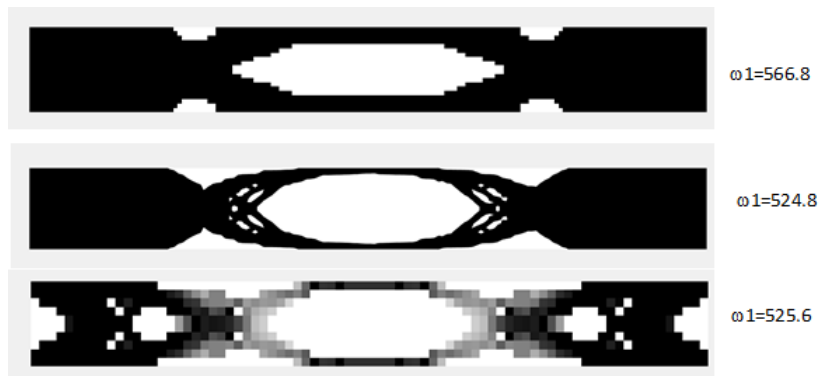


Figure 4.11: Optimum material layout of fixed beam

history of the objective and constraints is referred to as Figure 4.12. The optimization has converged, starting with an initial strain energy of $369000Nmm$ and reaching a final strain energy of $29632.3574Nmm$ at iteration 40. During this process, a volume fraction of 30% is maintained, and the displacement at the center of the beam has been successfully reduced to a final converged value of 0.77mm. The optimized layout of the beam is illustrated in Figure 4.13.

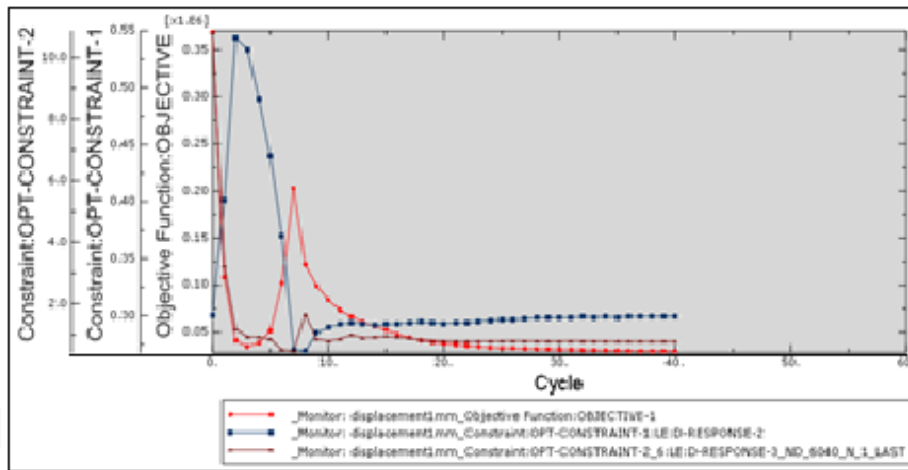


Figure 4.12: Optimization history with displacement as Constraint-2

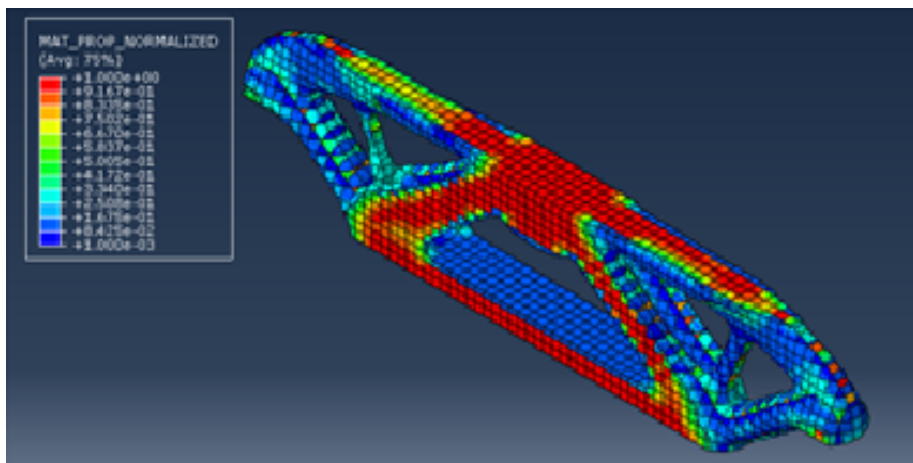


Figure 4.13: Optimum material layout)

Problem 2

The optimization process includes a constraint that ensures the eigen frequency of the first mode is greater than or equal to 10 rad/time. The initial strain energy, starting at 1.58e5, converges to 1.48e5 at iteration 34, while maintaining a volume fraction of 29.9%. The optimization successfully achieves the eigenfrequency constraint with a final value of 11.2249 rad/sec. Figure 4.14 displays the optimization history, showing the progress of the objective and constraints throughout the iterations. On the other hand, Figure 4.15 represents the optimized material layout resulting from the optimization process.

Problem 3

The optimization process incorporates a stress criterion, where the von Mises stress should not exceed the material strength of concrete, set at $35N/mm^2$. At iteration 48, the strain energy has decreased from 368500Nmm to 29074.5Nmm, while the von Mises stress

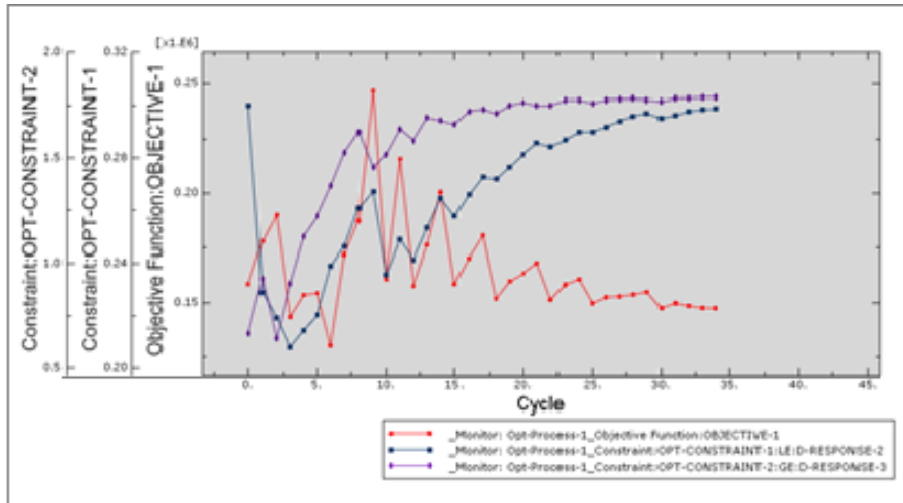


Figure 4.14: Optimization history with Eigen frequency as Constraint-2

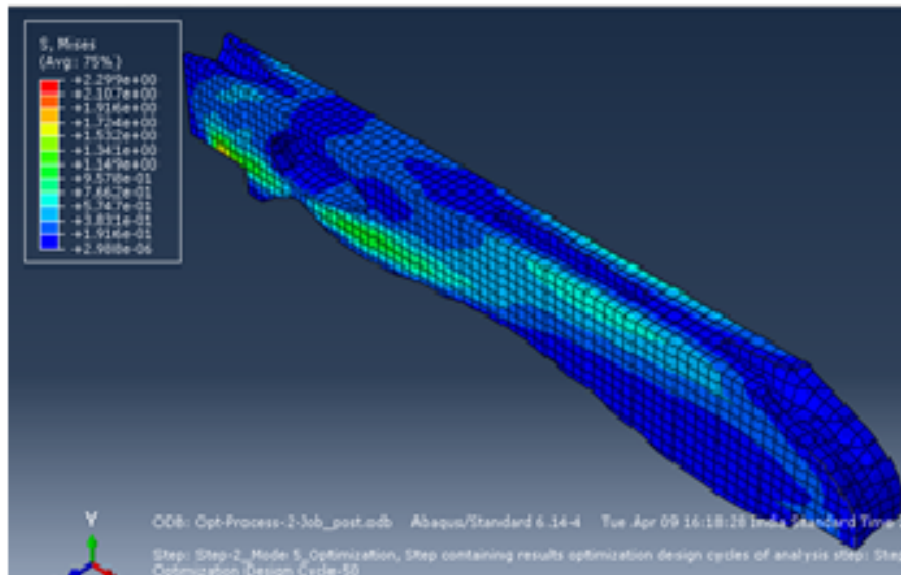


Figure 4.15: Optimum material layout

remains within the limit at $4.256N/mm^2$. The optimization history, depicting the changes in the objective and constraints during the iterations, is presented in Figure 4.16. Furthermore, Figure 4.17 illustrates the final material layout achieved through the optimization process.

Problem 4

Some convergence issues had occurred while selecting volume as an objective function with material strength as constraint. However a reasonable optimum material layout at iteration 56 with a von Mises stress of $30 N/mm^2$ is shown in Figure 4.18.

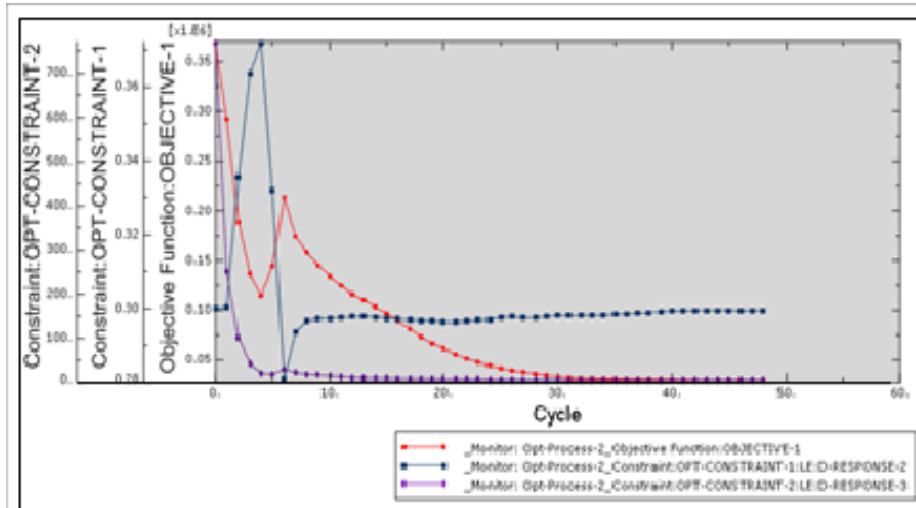


Figure 4.16: Optimization history with Stress as Constraint-2

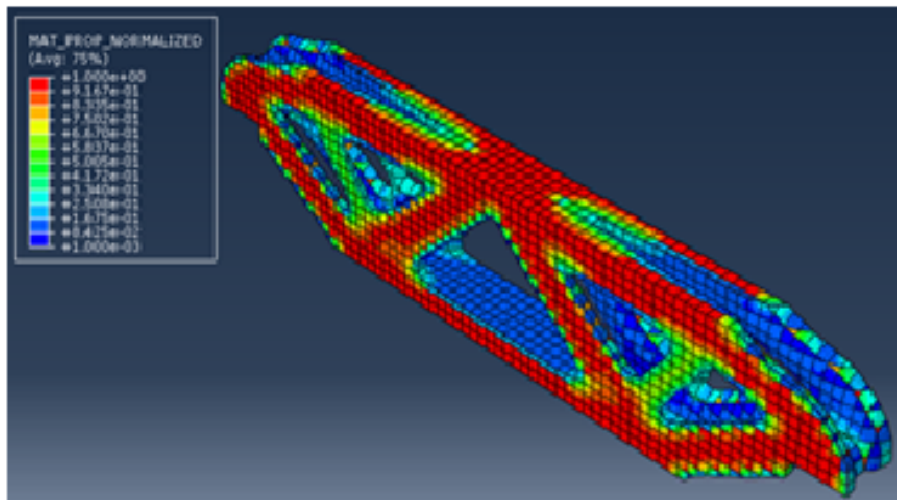


Figure 4.17: Optimum material layout

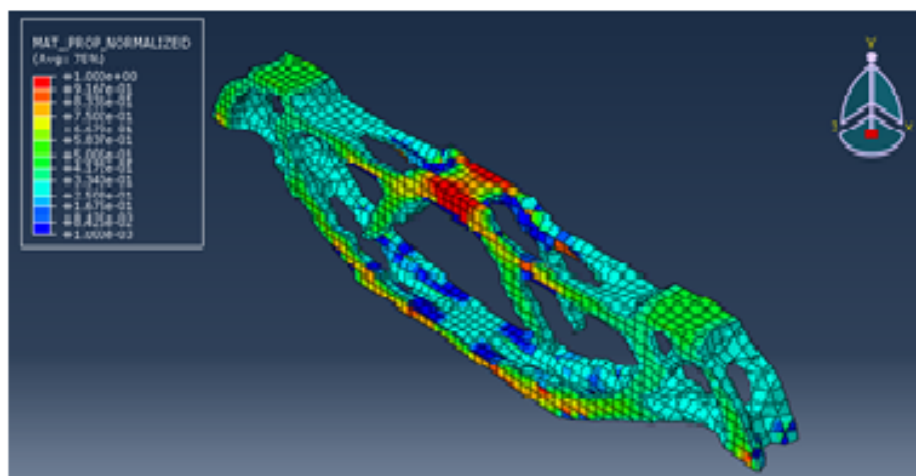


Figure 4.18: Optimum material layout

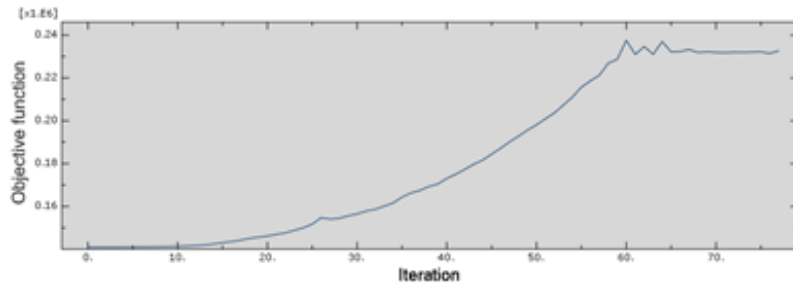


Figure 4.19: Objective history of Load case 1 in BESO

4.2.2 Dapped beams with different loads

This section focuses on the optimization of 3D Concrete dapped end beams (DEBs) using the BESO (Bi-directional Evolutionary Structural Optimization) method within the ABAQUS finite element software environment. The 3D concrete DEBs are modeled in ABAQUS, and loads, boundary conditions, and finite element discretization are applied. The optimization process involves sensitivity analysis, filtering, and updating of element status based on optimality criteria, all achieved using the ABAQUS Scripting Interface. Throughout the simulation, a mesh size of 40mm is utilized, and an evolutionary ratio of 2% is adopted. The filter radius is set at 120mm, and a fixed volume fraction of 30% is maintained in all load cases.

Load case 1

To analyze the behavior under unsymmetrical loading conditions, a load of 60kN has been applied 650mm from the left end of the structure. The iteration history of the objective function in both BESO and ABAQUS is presented in Figure 4.19 and Figure 4.20, respectively. The final topology obtained using the optimality criteria in BESO is shown in Figure 4.21.

In the BESO optimization, the final topology converges at iteration 77, resulting in a strain energy of 232632.85Nmm. On the other hand, in ABAQUS, the convergence is achieved in fewer iterations, with a strain energy of 213000Nmm.

Load case 2

Under a load of 300kN/mm applied throughout the supported span, the iteration history of the objective function is provided for both BESO and ABAQUS in Figure 4.22 and Figure 4.23 respectively. The final topology obtained through the BESO optimization, based on the specified optimality criteria, is shown in Figure 4.24.

In the BESO optimization, the final topology converges at iteration 53, resulting in a strain

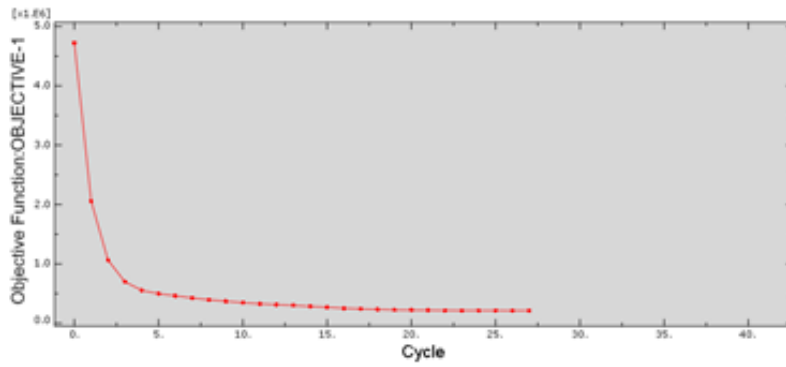


Figure 4.20: Objective history of Load case 1 in ABAQUS

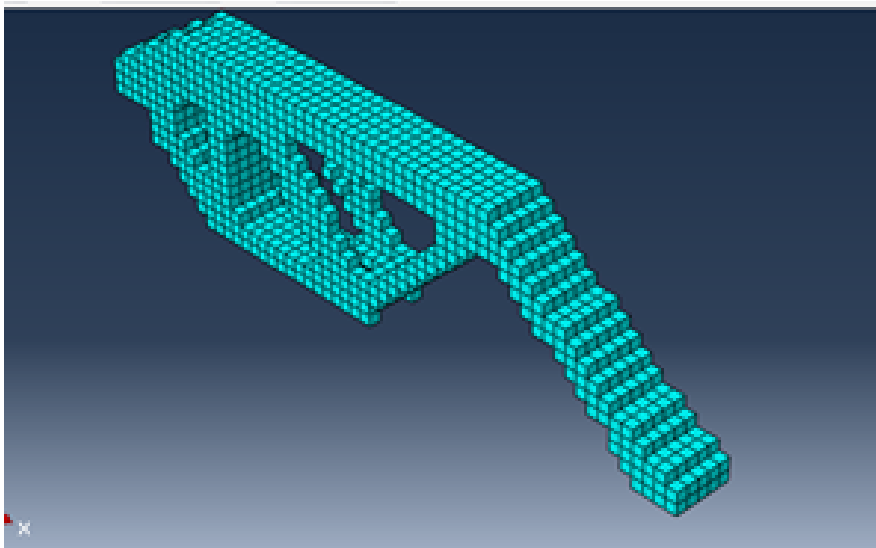


Figure 4.21: Optimum material layout in Load case 1

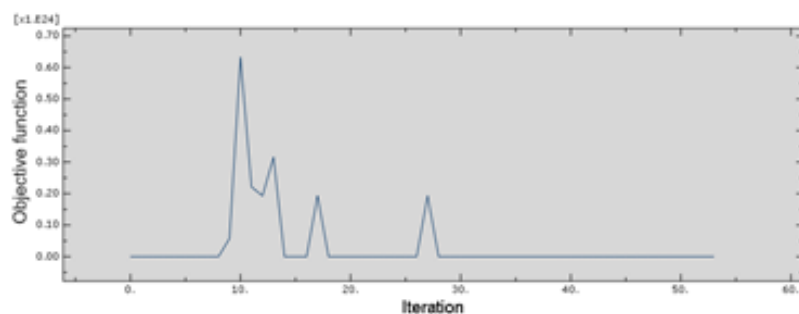


Figure 4.22: Objective history of Load case 2 in BESO

energy of $1.89e^{14}Nmm$. On the other hand, ABAQUS achieves convergence in 22 iterations, with a strain energy of $1.78e^{14}Nmm$. The discrepancies in the convergence behavior and the final strain energy values between BESO and ABAQUS can be attributed to the inherent differences in their optimization algorithms.

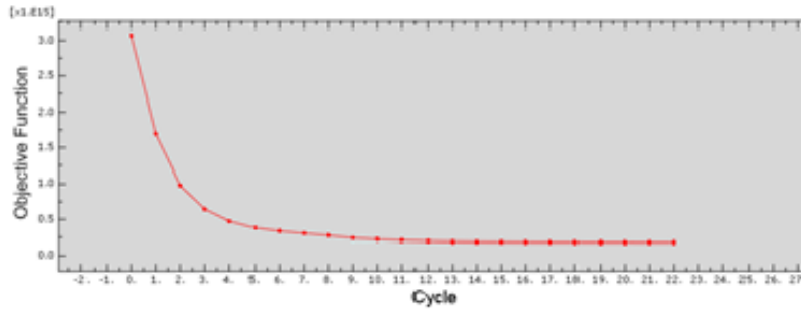


Figure 4.23: Objective history of Load case 2 in ABAQUS

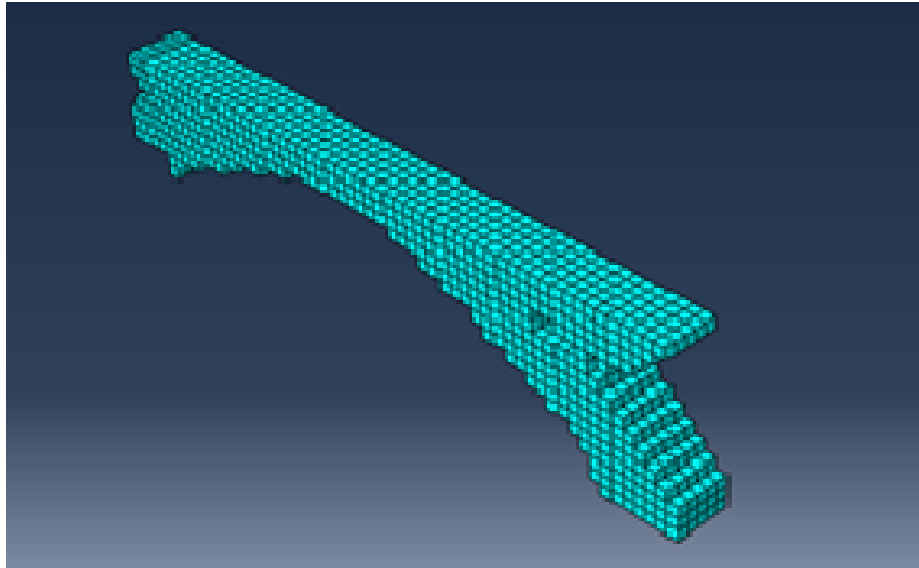


Figure 4.24: Optimum material layout in Load case 2

Load case 3

Under a load of 30kN/mm applied at the mid-third of the effective span, the iteration history of the objective function is shown for both BESO and ABAQUS in Figure 4.25 and Figure 4.26 respectively. The final topology obtained through the BESO optimization, based on the specified optimality criteria, is displayed in Figure 4.27. In the BESO optimization, the final topology converges at iteration 69, resulting in a strain energy of 4.88e15Nmm. On the other hand, ABAQUS achieves convergence in 31 iterations, with a strain energy of 3.97e15Nmm.

Load case 4

To simulate the effects of lateral loads such as wind and earthquake, a lateral load of 25kN has been applied at both ends of the beams. The iteration history of the objective function is provided for both BESO and ABAQUS in Figure 4.28 and Figure 4.29 respectively. The final topology obtained through the BESO optimization, based on the specified optimality

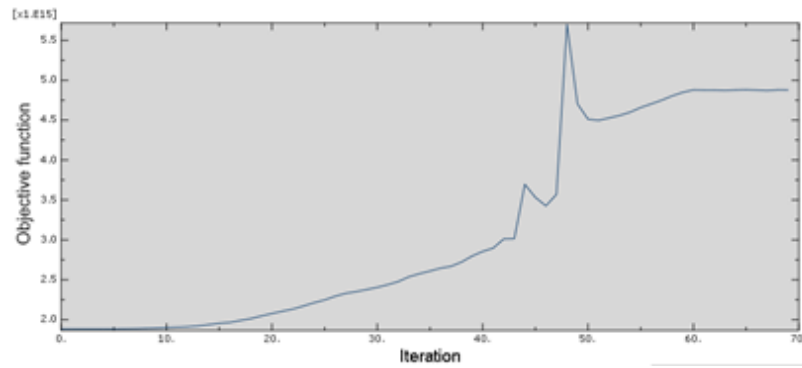


Figure 4.25: Objective history of Load case 3 in BESO

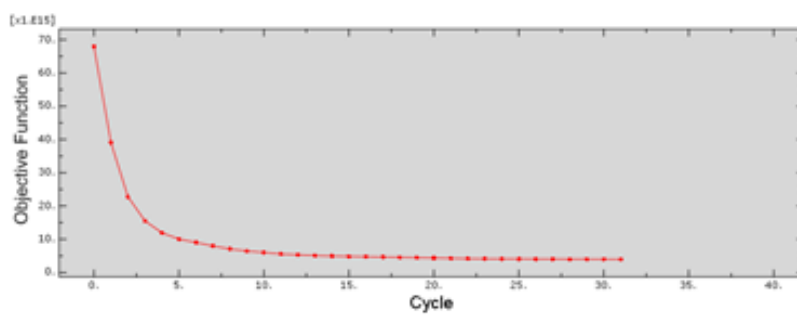


Figure 4.26: Objective history of Load case 3 in ABAQUS

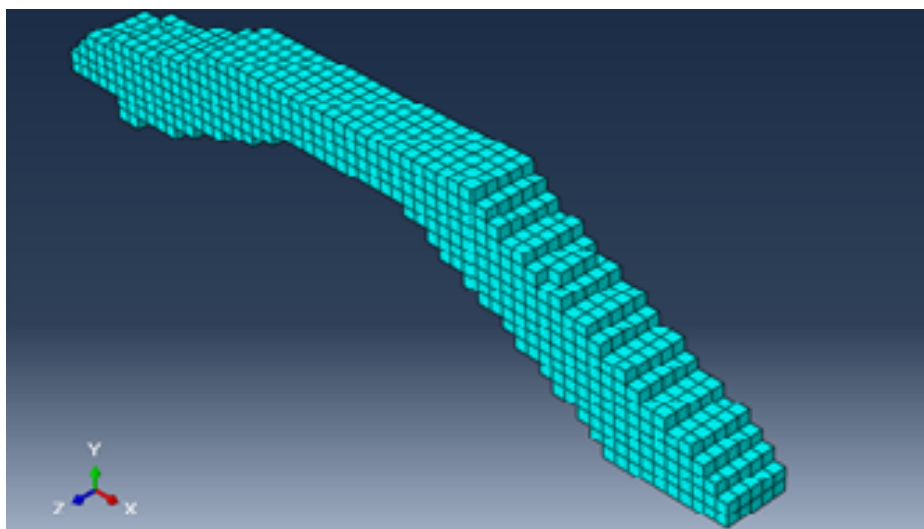


Figure 4.27: Converged layout in Load case 3

criteria, is shown in Figure 4.30. In the BESO optimization, the final topology converges at iteration 96, resulting in a strain energy of 241711.31Nmm. On the other hand, ABAQUS achieves convergence in 29 iterations, with a strain energy of 167000Nmm.

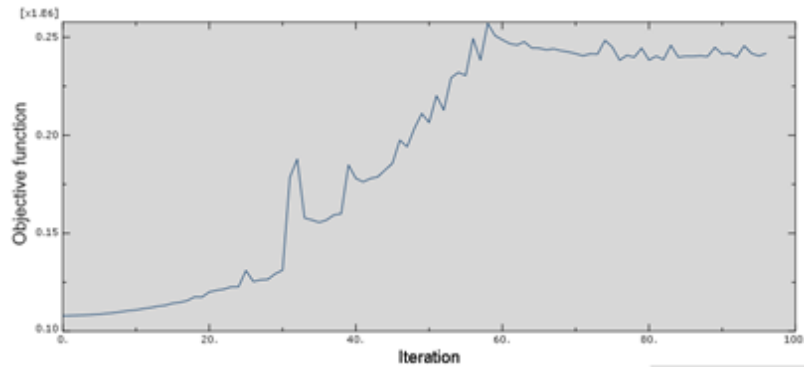


Figure 4.28: Objective history of Load case 4 in BESO

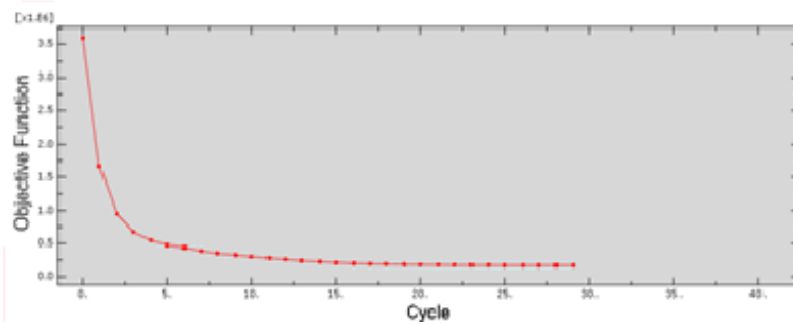


Figure 4.29: Objective history of Load case 4 in ABAQUS

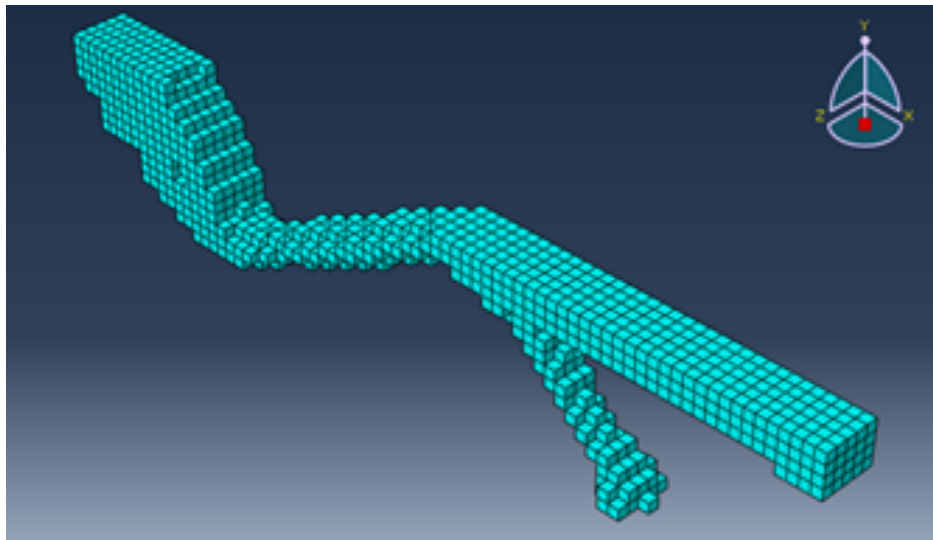


Figure 4.30: Converged layout in Load case 4

4.2.3 Topology Optimization with Concrete Damaged Plasticity model

ABAQUS finite element software is used to simulate the optimization problem using CDP model. Compliance minimization problem with a volume constraint of 30% is selected. A simply supported beam of 4m x 1m with a central load of 100kN is modeled in ABAQUS. The data for compressive behaviour in ABAQUS is calculated using the Hognes-

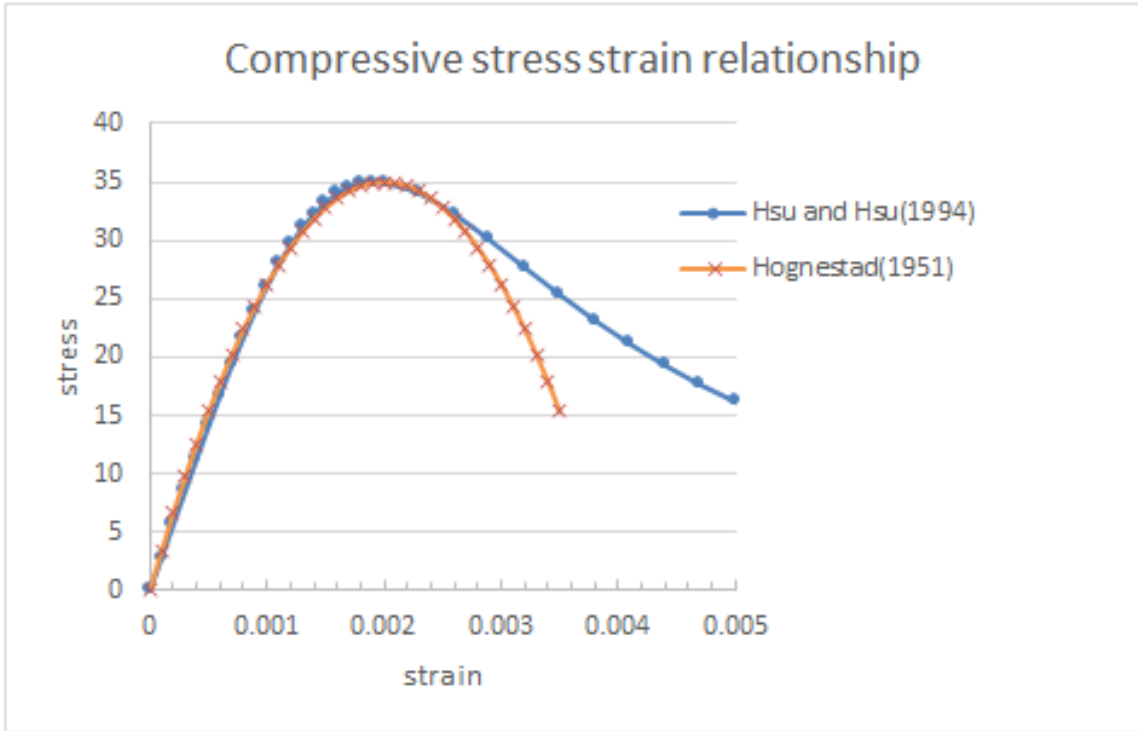


Figure 4.31: Stress-Strain behaviour in Compression

tad(1951)model and Hsu and Hsu(1994)model. Stress-strain curve of compressive behaviour using Hognestad model and Hsu model is shown in Figure 4.31. Tensile behaviour is modeled by Aslani and Jowkarmeimandi(2012) is shown in Figure 4.32. The input parameters of plasticity are : $\zeta=35$, $\varepsilon=0.1$, $K = \frac{2}{3}$, $\mu = 0$ and $\frac{\sigma_{ho}}{\sigma_{co}} = 1.16$

The history of convergence of objective function for both linear and CDP model doesn't show much difference. The information presented in the graph depicted in "Figure 4.33" is clear and apparent. From the final material layout after simulation shown in Figure 4.34, it is clear that the material distribution pattern is similar. Maximum von Mises stress in both models are $1.59e^6 N/m^2$ and the difference is there in the distribution of stress in the final layout. The intuition of this simulation is to verify whether non-linear material properties are compatible with topology optimization. Hognestad model and Hsu model can be consolidated as CDP model. Final converged value of objective in Hognestad model is 24.14Nm while that in linear model is 24.05Nm.

4.2.4 Higher order Elements

A Concrete grade of M35 has been selected for the study. Simply supported beam of 120mmx40mm with a central load 1000N is taken for example. The example problem taken for comparison, is modeled with 3 different finite elements and optimized using 3 element

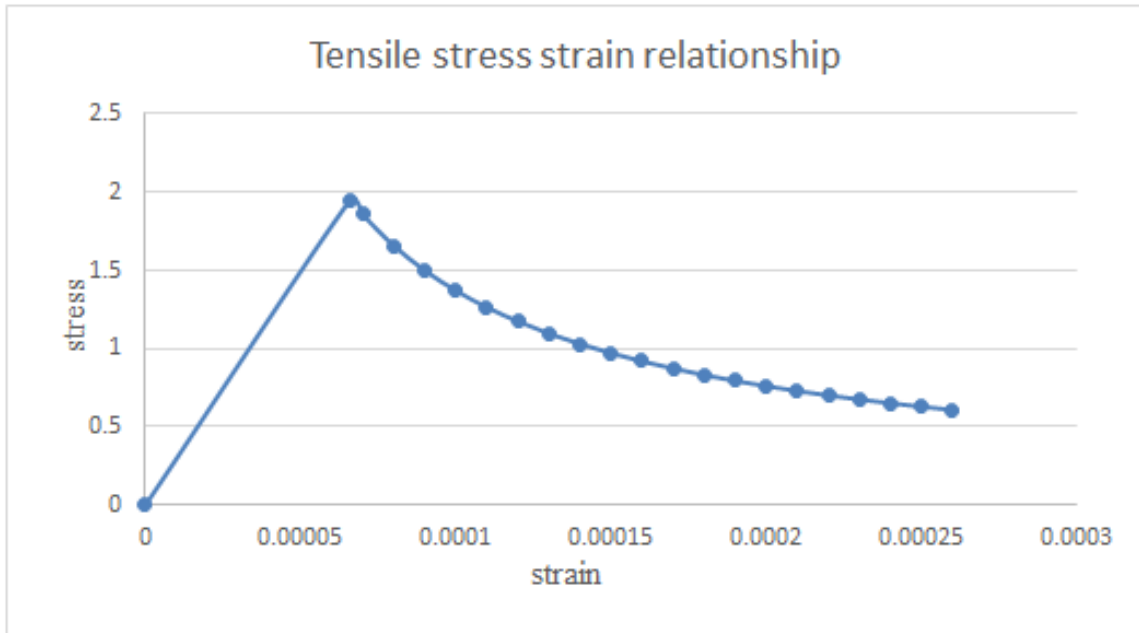


Figure 4.32: Stress-Strain behaviour in Tension

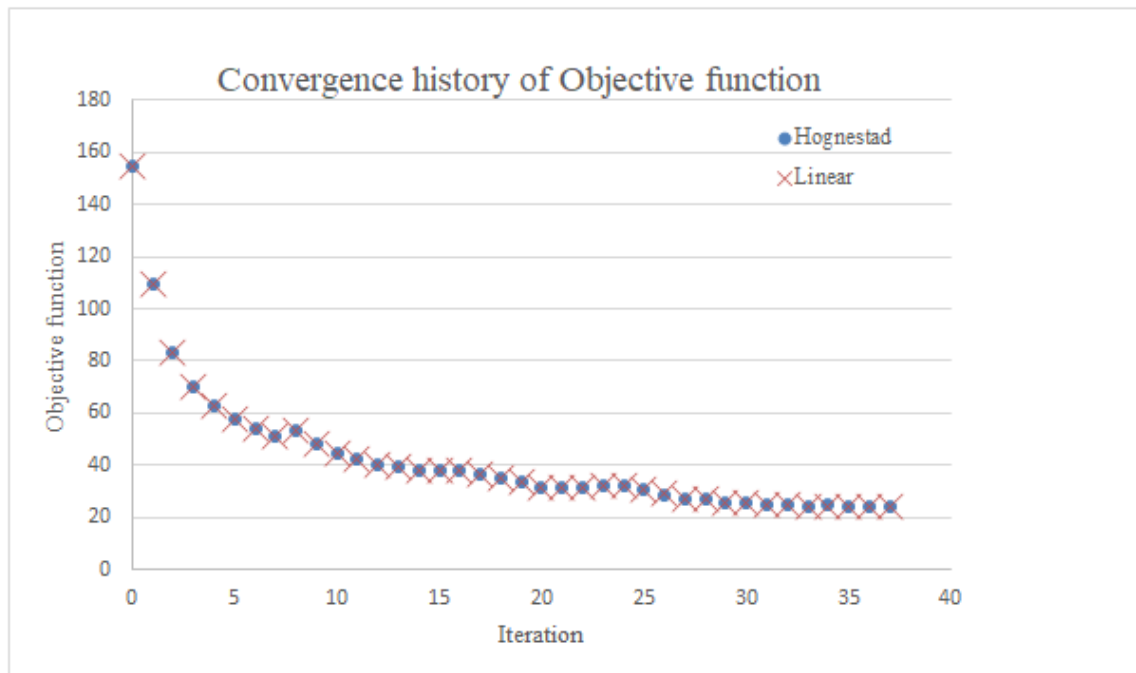


Figure 4.33: Convergence history of CDP model and linear model in ABAQUS

updating algorithm. Optimality criteria method, BESO method and MMA algorithm are used for element updation. BESO algorithm with 4-noded elements shows the fastest convergence with least time. MMA algorithm with 9-noded elements take the maximum computation time. Higher-order elements take more iterations to converge. The converged value of objective function lies in between 19Nmm to 23Nmm. The convergence history of dif-

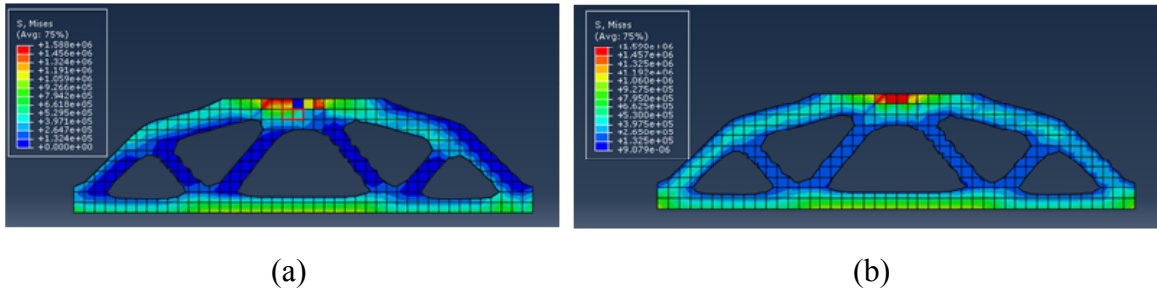


Figure 4.34: Final layout in ABAQUS (a)CDP model (b)Linear model

ferent finite elements using BESO algorithm is shown in Figure 4.35. The optimum layout of structure in OC and MMA is almost similar in all order finite elements. The fastest converged BESO algorithm shows a slight difference in optimum topology for higher-order elements. Optimum topology using BESO method is similar for 8 and 9-noded elements. BESO algorithm requires 14 to 18 times more computation time in 8 and 9-Noded elements than that in 4-noded elements. Optimum topology of simply supported beam in BESO for 4-noded element and higher order elements is shown in Figure 4.36. The final layout of beam using 3 kinds of finite elements in OC and MMA is represented by one figure because it is similar for 4-noded as well as higher-order elements. Convergence history and optimum layout of higher order elements in OC and MMA are represented in Figure 4.37 and Figure 4.38 respectively. OC method requires 9 to 13 times more computation time in 8 and 9-Noded elements than that in 4-noded elements. Element updation using MMA method requires 8 to 12 times more computation time when higher order elements are used.

Higher order elements extracts the layout with less checkerboard pattern in the absence of filter. It can be visible from the results shown in Table 4.1. A 2-D cantilever beam of size 120mm x 40mm with plane stress thickness of 40mm has taken. A concentrated load of 1000N has applied at the free end. Simulation took more time for convergence in the optimization without filtering. However in the example taken, the solution with 8-noded element shows better result with least checkerboard pattern. Anyway 9-noded element derives better solution than 4-noded element when the simulation lacks filtering technique. Converged values of Objective function with and without filter are listed in the table.

4.2.5 Displacement constrained optimization

The beam shown in Figure 4.39 is taken to simulate the optimization problem with displacement constraint. Concrete beam of grade M35 with a poisson's ratio of 0.2 and mass

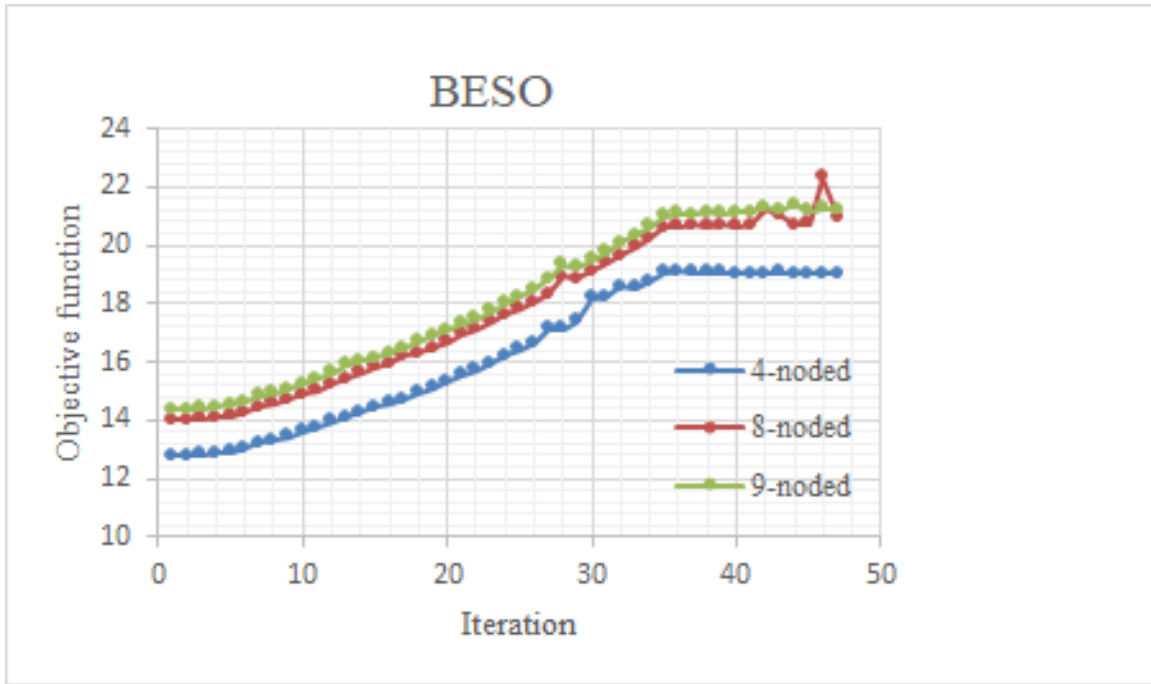


Figure 4.35: Convergence history of BESO method in higher order elements



Figure 4.36: Optimum Topology of BESO method (a)4-noded element (b)Higher order elements

density of $2400kg/m^3$ is taken. Right end of beam is roller supported and is denoted by point B where local displacement constraint is applied. The design domain is discretized using 100×50 quadrilateral plane stress elements. A simply supported beam with a central vertical load of $100N$ is optimized to maximize stiffness with a volume constraint of 45% and a displacement constraint of $0.02mm$. Penalty factor (p) = 3, Evolutionary ratio (ER) = 2% and a filter radius (r_{min}) = $3mm$ are selected for the study.

The horizontal displacement value at the right roller support is restricted to $0.02mm$. The convergence history of Objective function with and without displacement constraint is shown in Figure 4.40. Convergence history with and without extra constraint shows large variation in between. Displacement constrained problem converged with a value of compliance $5.89Nmm$ which shows a 25% variation from the problem without displacement constraint. The effect of Lagrange multiplier varies with the value of displacement at point B.

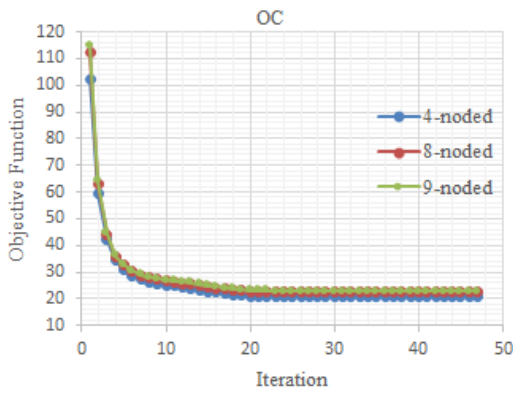


Figure 4.37: Convergence history and Optimum topology of OC method

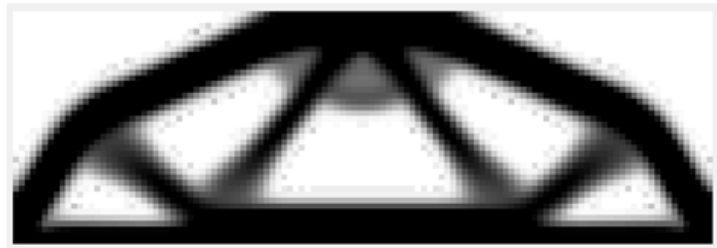
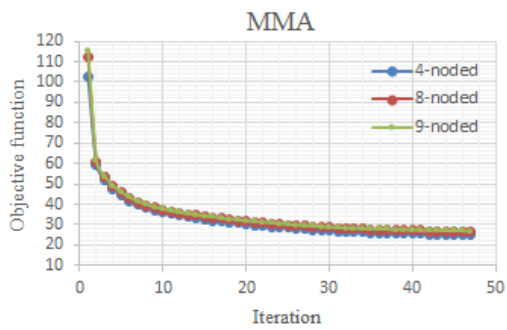


Figure 4.38: Convergence history and Optimum topology of MMA method

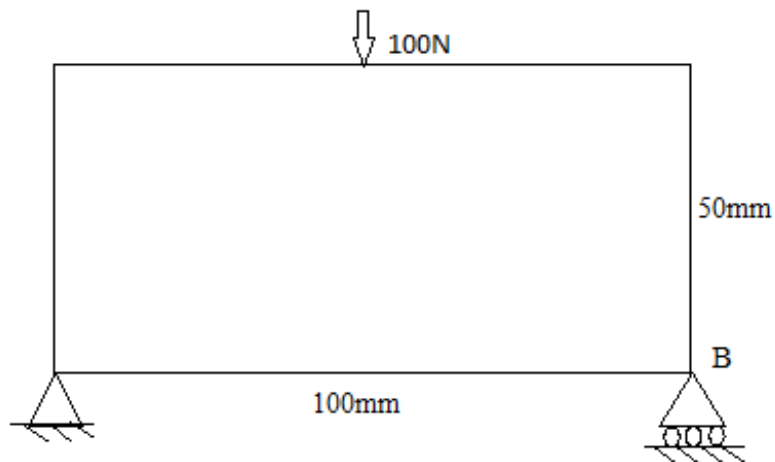








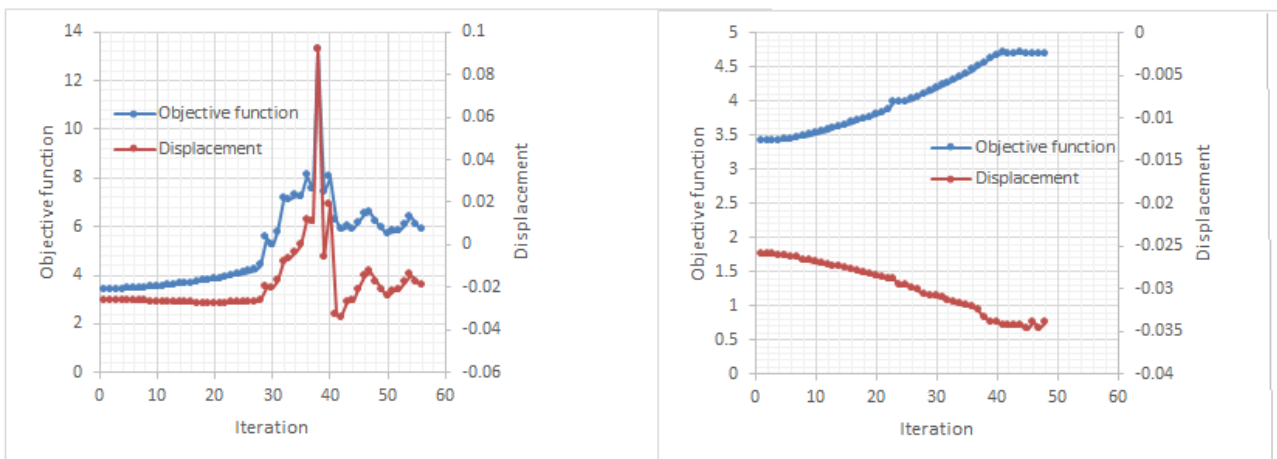
Figure 4.39: Example for displacement constrained problem

4.3 Stress Constrained Optimization

Two examples have been chosen to compare the Von Mises stress with the optimization algorithm. The first example involves a cantilever beam, while the second one is a simply supported beam, both using concrete grade M35 and a Poisson's ratio of 0.2. Two optimization problems are considered: one is a minimum compliance problem with volume constraint, and the other is a minimum compliance problem with stress constraint. For both

Table 4.1: Comparison of Higher Order Elements without filter

Element	solution with Filter	solution without Filter
4-node	 C=151.99	 C= 155.58
8-node	 C=154.81	 C=158.02
9-node	 C=155.54	 C=163.93



(a)

(b)

Figure 4.40: Convergence history of optimization (a) with displacement constraint (b) without displacement constraint

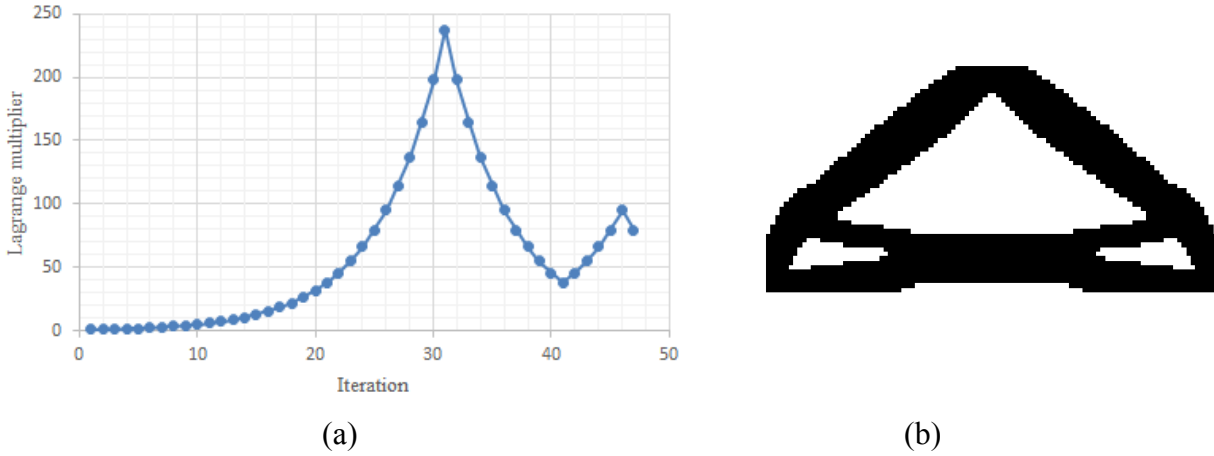


Figure 4.41: (a) Variation of lambda (b) Optimum layout in displacement constrained problem

examples, a mesh of 120 x 40 plane stress elements with a 3mm filter radius is used. To evaluate the validity of the optimization solutions, the maximum deflection and Von Mises stress of the cantilever beam and simply supported beam with a point load can be calculated using Equation 4.2 and Equation 4.3, respectively.

$$\delta = \frac{WL^3}{CEI} \quad (4.2)$$

$$\sigma_{vm} = \sqrt{f^2 + 3\tau_{xy}^2} \quad (4.3)$$

where $f = \frac{M}{Z}$ and $\tau_{xy} = \frac{VA_y}{Ib}$

W is the point load, C = 3 for cantilever and 48 for simply supported beam, f is the bending stress, M is the moment, Z is the section modulus, V is the shear force and y is the distance of the neutral axis from the point.

Cantilever beam

Cantilever beam of size 120mm x 40mm x 40mm is subjected to an edge load of 1000N at bottom. Bending stress and shear stress are obtained as 11.25N/mm² and 0.9375N/mm² respectively. Vonmises stress at fixed end and deflection at free end are calculated as 11.288N/mm² and 0.0913mm. The stresses and deflections at different length of the cantilever beam have listed in Table 4.2. Length has been taken from fixed support towards free end. Von Mises stress and deflection show a deviation of 16% and 13% respectively from the actual value. For a minimum compliance optimization, compliance has been converged from 839.017Nmm to 165.685Nmm. Final iteration shows a slight increase in stress and deflection values as the volume has been declined to 50% of initial volume. In the second optimization

Table 4.2: Von Mises stress and Deflection values for cantilever beam

Length from fixed end (mm)	Von Mises stress (N/mm^2)			Deflection (mm)		
	Initial stage	Final stage w/volume constraint	Final stage w/stress constraint	Initial stage	Final stage w/volume constraint	Final stage w/stress constraint
0	13.03	20.53	25.91	0	0	0
20	9.15	10.03	9.01	-0.0052	-0.0114	-0.0172
40	7.36	8.68	9.93	-0.0162	-0.0288	-0.0413
60	5.53	8.43	9.39	-0.0322	-0.0529	-0.0750
80	3.73	7.27	8.79	-0.0521	-0.0875	-0.115
100	2.49	6.29	8.24	-0.0745	-0.1249	-0.1571
120	32.91	32.92	32.94	-0.1049	-0.1657	-0.2046

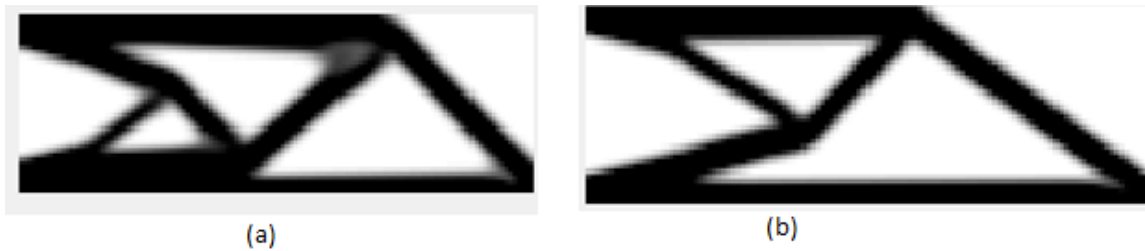


Figure 4.42: Optimum topology of Cantilever beam with volume constraint (a) and stress constraint (b)

problem for Cantilever beam, Von Mises stress is fixed as a constraint. The maximum value of stress at any point is restricted to exceed by a value of 35MPa. The algorithm of stress constrained problem is in accordance with Biyikli and Albert (2015). The optimum topology for minimum compliance problem and stress constrained problem is shown in Figure 4.42. Both of the figures show slight variation in topology. Compliance value has been converged from 839.02Nmm to 204.58Nmm with a volume fraction of 0.40.

Simply supported beam

Simply supported beam of size 120mm x 40mm x 40mm is subjected to a central load of 1000N at top. Von Mises stress and deflection at midpoint are calculated as 2.825N/mm² and 0.0057mm respectively. The values of Initial stage and final stage have been listed in Table 4.3. The values of compliance problem with stress constraint are also included in Figure 9. A value of 20MPa is fixed as stress constraint. In first problem compliance is converged from 69.02Nmm to 11.875Nmm. In the stress constrained problem, final converged value

Table 4.3: Von Mises stress and Deflection values for simply supported beam

Length from fixed end (mm)	Von Mises stress (N/mm^2)			Deflection (mm)		
	Initial stage	Final stage w/volume constraint	Final stage w/stress constraint	Initial stage	Final stage w/volume constraint	Final stage w/stress constraint
0	17.31	20.96	19.99	0	0	0
10	0.69	0.86	0.62	-0.0025	-0.0025	-0.0025
60	15.81	15.98	15.95	-0.0086	-0.0119	-0.0113
110	0.61	0.44	0.21	-0.0025	-0.0025	-0.0025
120	17.31	20.95	19.99	0	0	0

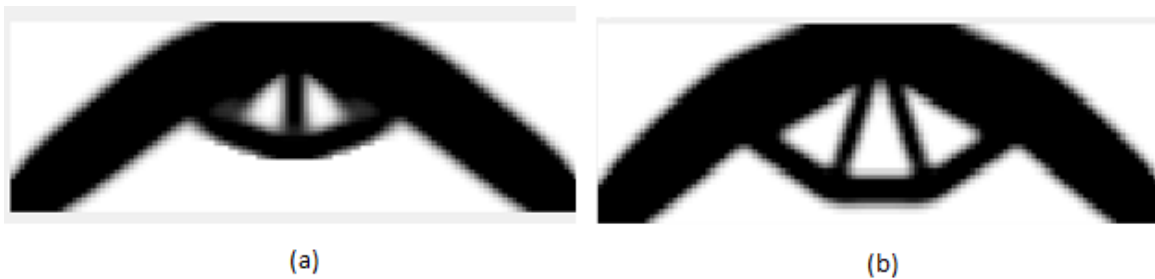


Figure 4.43: Optimum topology of Simply supported beam with (a) volume constraint (b) and stress constraint

is slightly changed to 11.34Nmm. The optimum topology for both kinds of problems are shown in Figure 4.43.

4.3.1 Drucker-prager stress criterion

Concrete grade of M35 has selected. Active number of constraints indicates the highest stressed elements is plotted with iteration. The lowest stressed elements are removed from the active constraints. The number of active constraints are gradually reduced and become almost constant in the later iterations. The variation of stress and the optimum layout are shown in Figure 4.44 and Figure 4.45. This equivalent stress criterion is more appropriate for concrete modeling.

4.3.2 Strut and Tie modeling

The experimental data is extracted from paper [Abdul-Razzaq and Jebur \(2017\)](#), wherein the deep beam is simulated following the guidelines of ACI 318-14. The steps related to strut and tie modeling of deep beam with two point loads are documented to understand the proce-

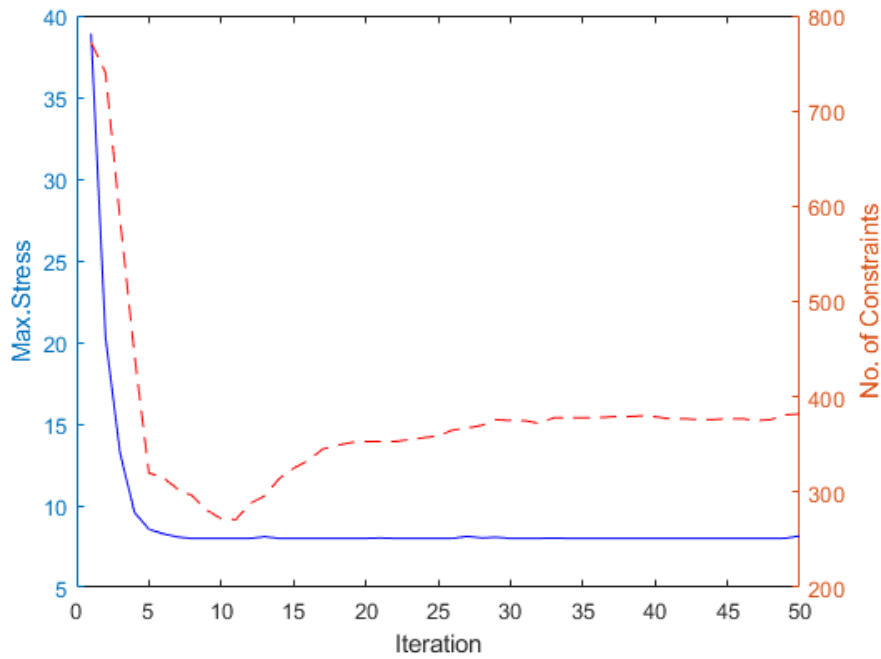


Figure 4.44: Variation of stress and number of constraints

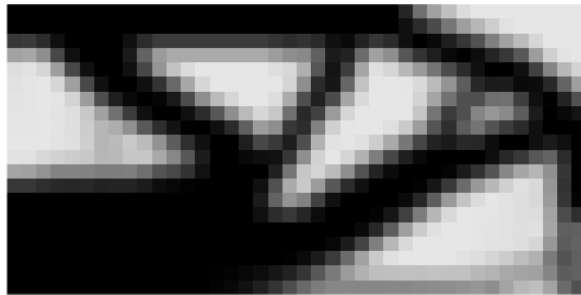


Figure 4.45: MBB using Drucker-Prager yield criteria

ture. It's important to note that topology optimization differs from the STM model. Topology optimization provides an exact arrangement of compression and tension areas. This can be used not only for the efficient reinforcement design but also for creating the Strut and Tie model. Topology optimization has been incorporated into the user-friendly software IDEA StatiCa Detail. Figure 4.46 displays the results of the deep beam analysis obtained from the software. The experimental setup depicted in Figure 4.47 is based on the model described in Abdul-Razzaq and Jebur (2017). The experimental investigation involved constructing and testing a beam measuring 1400mm in length, 400mm in height, and 150mm in width. Three self-compacting concrete (SCC) beams, each subjected to different load types, were specifically designed to fail due to shear forces. The SCC hardened concrete strength was

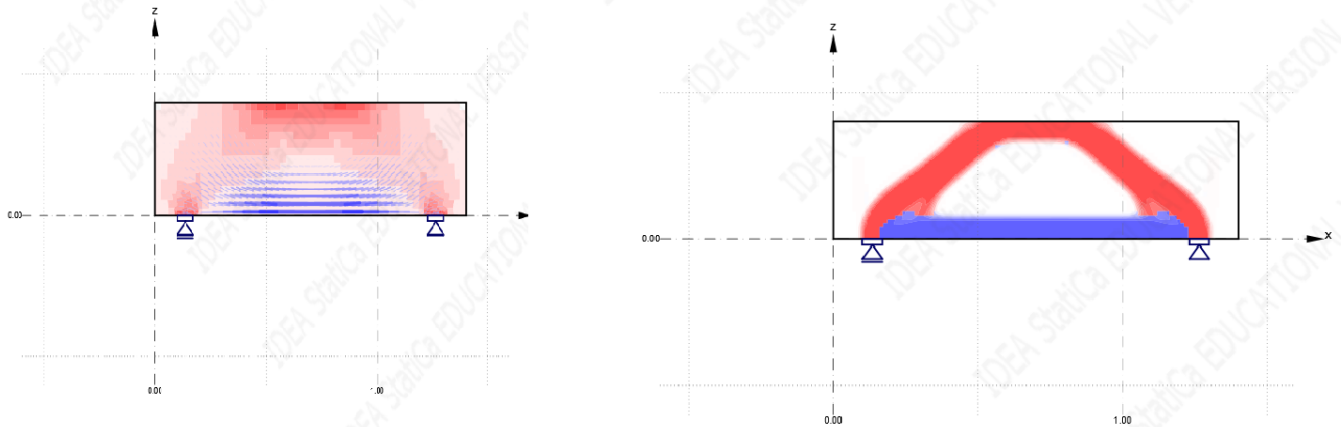


Figure 4.46: Linear Analysis and Topology optimization results from IDEA Statica

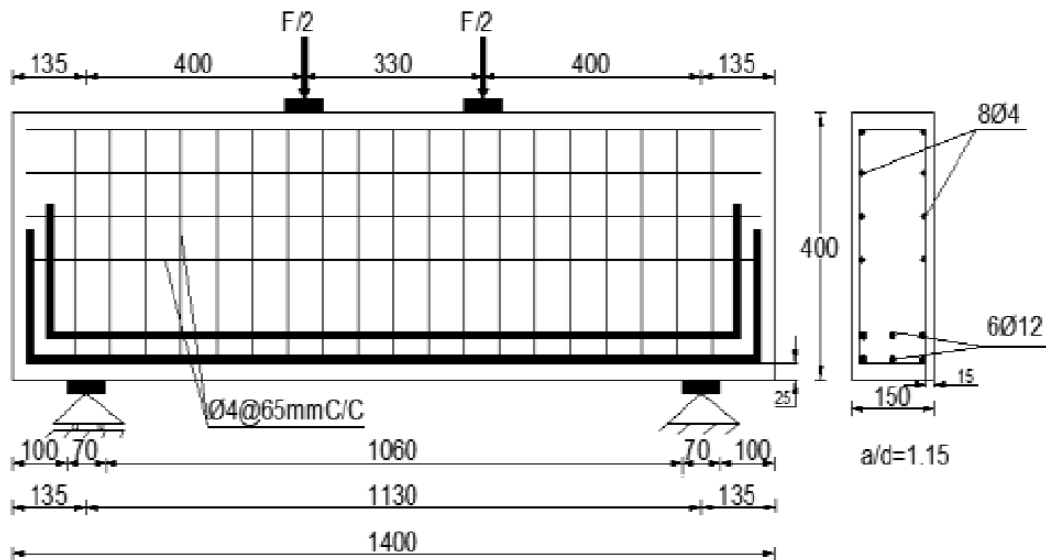


Figure 4.47: Experimental set up from Abdul-Razzaq and Jebur (2017)

evaluated at 35MPa, with a Modulus of Elasticity recorded as 27805MPa.

Steps of Strut and Tie modeling

1. The initial stage in STM modeling involves identifying and isolating D-regions. As depicted in Figure 4.48, the beam is entirely classified as a D region, indicating its suitability for STM. The subsequent step is to recognize the truss model within the beam, as illustrated in Figure 4.48.

2. A static analysis must be conducted to determine the reactions.

$$\text{Self weight of beam} = 2400 \times 150 \times 1400 \times 400 \times 9.81 = 1977.69 \text{ N}$$

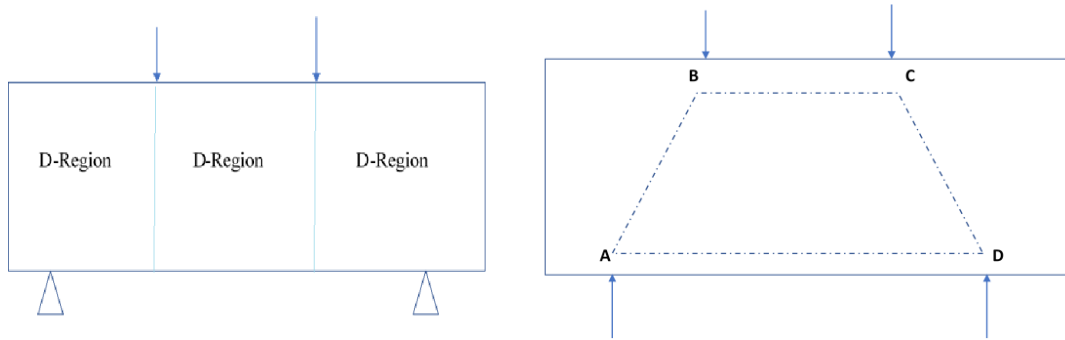


Figure 4.48: Identification of truss within beam

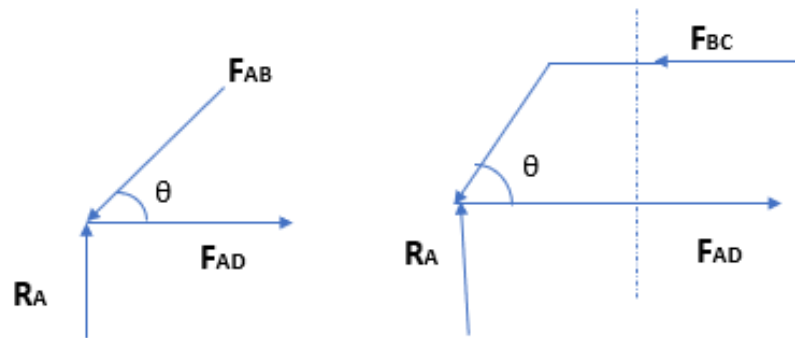


Figure 4.49: Member forces from the Method of joints

The load at failure from the experiment is 562kN.

Factored load, $F_u = 1.2[1.98 + 562] = 676.77kN$

Reactions, $R_A = P_u/2 = 339kN$

3. Third step is the check of deep beam

$$l_n/h = 1135/400 = 2.825 < 4$$

Therefore, It is a deep beam.

4. Determining width of struts and ties and Effective width(d)

The thickness of struts and tie is equal to width of beam ($b=150mm$). Assume the height of truss(z) is $0.8 \cdot h$ and effective depth(d) is $0.9 \cdot h$.

$$z = 0.8 * 400, d = 0.9 * 400, \tan\theta = \frac{z}{d}$$

Forces in each truss member can be calculated by the method of joints.

$$F_{AB} \sin 38.65 = 339$$

$$F_{AB} = 542.78kN$$

$$F_{AD} = F_{AB} \cos 38.65 = 423.898kN$$

$$\text{Bearing stress, } \sigma_b = \frac{F}{A} = \frac{339 * 1000}{70 * 70} = 69.18N/mm^2$$

Width of struts and tie can be determined based on the bearing stress.

$$w_{AB} = \frac{F_{AB}}{69.18 * 150} = 52.34mm$$

$$w_{BC} = w_{AD} = \frac{F_{AD}}{69.18 * 150} = 40.849mm$$

$$z = h - \frac{w_{AD}}{2} - \frac{w_{BC}}{2} = 400 - 40.849 = 359.151mm$$

Once more, begin with point A and repeat all the aforementioned procedures along with necessary iterations until θ stabilizes at a consistent value. Assess each component of the STM for potential failure, ensuring adequacy of nodes and struts while designing ties. As per the 23rd chapter of ACI 318-14, evaluate the safety of assumed nodes and struts. If all nodes and struts are deemed safe, proceed to expand the procedure to design reinforcement based on tie strength. This process involves a trial and error approach to achieve accuracy.

CHAPTER 5

CONCLUSIONS

1. The topology optimization of 3D concrete structures heavily relies on the modeling and analysis capabilities of the ABAQUS finite element software. For static problems, the optimization process involves compliance minimization while considering the volume constraint to obtain a truss-like pattern in the structure. On the other hand, for free vibration cases, the objective is to maximize the first-order eigen-frequency to achieve an optimized material layout. The study has effectively implemented the optimization procedure by utilizing a predetermined volume fraction as a constraint.
2. This study employed various constraints based on design requirements to ensure the practicality of topology optimization during the design phase. In many stages of the design process, dealing with multiple constrained problems is unavoidable. By selecting appropriate constraints, the structural performance can be evaluated, leading to material-saving designs that satisfy functional requirements in optimization problems. The topology optimization of concrete dapped beams was simulated using the BESO method within the ABAQUS software environment, considering the presence of discontinuity regions in some parts of the dapped beams. The Concrete Damage Plasticity model incorporates both tension damage and compression damage within the model.
3. Four different load cases were applied for simulation, allowing the examination of real load scenarios, including transverse and lateral loads. For all load cases, minimum compliance optimization with a volume constraint was adopted. The results showed that the objective history varied for each load case, with the lateral load case requiring more iteration steps to converge. However, after a reasonable number of iterations, a final topology resembling a truss pattern was obtained, which can be effectively used for the appropriate generation of strut and tie modeling.

4. Minimum compliance optimization with a volume constraint was chosen to compare higher-order elements. The observation revealed that switching from quadrilateral to quadratic elements for regular structural elements did not lead to increased efficiency. However, for highly irregular geometry structures, the use of higher-order elements may prove to be more efficient in problem-solving. Higher-order elements were found to produce layouts with fewer checkerboard patterns, particularly in the absence of a filter. Among the three finite elements considered, the 8-noded element showed the best results with the least checkerboard pattern.
5. Topology optimization problems have effectively addressed both stress and deflection control. In these problems, the final layout of the optimized structure is developed based on the fixed constraint values specified for stress and deflection. This ensures that the converged values never exceed the specified constraint values, thereby meeting the safety and aesthetic requirements of the design. Deflection control is also unavoidable to maintain the structural aesthetic appearance.
6. In both types of optimization problems, the final layout of the optimized structure is determined based on fixed constraint values specified for stress and deflection. This ensures that the optimized solution never exceeds the defined constraint values, guaranteeing that the structural integrity and safety requirements are met.
7. Concrete is considered a quasi-brittle material with distinct limits in tension and compression behavior. To accurately model concrete structures, the Drucker-Prager yield criterion for stress is well-suited for such materials, although it demands additional computational effort. This criterion provides precise modeling of concrete structures. Topology optimization offers a powerful approach to optimize the material distribution within the structure, ensuring more accurate and efficient modeling of concrete structures.

5.1 Future scope of research

1. Topology optimization results can be extended to STM modeling of structures dominated with D-regions.
2. The results of topology optimization can be validated with experimental procedures
3. This work can be extended to the design procedures of reinforcement layout of real life structures with D-regions.

4. Modified designs can be checked for fracture and failure to verify adaptability of the Topology optimization in the design.

5.2 PUBLICATIONS

Resmy, V. R. and Rajasekaran, C. (2021).“ Stiffness maximization of concrete structures using topology optimization in static and dynamic problems”. Journal of Structural Engineering, Vol.48, No.1, pp.51-60 (SCOPUS indexed)

Resmy, V. R. and Rajasekaran, C. (2021).“Evolutionary Topology Optimization of Structural Concrete under Various Load Cases”.Advances in Civil Engineering, Lecture Notes in Civil Engineering 83, 369-380 (SCOPUS indexed)

https : //doi.org/10.1007/978 – 981 – 15 – 5644 – 9_2

Resmy, V. R. and Rajasekaran, C.(2020). “Topology Optimization of Concrete Dapped Beams Under Multiple Constraints”., Numerical Optimization in Engineering and Sciences,Advances in Intelligent Systems and Computing 979,43-52 (SCOPUS indexed)

https : //doi.org/10.1007/978 – 981 – 15 – 3215 – 3_5

Resmy, V. R. and Rajasekaran, C.“ Topology optimization of Concrete Structures using Stress Criterion .” Computers and Concrete. (Communicated)

Resmy, V. R. and Rajasekaran, C. (2023). ”Topology Optimization of Concrete beam using Higher Order Finite Elements ”(Accepted for publication in Springer series)

CONFERENCES

Resmy, V. R. and Rajasekaran, C. (2019). “Structural Topology Optimization for Static and Dynamic Load Cases”. 3rd National Conference on Emerging Trends in Science and Engineering(NCETSE-2019),SMVITM,Udupi.

Resmy, V. R. and Rajasekaran, C. (2023). ”Topology Optimization of Concrete beam using Higher Order Finite Elements ”.International Conference on Sustainable Infrastructure (SIIOC-2023),NITK, Suarthkal.

Bibliography

- Abdul-Razzaq, K. S. and Jebur, S. F. (2017). “Experimental verification of strut and tie method for reinforced concrete deep beams under various types of loadings”. *Journal of Engineering and Sustainable Development*, 21(6):39–55. [ix](#), [70](#), [71](#), [72](#)
- Allaire, G. and Jouve, F. (2005). “A level-set method for vibration and multiple loads structural optimization”. *Computer methods in applied mechanics and engineering*, 194(30-33):3269–3290. [19](#)
- Allaire, G. and Jouve, F. (2008). “Minimum stress optimal design with the level set method”. *Engineering analysis with boundary elements*, 32(11):909–918. [19](#)
- Allaire, G., Jouve, F., and Toader, A.-M. (2004). “Structural optimization using sensitivity analysis and a level-set method”. *Journal of computational physics*, 194(1):363–393. [19](#)
- Almeida, V. S., Simonetti, H. L., and Neto, L. O. (2013). “Comparative analysis of strut-and-tie models using smooth evolutionary structural optimization”. *Engineering Structures*, 56:1665–1675. [21](#)
- Amir, O. and ole Sigmund, O. (2013). “Reinforcement layout design for concrete structures based on continuum damage and truss topology optimization”. *Structural and Multidisciplinary Optimization*, 47(2):157–174. [21](#)
- Aslani, F. and Jowkarmeimandi, R. (2012). “Stress–strain model for concrete under cyclic loading”. *Magazine of concrete research*, 64(8):673–685. [36](#)
- Baumgartner, A., Harzheim, L., and Mattheck, C. (1992). “Sko (soft kill option): the biological way to find an optimum structure topology”. *International Journal of Fatigue*, 14(6):387–393. [22](#)
- Beckers, M. (1999). “Topology optimization using a dual method with discrete variables”. *Structural optimization*, 17(1):14–24. [14](#)

- Beghini, L. L., Beghini, A., Katz, N., Baker, W. F., and Paulino, G. H. (2014). “Connecting architecture and engineering through structural topology optimization”. *Engineering Structures*, 59:716–726. [6](#)
- Bends, M. P., Sigmund, O., et al. (2003). “Topology optimization-theory, methods, and applications”. [3](#), [7](#), [8](#), [28](#), [30](#)
- Bendsøe, M. P. (1989). “Optimal shape design as a material distribution problem”. *Structural optimization*, 1:193–202. [13](#), [15](#)
- Bendsoe, M. P. and Querind, O. (2003). *Topology optimization: theory, methods, and applications*. Springer Science & Business Media. [14](#), [16](#)
- Borkowski, A. and Jendo, S. (1990). “Structural optimization”. *Mathematical programming*, 2. [12](#)
- Bruggi, M. (2008). “On an alternative approach to stress constraints relaxation in topology optimization”. *Structural and multidisciplinary optimization*, 36:125–141. [23](#)
- Bruggi, M. (2009). “Generating strut-and-tie patterns for reinforced concrete structures using topology optimization”. *Computers & Structures*, 87(23-24):1483–1495. [21](#)
- Bruggi, M. (2016). “A numerical method to generate optimal load paths in plain and reinforced concrete structures”. *Computers & Structures*, 170:26–36. [21](#)
- Buhl, T., Pedersen, C. B., and Sigmund, O. (2000). “Stiffness design of geometrically non-linear structures using topology optimization”. *Structural and Multidisciplinary Optimization*, 19(2):93–104. [15](#)
- Chan, C.-M. and Liu, P. (2000). “Design optimization of practical tall concrete buildings using hybrid optimality criteria and genetic algorithms”. In *8th International Conference on Computing in Civil & Building Structures*. [13](#)
- Chen, S. and Chen, W. (2011). “A new level-set based approach to shape and topology optimization under geometric uncertainty”. *Structural and Multidisciplinary Optimization*, 44(1):1–18. [20](#)
- Cheng, G. and Jiang, Z. (1992). “Study on topology optimization with stress constraints”. *Engineering Optimization*, 20(2):129–148. [23](#)

- Cheng, G. D. and Guo, X. (1997). “ ε -relaxed approach in structural topology optimization”. *Structural optimization*, 13:258–266. [23](#)
- Chu, D. N., Xie, Y., Hira, A., and Steven, G. (1996). “Evolutionary structural optimization for problems with stiffness constraints”. *Finite elements in analysis and design*, 21(4):239–251. [17](#)
- Deng, H., Vulimiri, P. S., and To, A. C. (2021). “An efficient 146-line 3d sensitivity analysis code of stress-based topology optimization written in matlab”. *Optimization and Engineering*, pages 1–29. [24](#)
- Dorn, W. (1964). “Automatic design of optimal structures”. *J. de Mecanique*, 3:25–52. [7](#)
- Duysinx, P. and Bendsøe, M. P. (1998). “Topology optimization of continuum structures with local stress constraints”. *International journal for numerical methods in engineering*, 43(8):1453–1478. [22](#), [23](#)
- Duysinx, P. and Sigmund, O. (1998). “New developments in handling stress constraints in optimal material distribution”. In *7th AIAA/USAF/NASA/ISSMO symposium on multidisciplinary analysis and optimization*, page 4906. [23](#)
- Duysinx, P., Van Miegroet, L., Lemaire, E., Brùls, O., and Bruyneel, M. (2008). “Topology and generalized shape optimization: Why stress constraints are so important?”. *International Journal for Simulation and Multidisciplinary Design Optimization*, 2(4):253–258. [11](#)
- Eiben, A. E. and Schoenauer, M. (2002). “Evolutionary computing”. *Information Processing Letters*, 82(1):1–6. [19](#)
- Fogel, D. B. (1998). *Artificial intelligence through simulated evolution*. Wiley-IEEE Press. [19](#)
- Grierson, D. E. and Chan, C.-M. (1993). “Design optimization of tall steel building frameworks”. In *Optimization of large structural systems*, pages 863–872. Springer. [12](#)
- Guo, X., Zhang, W. S., Wang, M. Y., and Wei, P. (2011). “Stress-related topology optimization via level set approach”. *Computer Methods in Applied Mechanics and Engineering*, 200(47-48):3439–3452. [23](#)

- Haftka, R. T. and Grandhi, R. V. (1986). “Structural shape optimization—a survey”. *Computer methods in applied mechanics and engineering*, 57(1):91–106. 13
- Herranz, J. P., Santa María, H., Gutierrez, S., and Riddell, R. (2012). “Optimal strut-and-tie models using full homogenization optimization method”. *ACI Structural Journal*, 109(5):605. 21
- Hognestad, E. (1951). “Study of combined bending and axial load in reinforced concrete members”. Technical report, University of Illinois at Urbana Champaign, College of Engineering 36
- Hsu, L. and Hsu, C.-T. (1994). “Complete stress—strain behaviour of high-strength concrete under compression”. *Magazine of concrete research*, 46(169):301–312. 36
- huang, O., Young, V., Steven, G., and Xie, Y. (2000). “Computational efficiency and validation of bi-directional evolutionary structural optimisation”. *Computer methods in applied mechanics and engineering*, 189(2):559–573. 17
- Huang, P.-C. and Nanni, A. (2006). “Dapped-end strengthening of full-scale prestressed double tee beams with frp composites”. *Advances in Structural Engineering*, 9(2):293–308. 32
- Huang, X. and Xie, Y. (2007). “Convergent and mesh-independent solutions for the bi-directional evolutionary structural optimization method”. *Finite elements in analysis and design*, 43(14):1039–1049. 17
- Jh, H. (1975). “Adaptation in natural and artificial systems”. *Ann Arbor*. 18
- Kirsch, U. (1990). “On singular topologies in optimum structural design”. *Structural optimization*, 2:133–142. 23
- Koza, J. R. (1994). *Genetic programming II: automatic discovery of reusable programs*. MIT press. 19
- Larsen, U. D., Signund, O., and Bouwsta, S. (1997). “Design and fabrication of compliant micromechanisms and structures with negative poisson’s ratio”. *Journal of microelectromechanical systems*, 6(2):99–106. 15

- Le, C., Norato, J., Bruns, T., Ha, C., and Tortorelli, D. (2010). “Stress-based topology optimization for continua”. *Structural and Multidisciplinary Optimization*, 41(4):605–620. [23](#)
- Lee, D.-K., Yang, C.-J., and Starossek, U. (2012). “Topology design of optimizing material arrangements of beam-to-column connection frames with maximal stiffness”. *Scientia Iranica*, 19(4):1025–1032. [22](#), [25](#)
- Liang, Q. Q., Uy, B., and Steven, G. P. (2002). “Performance-based optimization for strut-tie modeling of structural concrete”. [20](#), [21](#)
- Liu, S. and Qiao, H. (2011). “Topology optimization of continuum structures with different tensile and compressive properties in bridge layout design”. *Structural and Multidisciplinary Optimization*, 43(3):369–380. [21](#)
- Liu, X., Yi, W.-J., Li, Q., and Shen, P.-S. (2008). “Genetic evolutionary structural optimization”. *Journal of constructional steel research*, 64(3):305–311. [18](#)
- Luo, Z., Wang, M. Y., Wang, S., and Wei, P. (2008). “A level set-based parameterization method for structural shape and topology optimization”. *International Journal for Numerical Methods in Engineering*, 76(1):1–26. [19](#)
- Maar, B. and Schulz, V. (2000). “Interior point multigrid methods for topology optimization”. *Structural and Multidisciplinary Optimization*, 19(3):214–224. [15](#)
- Makhija, D. and Maute, K. (2014). “Numerical instabilities in level set topology optimization with the extended finite element method”. *Structural and Multidisciplinary Optimization*, 49(2):185–197. [19](#)
- Maxwell, J. C. (1864). “L. on the calculation of the equilibrium and stiffness of frames”. *The London, Edinburgh, and Dublin Philosophical Magazine and Journal of Science*, 27(182):294–299. [12](#)
- Michell, A. G. M. (1904). “Lviii. the limits of economy of material in frame-structures”. *The London, Edinburgh, and Dublin Philosophical Magazine and Journal of Science*, 8(47):589–597. [11](#), [13](#)

- Mueller, K. M. and Burns, S. A. (2001). “Fully stressed frame structures unobtainable by conventional design methodology”. *International journal for numerical methods in engineering*, 52(12):1397–1409. [12](#)
- Nagarajan, P. and Pillai, T. M. (2008). “Development of strut and tie models for simply supported deep beams using topology optimization”. *Sonklanakarin Journal of Science and Technology*, 30(5):641. [21](#)
- Ohmori, H. (2011). “Computational morphogenesis: its current state and possibility for the future”. *International Journal of Space Structures*, 26(3):269–276. [6](#)
- Osher, S. and Sethian, J. A. (1988). “Fronts propagating with curvature-dependent speed: Algorithms based on hamilton-jacobi formulations”. *Journal of computational physics*, 79(1):12–49. [19](#)
- Palmisano, F. and Elia, A. (2015). “Shape optimization of strut-and-tie models in masonry buildings subjected to landslide-induced settlements”. *Engineering Structures*, 84:223–232. [21](#)
- Pedersen, P. (2003). “Optimal designs-structures and materials-problems and tools”. [1](#), [11](#)
- Pereira, J. T., Fancello, E. A., and Barcellos, C. (2004). “Topology optimization of continuum structures with material failure constraints”. *Structural and Multidisciplinary Optimization*, 26(1-2):50–66. [22](#)
- Prager, W. and Rozvany, G. I. (1977). “Optimization of structural geometry”. *Dynamical systems*, pages 265–293. [13](#)
- Pucker, T. and Grabe, J. (2011). “Structural optimization in geotechnical engineering: basics and application”. *Acta Geotechnica*, 6(1):41–49. [5](#)
- Querin, O., Steven, G., and Xie, Y. (2000). “Evolutionary structural optimisation using an additive algorithm”. *Finite elements in Analysis and Design*, 34(3-4):291–308. [17](#)
- Querin, O. M., Steven, G. P., and Xie, Y. M. (1998). “Evolutionary structural optimisation (eso) using a bidirectional algorithm”. *Engineering computations*. [17](#)
- Rechenberg, I. (1965). “Cybernetic solution path of an experimental problem”. *Royal Aircraft Establishment Library Translation 1122*. [19](#)

- Rozvany, G. I. (2009). “A critical review of established methods of structural topology optimization”. *Structural and multidisciplinary optimization*, 37(3):217–237. [16](#)
- Rozvany, G. I. (2012). *Structural design via optimality criteria: the Prager approach to structural optimization*, volume 8. Springer Science & Business Media. [12](#)
- Rozvany, G. I., Zhou, M., and Birker, T. (1992). “Generalized shape optimization without homogenization”. *Structural optimization*, 4:250–252. [22](#)
- Schlaich, J., Schäfer, K., and Jennewein, M. (1987). “Toward a consistent design of structural concrete”. *PCI journal*, 32(3):74–150. [20](#)
- Senhora, F. V., Giraldo-Londono, O., Menezes, I. F., and Paulino, G. H. (2020). “Topology optimization with local stress constraints: a stress aggregation-free approach”. *Structural and Multidisciplinary Optimization*, 62:1639–1668. [24](#)
- Sethian, J. A. and Wiegmann, A. (2000). “Structural boundary design via level set and immersed interface methods”. *Journal of computational physics*, 163(2):489–528. [19](#)
- Stolpe, M. and Svanberg, K. (2001). “On the trajectories of penalization methods for topology optimization”. *Structural and Multidisciplinary Optimization*, 21(2):128–139. [16](#), [22](#)
- Tenek, L. H. and Hagiwara, I. (1993). “Optimization of material distribution within isotropic and anisotropic plates using homogenization”. *Computer methods in applied mechanics and engineering*, 109(1-2):155–167. [15](#)
- Tjhin, T. and Kuchma, D. (2002). “Computer-based tools for design by strut-and-tie method: Advances and challenges”. *ACI Structural Journal*, 99(5). [22](#)
- Tsavidaridis, K. D. (2015). “Applications of topology optimization in structural engineering: High-rise buildings and steel components”. *Jordan Journal of Civil Engineering*, 9(3):335–357. [6](#)
- Van Mieghroet, L. and Duysinx, P. (2007). “Stress concentration minimization of 2d filets using x-fem and level set description”. *Structural and Multidisciplinary Optimization*, 33:425–438. [23](#)

- Vanderplaats, G. N. (1993). “Thirty years of modern structural optimization”. *Advances in Engineering Software*, 16(2):81–88. [11](#)
- Wang, M. Y., Wang, X., and Guo, D. (2003). “A level set method for structural topology optimization”. *Computer methods in applied mechanics and engineering*, 192(1-2):227–246. [19](#)
- Xia, L., Fritzen, F., and Breitkopf, P. (2017). “Evolutionary topology optimization of elastoplastic structures”. *Structural and Multidisciplinary Optimization*, 55:569–581. [17](#)
- Xia, L., Xia, Q., Huang, X., and Xie, Y. M. (2018a). “Bi-directional evolutionary structural optimization on advanced structures and materials: a comprehensive review”. *Archives of Computational Methods in Engineering*, 25:437–478. [17](#)
- Xia, L., Zhang, L., Xia, Q., and Shi, T. (2018b). “Stress-based topology optimization using bi-directional evolutionary structural optimization method”. *Computer Methods in Applied Mechanics and Engineering*, 333:356–370. [23](#), [24](#)
- Xia, Q., Shi, T., Liu, S., and Wang, M. Y. (2012). “A level set solution to the stress-based structural shape and topology optimization”. *Computers & Structures*, 90:55–64. [23](#)
- Xie, Y. M. and Steven, G. P. (1993). “A simple evolutionary procedure for structural optimization”. *Computers & structures*, 49(5):885–896. [17](#), [21](#), [24](#)
- Yang, R. and Chen, C. (1996). “Stress-based topology optimization”. *Structural optimization*, 12(2-3):98–105. [23](#), [24](#)
- Yang, X. (1999). *Bi-directional evolutionary method for stiffness and displacement optimization*. PhD thesis, Victoria University of Technology. [21](#)
- Zhao, J. and Wang, C. (2014). “Robust structural topology optimization under random field loading uncertainty”. *Structural and Multidisciplinary Optimization*, 50(3):517–522. [6](#)
- Zhong, J., Wang, L., Deng, P., and Zhou, M. (2017). “A new evaluation procedure for the strut-and-tie models of the disturbed regions of reinforced concrete structures”. *Engineering Structures*, 148:660–672. [22](#)

SCHOLAR DETAILS

Name : Resmy V R
Student Registration Number : 165112CV16F16
Contact No : + 91-7022087177
E-mail : resmy.raveendra@gmail.com
Research Interests : Finite element Modeling, Reinforced Concrete Structures,
Structural Optimization , Fracture Mechanics
Address : Varuvilaveedu, Nedungolam P.O, Paravur, Kollam -691334

